Proteome characterization of *Escherichia coli* cells evolved to tolerate elongation factor P deletion

Vorgelegt von

M.Sc. in Biochemie und Molekularbiologie

Mingjian Wang

Geb. In Lanzhou, Gansu, China

Von der Fakultät II – Mathematik und Naturwissenschaften

der Technischen Universität Berlin

Zur Erlangung des akademischen Grades

Doktor der Naturwissenschaften

Dr. rer. nat

genehmigte Dissertation

Promotionsausschuss:

Vorsitzender: Prof. Dr. Reinhard Schomäcker

Erstgutachter: Prof. Dr. Nediljko Budisa

Zweitgutachter: Prof. Dr. Daniel Wilson

Drittgutachter: Dr. Verónica Dumit

Tag der wissenschaftlichen Aussprache: 26. Oktober 2017

Berlin 2017

Abstract

Elongation factor P (EF-P) is an essential translation factor in bacteria, it has been reported that EF-P plays an important role in rescuing the translation stalling caused by the oligo-proline containing peptides stretch. The growth rate of *E. coli* was significantly restricted when EF-P was knocked out. However, through a continuous directed evolution in the turbidostatic model, both the wildtype and the EF-P knock-out strains grow robustly. To elucidate possible mechanism behind the robust growth established during the adaptation in under the conditions of continuous cultivation, we employed a high-throughput proteome approach, which involves mass spectrometry (MS) and stable isotope labeling by amino acids in cell culture (SILAC). In addition, YeiP has been considered as a paralog of EF-P. In order to reveal whether YeiP's function overlaps those of EF-P, the proteomics study was also performed on YeiP knock-out strains and on an EF-P and YeiP double knock-out strain. In order to employ SILAC-based MS, *argA* and *lysA* genes had to be knock-out from all strains studied.

Continuous directed evolution proved to have a negative effect on the level of a large amount of proteins involved in ATP-dependent biosynthetic pathways, chemotaxis and flagellar assembly.

In the comparison of the EF-P knock-out strain and the control strain, the most interesting change is the down-regulation of the iron metabolism related proteins, which are involved in enterobactin biosynthesis and the sulfur mobilization (SUF) system for Fe-S cluster assembly. After the evolution, the level of the proteins participating in the enterobactin biosynthesis pathway was not significantly changed, but the proteins from the SUF system were significantly up-regulated.

Additionally, MS data on oligo-proline containing proteins revealed that the absence of EF-P did not globally decrease the level of the PP-containing proteins, even up-regulated some of them. Approximately one-third of the quantified PPP-containing proteins were significantly down-regulated by the absence of EF-P. After the evolution process, a partial recovery of these proteins' values was observed.

The YeiP knock-out strain did not show the same behavior regarding its growth rate and proteome changes as the EF-P knock-out strain when compared to the control. The only significant change that was detected was the up-regulation of MgtA (magnesium-transporting ATPase). The double EF-P and YeiP knock-out strain displayed a lower growth rate but similar proteome changes as the EF-P knock-out strain. It indicates that YeiP does not strictly overlap its function to the one of EF-P.

Zusammenfassung

Der Elongationsfaktor P (EF-P) ist ein essentieller Translationsfaktor in Bakterien. Es wurde berichtet, dass EF-P eine wichtige Rolle beim Verhindern von ribosomalem stalling spielt, die durch Oligoprolinabschnitte in Peptiden verursacht werden. Die Wachstumsrate von *E. coli* war signifikant verringert wenn EF-P knockout war. Jedoch wuchsen durch kontinuierliche gerichtete Evolution des turbidostatischen Models sowohl der Wildtyp als auch der EF-P-Knockout-Stamm robust. Um die Mechanismen dieses robusten Wachstums aufzudecken, wurde ein high-throughput Proteomansatz etabliert, der Massenspektrometrie (MS) und „stable isotope labeling by amino acids in cell culture“ (SILAC) enthält. Zusätzlich wurde YeiP als Paralog von EF-P betrachtet. Um herauszufinden, ob die Funktion von YeiP die von EF-P überschneidet wurden die proteomischen Untersuchungen auch an YeiP-Knockout-Stämmen und an YeiP- und EF-P-Doppelknockout-Stämmen durchgeführt. Um die SILAC-basierte MS einzuführen, mussten *argA* und *lysA* Gene von allen untersuchten Stämmen knockout werden.

Es ist bewiesen, dass die kontinuierliche gerichtete Evolution einen negativen Effekt auf den Gehalt von vielen Proteinen hat, die in den ATP-abhängigen Biosytheseweg und Chemotaxis involviert sind.

Im Vergleich zwischen EF-P-Knockout und dem Kontrollstamm ist die interessanteste Veränderung die Runterregulierung von Proteinen, die mit dem Eisenmetabolismus zusammenhängen. Diese Proteine sind an der Enterobaktinbiosynthese und dem Schwefelmobilisierungssystem (SUF) für Fe-S Cluster beteiligt. Nach der Evolution war der Gehalt an Proteinen die in der Enterobaktinbiosynthese beteiligt sind nicht signifikant verändert, allerdings waren die Proteine des SUF-Systems signifikant hoch reguliert.

Außerdem wurde über die MS Daten von Oligoprolinhaltigen Proteinen erkannt, dass die Abwesenheit von EF-P den Gehalt von PP-haltigen Proteinen nicht global verringert, sondern einige sogar hoch reguliert. Ungefähr ein Drittel der quantifizierten PPP-haltigen Proteine waren durch die Abwesenheit von EF-P signifikant runter reguliert. Nach dem Evolutionsprozess wurde eine partielle Wiederherstellung dieser Proteingehalte festgestellt.

Der YeiP-Knockout-Stamm zeigte nicht das gleiche Verhalten in Bezug auf Wachstumsrate und Veränderung des Proteoms wie der EF-P-Knockout-Stamm im Vergleich zur Kontrolle. Die einzige signifikante Veränderung die festgestellt werden konnte war die Hochregulierung von MgtA (Magnesium-transportierende ATPase). Der EF-P-YeiP-Doppelknockout-Stamm zeigte eine geringere Wachstumsrate, aber ähnliche Veränderungen des Proteoms wie der EF-P-Knockout-Stamm. Dies deutet an, dass die Funktion von YeiP nicht zwingend die Funktion von EF-P überschneidet.

Table of Contents

List of Tables

List of Figures

List of Abbreviations

(4S/R-) Flp	*cis/trans*-4-fluoroproline
[3,2]Tp	β-thieno[3,2-b]pyrrole
[3,2]Tpa	L-β-(thieno [3,2-b]pyrrolyl) alanine
µ	micro
1, 3 BPG	1, 3-Bisphosphoglyceric acid
2D	two-dimensional
2PG	2-Phosphoglyceric acid
3-L-CHOP	*cis*-3-hydroxy-L-proline
3-L-THOP	*trans*-3-hydroxy-L-proline
3PG	3-Phosphoglyceric acid
4-D-CHOP	*cis*-4-hydroxy-D-proline
4FTrp	4-fluorotrytophan
4-L-CHOP	*cis*-4-hydroxy-L-proline
4-L-THOP	(2S, 4R)-4-hydroxyproline
a/eIF-5A	archaeal and eukaryotic initiation factor 5A
ABC	ATP-binding cassette
Ac-Pro-NHMe	*N*-acetyl-L-proline-*N'*-methylamide
Ala, A	alanine
AMP	antimicrobial peptide
amp	ampicillin
ampR	ampicillin resistance
Arg, Arg-0, R	arginine
Arg-10	L-[$^{13}C_6$, $^{15}N_4$] arginine
Arg-6	L-[$^{13}C_6$] arginine
Asn, N	asparagine
Asp, D	aspartate
ATT	attractant
Aze	azetidine-2-carboxylic acid
cAA	canonical amino acid
CCW	counter-clockwise
CW	clockwise
Cys, C	cysteine
Da	dalton
ddH_2O	double distilled water
DHAP	dihydroxyacetone phosphate
DHP	dihydroxyproline
dNTP	deoxyribonucleotide triphosphate
Dpp	dipeptide permease
Dtp	dipeptide and tripeptide permease
DTT	dithiothreitol
E. coli	*Escherichia coli*
EDTA-2Na	Ethylenediaminetetraacetic acid disodium salt dihydrate
EF-P	elongation factor P
ELP	elastin-like polypeptide
et al.	*et alii*

Evo	evolved
F6P	D-fructose 6-phosphate
FDP	D-fructose 1, 6-bisphosphate
Fe^{2+}	ferrous
Fe^{3+}	ferric iron
Fe-S	Iron-sulfur
Flp	flippase
g	gram
G1P	glucose-1-phosphate
G3P	D-glyceraldehyde 3-phosphate
G6P	D-glucose 6-phosphate
Gat1P	galactitol 1-phosphate
Gln, Q	glutamine
Glu, E	glutamic acid
Gly, G	glycine
His, H	histidine
HOP	hydroxyproline
HPLC	High-performance liquid chromatography
Hyp	(2S, 4R)-4-hydroxyproline
IAA	iodoacetamide
Ile, I	isoleucine
IMP	inosine monophosphate
Ind	indole
ISC	iron-sulfur cluster
kan	kanamycin
kanR	kanamycin resistance
kb	kilobase pairs
KO	knock-out
Leu, L	leucine
LTEE	long-term evolution experiment
Lys, Lys-0, K	lysine
Lys-4	L-[$^{2}H_{4}$] lysine
Lys-8	L-[$^{13}C_{6}$, $^{15}N_{2}$] lysine
m	milli
M	molar
MCP	methyl-accepting chemotaxis protein
Met, M	methionine
MePro	methanoprolines
MgtA	magnesium-transporting ATPase
MS	mass spectrometry
NADH	Nicotinamide adenine dinucleotide
NAP	nitrate reductase
ncAA	non-canonical amino acid
O/N	overnight
OD_{600}	optical density at 600 nm
Opp	oligopeptide permease

P4H	prolyl 4-hydroxylase
PAGE	polyacrylamide gel electrophoresis
PAP	3'(2')-phosphoadenosine 5'-phosphate
PCR	polymerase chain reaction
PDB	Protein Data Bank
PEP	phosphoenolpyruvate
PES	potential energy surface
Pfk	phosphofructokinase
Phe, F	phenylalanine
Pip	pipecolic acid
Pro	proline
Pro*	Pro analogue
Pro, P	proline
PTC	peptidyl transferase center
PTM	post-translationally modification
PTR	peptide transporter
PTS	phosphotransferase system
Pyl	pyrrolysine
RiPP	ribosomally synthesized and post-translationally modified peptide
RPM	revolutions per minute
RT	room temperature
S. typhimurium	*Salmonella typhimurium*
SCS	stop codon suppression
SDS	sodium dodecyl sulfate
Sec	selenocysteine
Ser, S	serine
SILAC	stable isotope labeling by amino acids in cell culture
SPI	supplementation-based incorporation
SUF	sulfur mobilization
T. thermophilus	*Thermus thermophilus*
Tag6P	D-tagatose 6-phosphate
TagBP	D-tagatose 1, 6-bisphosphate
Taq	Taq DNA Polymerase
TCA-cycle	tricarboxylic acid cycle
Thr, T	threonine
T_m	melting temperature
Tris	Tris (hydroxymethyl) aminomethane
Trp, W	tryptophan
TrpBA	Trp synthase
Tt	transition temperature
Tyr, Y	tyrosine
UMP	uridine monophosphate
Val, V	valine
vs.	versus
WT	wildtype

1 Introduction

1.1 Amino acid proline appearance in protein

Ramachandran plot is a powerful tool for proteins structure research, by which torsion angles (φ and ψ) are used to describe the conformation of polypeptide and protein. The parameters φ and ψ represent the two dihedral angles of the rotation that occurs at the bond N-C^{α} and C^{α}-C′, respectively [1, 2]. Among the 20 canonical amino acids (cAAs), proline (Pro) is unique because of the N-alkyl cyclic structure, pyrrolidine ring (Figure 1A). The pyrrolidine ring restricts the φ angle to the average value around -65°. And as a five-membered ring, the structure of pyrrolidine ring could be two different down- (C^{γ}-*endo*) and up-puckered (C^{γ}-*exo*) conformations (Figure 2). The down-puckered conformation is defined as that the Pro residue's C^{γ} atom is located on the same side with the C′=O group, in contrast, the C^{γ} atom and the C′=O group are distributed on the opposite sides in the up-puckered conformation. The three atoms C^{δ}, N, and C^{α} define the pucker plane, which torsion angle χ1 is defined for the N-C^{α}-C^{β}-C^{γ} sequence [3, 4, 5] (Figure 1B). The vast majority of the planar peptide bonds in protein structures are *trans*-conformation. There are only around 0.03% of the reported non-Pro peptide bond is in *cis*- formation. Unusually, more than 5% X-Pro bond is in *cis*- formation [6] (Figure 3). The significant population of *cis*- Pro is owing to the tertiary amide bonds, which is only formed by Pro in the proteinogenic amino acids [7]. In the studies on the conformational preferences and transition states for the X-Pro isomerization, *N*-acetyl-L-proline-*N'*-methylamide (Ac-Pro-NHMe) is widely used as a model. From the potential energy surface (PES), the energy barrier of the ring flips from down- to up- puckered conformation is 2.5 kcal/mol for *trans*-conformational Ac-Pro-NHMe, and it is 3.2 kcal/mol for *cis*-confirmation [4]. There is a high energy barrier around 20 kcal/mol between *cis*- and *trans*- conformers for an 180° rotation around the peptide bond, which restricts the interconversion rate of the two confirmations [4, 8, 9]. The dihedral angle of the peptide bond is represented with ω, of which the value of prolyl peptide bond is at ω′≈120° and -70°. The energy barrier of prolyl peptide bond rotation for Ac-Pro-NHMe is increased with the increasing polarity of the solvent, which is mainly attributed to the relative free energy reducing for transition states. The population of *cis* conformation is increased with the same trend [4].

The unique structure and properties of Pro attribute specific characteristics to proteins [10]. The incorporation of the tertiary amide leads to the disintegration of α-helices and β-sheet structures in proteins. In a large number of plants and bacteria, the accumulation of Pro plays an essential role in response to osmotic stresses [11, 12]. In addition to the osmo-protection role, in vitro and Pro-overproducing studies show that Pro is involved in multiple biological functions: enhancement of the protein stress tolerance to freezing [13, 14] and dehydration [15], of thermal stability [16], and as antioxidant [17]. The solubility of sparingly soluble proteins could be improved by Pro solution [18]. During proteins folding and refolding, Pro could prevent the aggregation [19, 20].

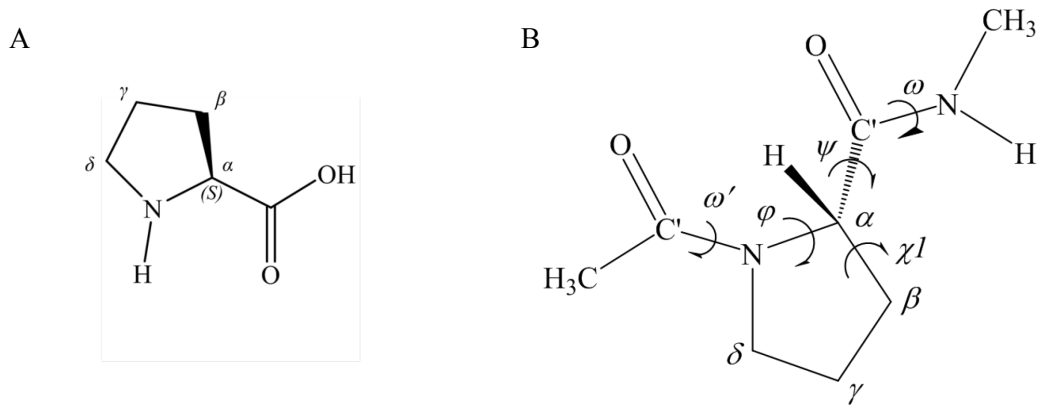

Figure 1. Structure parameters and torsion angles of proline and proline dipeptide [4, 5]. A. Structure of proline. B. Definition of torsion angles and structural parameters for Ac-Pro-NHMe.

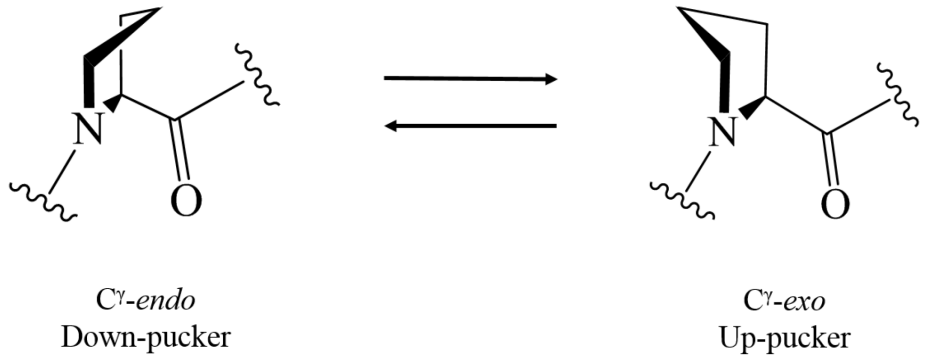

Figure 2. C$^{\gamma}$-*endo* and C$^{\gamma}$-*exo* puckers of proline [21].

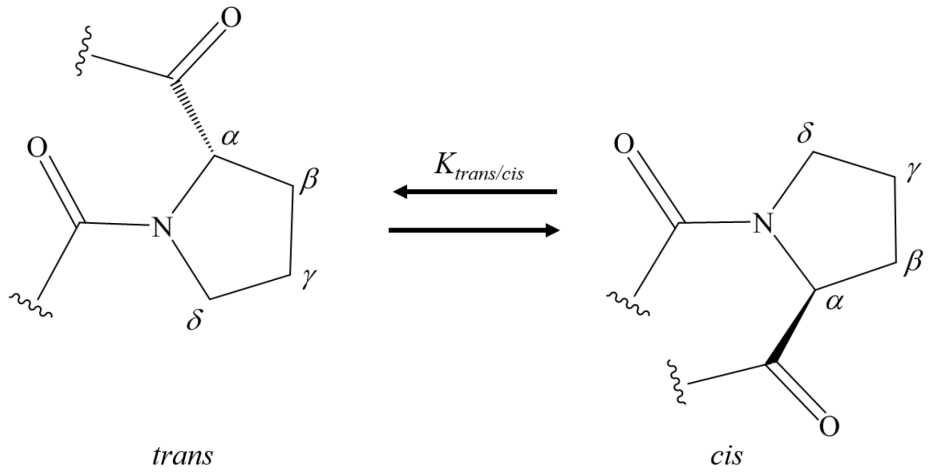

Figure 3. Proline *cis-trans* isomerization.

1.2 Ribosome stalling caused by oligo-proline stretches and rescued by elongation factor P

Ribosome serves as a platform for protein synthesis in cells. The peptidyl transferase center (PTC) is the active site of ribosome. PTC catalyzes two reactions, peptide bond formation and peptidyl-tRNA releasing. The peptide-bond formation occurs between an aminoacyl-tRNA in the ribosomal A-site and a peptidyl-tRNA in the P-site. The peptidyl-tRNA is hydrolyzed with the auxiliary of release factors [22, 23]. However, the efficiency of the peptide bonds among all the amino acids formed by ribosome is different. Especially for Pro, the unique pyrrolidine ring structure makes it different from other the 19 amino acids. On one hand, the privilege cyclic structure of Pro promotes protein folding, on the other hand, it remarkably impedes the rate of peptide bond formation by ribosome. During the protein synthesis, Pro is both a poor peptidyl acceptor in A-site and poor donor in P-site. These properties lead to the notably slower installation than other amino acids. Therefore, the ribosomal stalling caused by Pro-containing motifs is an essential constraint for elongation and termination [23, 24, 25, 26, 27, 28]. In addition, the ribosome stalling is progressively increased when consecutive (two or more) Pro residues participate in translation by ribosome. However, ribosome stalling caused by Pro or oligo-proline stretch can be alleviated by the elongation factor P (EF-P) [29, 30, 21, 31, 32].

EF-P is prevalent in bacteria, and it is orthologous to archaeal and eukaryotic initiation factor 5A (a/eIF-5A). In 1975, EF-P has been characterized as an initiation factor, which was known to bind to ribosome and stimulates the peptide bond formation [33, 34, 35]. Since 2013, numerous studies have shown that EF-P plays an essential role in rescuing the ribosome stalling induced by Pro or oligo-proline stretch [29, 30, 21, 31, 32].

EF-P consists 188 amino acid residues (See Appendix), and is codified by *efp* gene (567 bps). The amount of EF-P molecules in one *E. coli* cell is around 800-900, whose ratio is 1/10 to ribosome copies [36]. The crystal structure of EF-P from *Thermus thermophilus* HB8 strain shows that three β-barrel domains (I, II, and III) are arranged in an "L" shape (Figure 4). The overall shape, molecule size and charge distribution of EF-P are extraordinarily similar to a tRNA (Figure 4) [37].

The crystal structure of *T. thermophilus* 70S ribosome bound with EF-P and tRNA shows that EF-P joints 50S and 30S ribosome subunits, in combination with a tRNA (Figure 5). The binding site of EF-P at 70S ribosome is located between the P-site and the exiting tRNA (E-site). The D-loop and acceptor stem of the P-site tRNA is fixed to 50S subunit with EF-P domain I. And the EF-P domain III binds to the P-site tRNA near the anticodon stem-loop. Additionally, the domain II combines EF-P to the ribosomal protein L1 [38, 22].

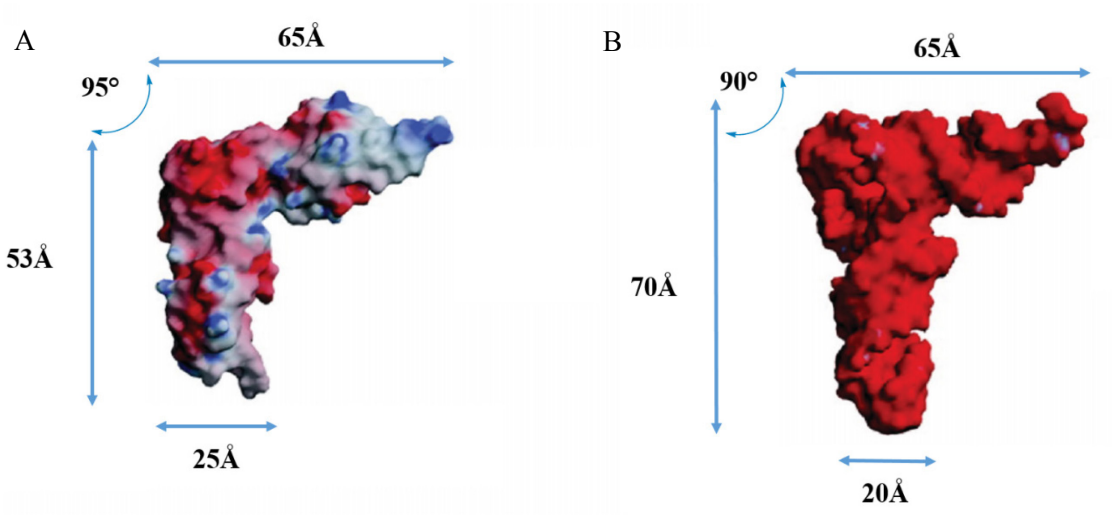

Figure 4. Structure comparison of EF-P and tRNA. A. EF-P from *T. thermophilus* (PDB ID code: 1UEB). B. $tRNA^{Phe}$ from Saccharomyces cerevisiae (PDB ID code: 1EFG). Modified from Hanawa-Suetsugu, et al. [37].

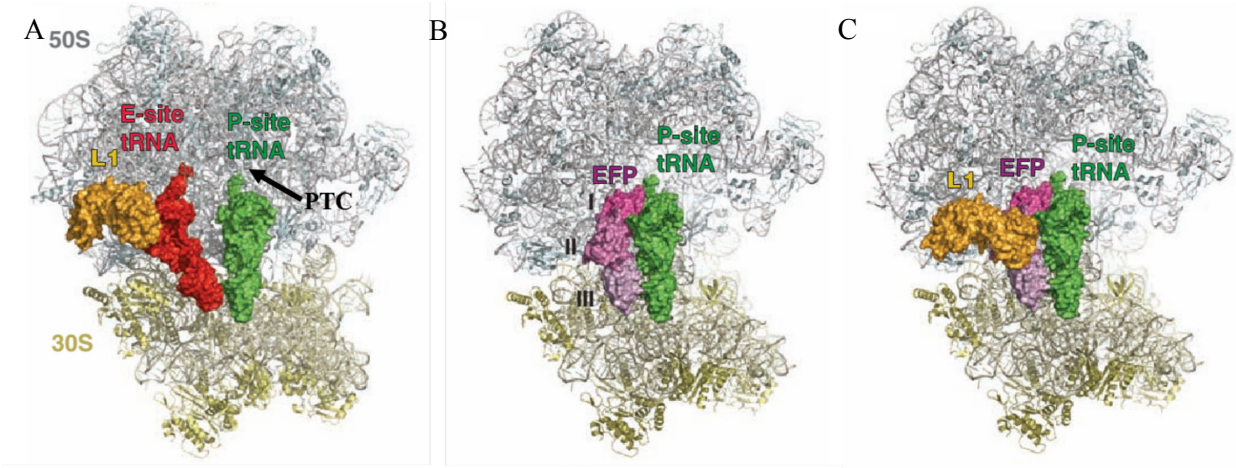

Figure 5. The structure of EF-P bound to 70S ribosome. A. E-site and P-site tRNA bound to the ribosome. B. EF-P and P-site tRNA bind to the ribosome. C. Same as B, but L1 is shown binding with domain II of EF-P. Note that the 50S subunit is shown in gray, the 30S subunit is shown in yellow, E-site tRNA is colored in red, P-site tRNA is colored in green, L1 is colored in golden, and the three domains of EF-P are shown in gradient magenta. Modified from Blaha et al. [38].

The activation of EF-P by post-translationally modifications (PTMs) is crucial for the rescuing of ribosome stalling caused by oligo-proline stretches. So far, there are two PTM pathways have been described. In the first strategy, the modification includes two steps by three enzymes, the Lys-34 (K34) residue in domain I is initially β-lysylted by lysine aminomutase EpmB (synonym is YjeK) and lysyl-transferase EpmB (synonyms include YjeA, PoxA, and GenX), and subsequent hydroxylation is performed by the hydroxylase EpmC (synonym is YfcM) [39, 40, 41, 42]. But in the cases of *Escherichia coli* and *Salmonella typhimurium*, it was indicated that the hydroxylation catalyzed by EpmC is not crucially required for EF-P activity [42]. From the crystallographic structure, it can be seen that the

length of the K34 residue is extended to reach the PTC, where it stimulates peptide bond formation. In the second active pathway for EF-P, the Arg-32 (R32) is rhamnosylated by a glycosyltransferase (EarP), and dTDP-L-rhamnose is utilized as a substrate [43]. This arginine-rhamnosylated strategy has been discovered in some clinically relevant bacteria, *Shewanella oneidensis* and *Pseudomonas aeruginosa* [43, 44]. In addition, a recent investigation about *Neisseria meningitidis* demonstrated that the rhamnosyl modified EF-P is essential for rescuing the ribosomal stalling caused by proline stretches [45]. Therefore, the rhamnosyl modification enzyme EarP and the dTDP-L-rhamnose biosynthetic enzymes are expected to be potential targets for antibacterial medicine development.

In recent five years, numerous studies have determined the most important function of EF-P, which is the rescuing of translation stalls caused by oligo-proline motifs containing sequence. In the case of the membrane-integrated sensor and transcriptional regulator CadC [29], which contains an oligo-proline motif (PPPIP), the expression of CadC was significantly reduced in an EF-P knock-out (KO) strain, and the translational stalling was relieved when EF-P was present. On the other side, EF-P does not significantly affect the translation when the sequence of the motif mutated to PAPIP or AAAIS. And it has been verified that the translation of oligo-proline containing motifs PPG, PPP, and longer Pro strings could be promoted by EF-P [30]. The high throughput proteomics research about EF-P mutant *S. typhimurium* strain revealed that APP is also a target tripeptide motifs for EF-P. Additionally, some motives without oligo-proline sequence like YIPYIP and GSCGPG are also regulated by EF-P. Only one fifth oligo-proline motifs containing proteins were down-regulated in the EF-P mutant *S. typhimurium*, this result suggested that the oligo-proline motifs are not extensively regulated by EF-P [46]. A study on XPPX sequence motifs revealed that the context of oligo-proline (both of XPP and PPX) have different consequences of translational stalling induced by the mutant of *efp* [32].

1.3 Proline analogues and their incorporation into proteins

Since the unique behavior endowed by Pro to structure and folding of proteins, a number of Pro analogues (Pro*) are researched and developed in order to alter protein features. The typical Pro* are (Figure 6): hydroxyproline (HOPs), azetidine-2-carboxylic acid (Aze), pipecolic acid (Pip), α-methyl-L-proline, α-benzyl-L-proline, 4-oxa-L-proline, thia-prolines, and fluorinated prolines. These Pro* have the potential to improve the physicochemical, biological, or pharmaceutical characteristics of natural or *de novo* designed peptides.

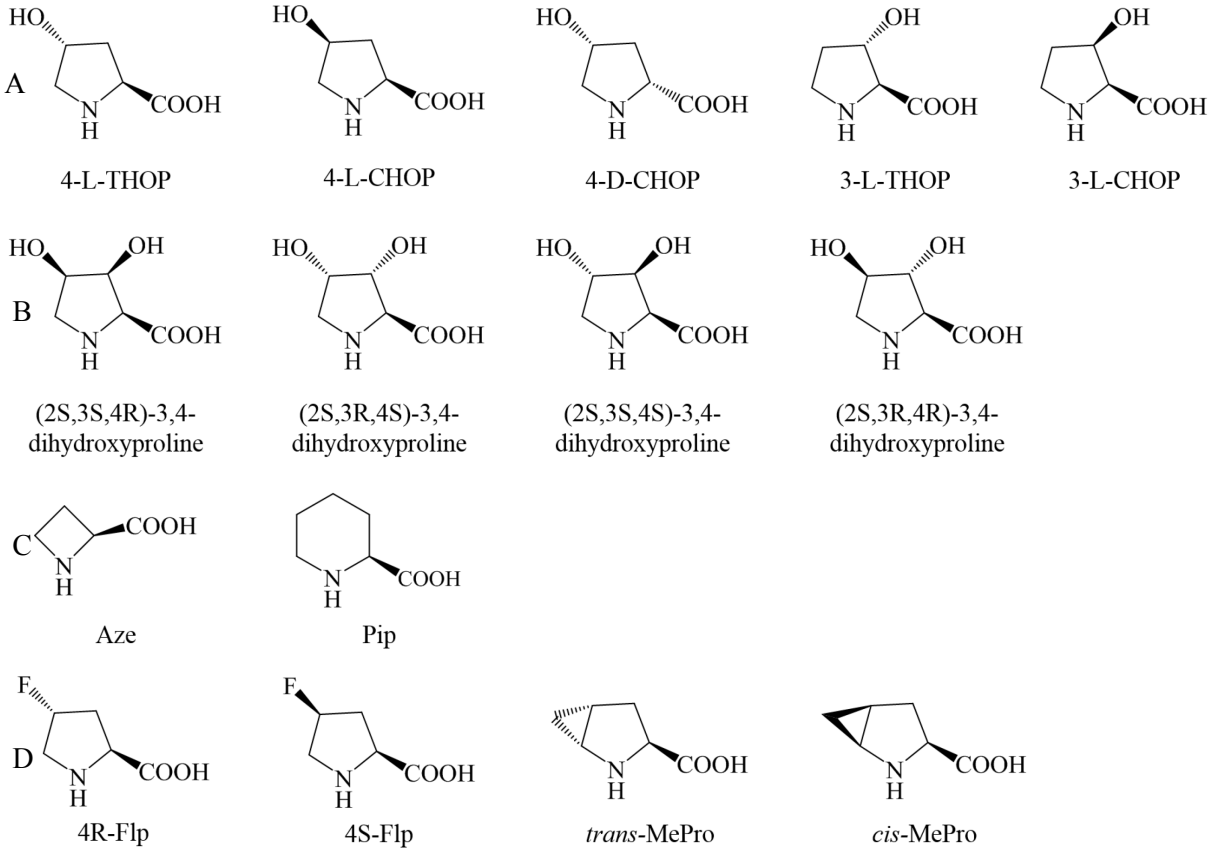

Figure 6. The structures of typical proline analogues. A. Natural HOPs. B. Possible stereoisomers of DHPs. C. Pro's four-membered ring analogue Aze and six-membered ring analogue Pip. D. (4S/R-) Flp and *trans/cis*-MePro.

HOPs are representative group analogues of Pro. Among HOPs, *trans*-4-hydroxy-L-proline (abbreviated as Hyp, or 4-L-THOP) (Figure 7) is the most common in nature, which is produced from Pro by the catalysis of prolyl 4-hydroxylase (P4H) in human cells [47]. P4H belongs to the non-heme Fe^{2+} and α-ketoglutarate dependent dioxygenase family. In addition, a molecule of oxygen (O_2) is necessary for the reaction. As a result, succinate and CO_2 are produced (Figure 7) [48, 49]. The 4R hydroxyl group leads to the structure predilection for up-puckering and *trans*- peptide bond (Figure 8). P4Hs not only exist in animal cells but also widely present in various plants and microbes. A series of prolyl and Pro hydroxylases have been reported, the substrates have multiple sequences, and the only common characteristic is the presence of Pro residues. Hyps are involved in proteins folding, structure

stabilization, molecular recognition, activation of other PTMs, and antibacterial activity of bacterial nonribosomal peptide [47].

Based on the positions of the hydroxyl group at 3 and 4, and the chirality (L-form and D-form), HOPs include eight kinds of heterocyclic stereoisomers (Figure 6A). In addition to the 4-L-THOP mentioned above, the remaining HOPs include *cis*-4-hydroxy-L-proline (4-L-CHOP), *trans*-4-hydroxy-D-proline, *cis*-4-hydroxy-D-proline (4-D-CHOP), *trans*-3-hydroxy-L-proline (3-L-THOP), *cis*-3-hydroxy-L-proline (3-L-CHOP), *trans*-3-hydroxy-D-proline, and *cis*-3-hydroxy-D-proline. Among these HOPs, 4-L-CHOP which is rare in nature has been clinically evaluated as an anticancer drug [50]. The basic principle is that the 4-L-CHOP leads to incorrect folding of the procollagen protein when it is incorporated into the protein, therefore the fibroblast growth of cells can be inhibited through a large number of collagen deposition [51]. 4-D-CHOP has been found in bacterial secondary metabolites as the example of antibiotic etamycin. 3-L-THOP presents in collagen types I, II, and III, which is hydroxylated by prolyl 3-hydroxylase. 3-L-CHOP has been established as a drug for anticancer and treatment for collagen disorder, which is hydroxylated post-translationally by proline 3-hydroxylase. Both of trans-3-hydroxy-D-proline and *cis*-3-hydroxy-D-proline have been synthesized from D-mannitol, but not been found in nature [10].

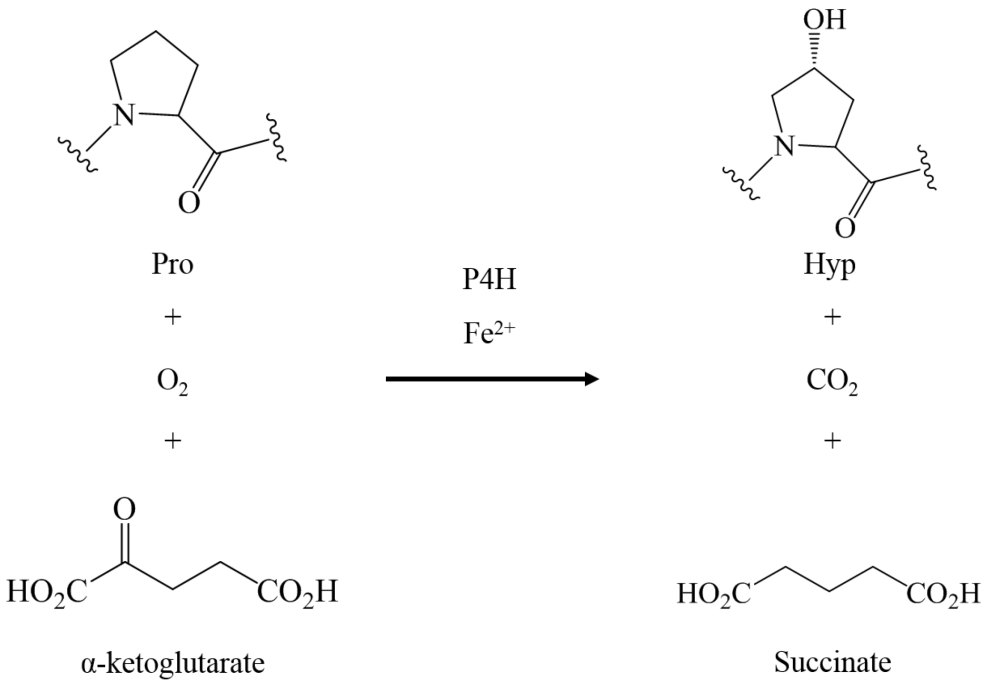

Figure 7. Conversion of Pro to Hyp catalyzed by P4H [47].

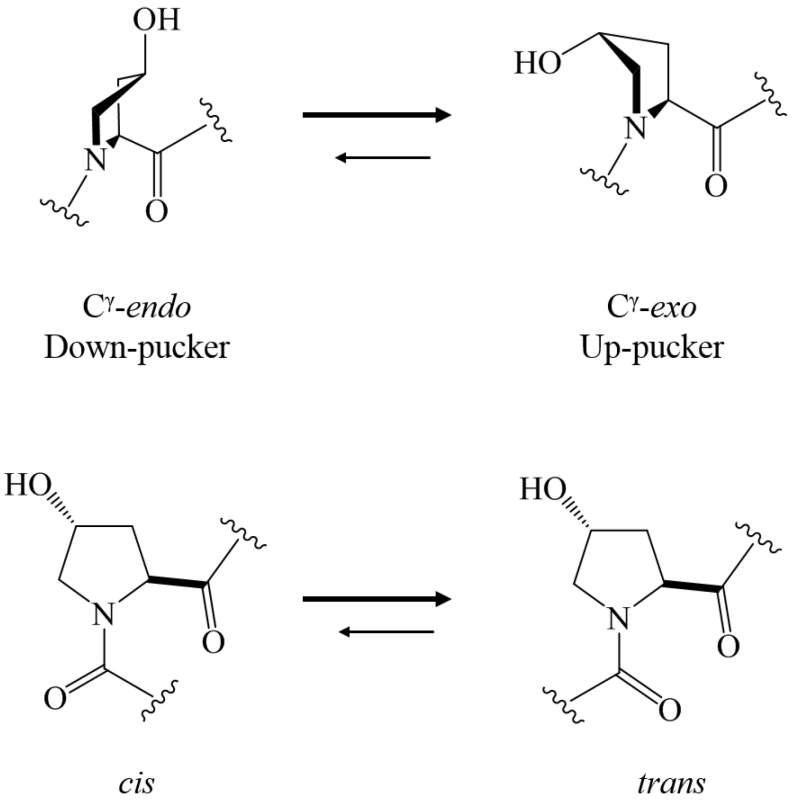

Figure 8. The hydroxylation at the 4R position makes the preference for a Cγ-exo-puckered pyrrolidine ring and *trans*-form peptide bind [47].

Dihydroxyprolines (DHPs) are formed by two hydroxylations at both position 3 and 5 of Pro. There are four possible L-form DHPs stereoisomers (Figure 6B) as follows, (2S,3S,4R)-3,4-dihydroxyproline, (2S,3R,4S)-3,4-dihydroxyproline, (2S,3S,4S)-3,4-dihydroxyproline, and (2S,3R,4R)-3,4-dihydroxyproline. In nature, the following L-form DHPs have been isolated: (2S,3S,4S)-3,4-dihydroxyproline has been identified from the cell wall proteins of diatom [52], (2S,3R,4R)-3,4-dihydroxyproline has been identified from the urotoxin peptide from the *Amanita virosa* mushroom [53]. The (2S,3R,4S)-3,4-dihydroxyproline has been found in an adhesive protein of the marine mussel *Mytilus edulis* [54], and it has been identified as a glycosylation inhibitor for the replication of HIV [55].

In addition to HOPs and DHPs, Aze is another important Pro* (Figure 6C), which widely presents in the *Liliaceae* family plants. Aze has the biological activity as an inhibitor for various cells growth [10].

As a unique group of non-canonical amino acids (ncAAs), Pro* plays an essential role in changing the structural properties of peptides, such as ribosomally synthesized and post-translationally modified peptides (RiPPs) and recombinant antimicrobial peptides (AMPs) [56]. Incorporation of Pro* is an excellent way to expand the structural diversity and develop the biological activities of peptides.

Two in vivo methodologies are currently available utilized for insertion of desirable ncAAs [57]: The first approach is based on stop codon suppression (SCS), the site-specific addition of ncAAs to the existing amino acid repertoire during translation by reassignment of termination or non-triplet coding

units through orthogonal-pairs. It is achieved by read-through of an in-frame stop codon with specific orthogonal ncAAs, which is then directly incorporated by ribosomal translation machinery into the core peptide. In addition to 20 cAAs, two more natural amino acids could be translated by ribosome in nature. Selenocysteine (Sec) and pyrrolysine (Pyl) could be co-translated as the 21st and 22nd amino acid by reprogrammed opal stop codon UGA [58] and amber codon UAG [59], respectively. The second approach is supplementation-based incorporation (SPI), which involves residue-specific incorporation of different ncAAs into target proteins via sense codon reassignment based on the auxotrophic host strains that take advantage of wide substrate tolerance in various amino acid analogs and surrogates [60].

The SPI methodology has been utilized in several cases of Pro* incorporation. The first example is the classic class I lantibiotic nisin, where the Pro in the core peptide position 9 (Pro-9, P9) was replaced a series of Pro*, such as *cis/trans*-4-fluoroproline ((4S/R-)Flp), 4-L-THOP, 4-L-CHOP, and *cis/trans*-methanoproline (*cis/trans*-MePro) (Figure 6D). These Pro* modified nisin variants represent different bioactivities in the antimicrobial activity assay [56]. In the case of incorporating 4-L-THOP to *E. coli* produced proteins, the intracellular concentration of 4-L-THOP is increased by the up-regulation of the endogenous Pro transporters codified by the *putP, proP,* and *proU* genes, which are up-regulated through the osmotic shock [61, 62]. In the case of cell-free synthesis of elastin-like polypeptides (ELPs) based on *E. coli* extract, a series of Pro* have been incorporated into the ELPs through the substitution of Pro to Pro* during the culture. The replacements of Pro by Pro* lead to the changes of phase transition temperature (Tt), the incorporations of 3,4-dehydro-L-proline, Aze, and (4R)-Flp are decreased the Tt of ELP-8 from 80°C to around 60°C, the incorporation of (4S)-Flp increased the Tt a little bit to 83°C, however, the incorporation of 1,3-thiazoidine-4-carboxylic significantly down-regulated the Tt to 18°C [63]. The low Tt is important to the solubility and delivery of pharmaceuticals in the human body.

During the translation of various Pro*, EF-P also plays the role of alleviating the ribosome stalling. At the free energy level study, it reveals that EF-P reduces the activation energy of the reactions by an average value of 2.5 kcal/mol in 10 of the 12 Pro*. EF-P leads to the favorable entropy change for the reactions, which drives the Pro-tRNA toward the direction of catalytic production in the ribosome PTC [21].

1.4 Bacterial adaptation during continuous cultivation experiments

Through the methodology of SPI, a certain cAA would be globally substituted by its own related analogues in an auxotrophic host cell. As early as in 1983, an analogue of tryptophan (Trp), 4-fluorotryptophan (4FTrp) has successfully substituted Trp in the Trp-auxotrophic *Bacillus subtilis* strains under the culture of the rich medium, which contains additional vitamins, nucleobases, and amino acids [64]. But the additives of the rich medium and the using of a mutagenic agent led to some debates in the results. The issues are mainly about that the potentially harmful effects of 4FTrp on protein function might be compensated and the proteome-wide selection pressure might be reduced.

In order to avoid the potential effects of the rich medium, the Lenski-type long-term evolution experiment (LTEE) has been applied in numerous research for bacterial adaptation for unusual nutrients or ncAAs. At the beginning, LTEE was performed on 12 populations of *E. coli* from the same clone. *E. coli* was cultured in a glucose-limited but high citrate medium. Until the 31,500 generation, there was no citrate-using (Cit^+) variant resulting from the evolution experiment [65]. Following this strategy, *E. coli* was continuous batch cultured by a series of dilution of 4FTrp (from low to high concentration) with the pure mineral medium. As a result of the LTEE, although Trp is the preference for the evolved *E. coli*, 4FTrp could be utilized and completely substituted Trp in the proteome of the strain [66]. In another case, L-β-(thieno [3,2-b]pyrrolyl) alanine ([3,2]Tpa) has successfully substituted Trp in *E. coli* proteome through LTEE. The uptake of Trp and its analogues in Trp-auxotrophic strain is mediated by a transporter, and in order to avoid the hindering or closing of them, the precursors indole (Ind) and β-thieno[3,2-b]pyrrole ([3,2]Tp), which are incorporated by passive diffusion into cells, were used in the cultures. Ind and [3,2]Tp were converted to Trp and [3, 2]Tpa by a Trp synthase (TrpBA) from *S. typhimurium* via a pSTB7 plasmid. During the LTEE, the amount of Ind was gradually reduced from 1 μM to 0 while the [3,2]Tp was maintained at 25 μM in the medium, by which the *E. coli* strains were forced to lose the dependence for Trp and finally the full adaptation for [3,2]Tpa happened in 506 days cultivation [67]. In a further study and application, the [3,2]Tpa adaptation *E. coli* strain has been employed as heterologous host bacterial strain for RiPPs, by which [3,2]Tpa was successfully incorporated to the molecular of lantibiotic lichenicidin [68].

The laboratory evolution is essential for bacterial adaptation for robust growth in various cultivation environments and the discovery and development of novel biomolecules. As a class of high-efficiency methods and an alternative of LTEE, continuous directed evolution methods have rapidly developed over the past few decades. Different from the traditional evolution methods, the highlight of continuous evolution is the novel and excellent characteristics of an uninterrupted cycle. Nowadays, continuous directed evolution has been developed using various organisms, ranging from viruses to higher eukaryotes. The applications of continuous directed evolution are involved in studies on antibiotic resistance, organismal adaptation, rapid generation of useful proteins and nucleic acids, and tailored properties [69, 70]. Depending on the requirement of long-term screening for the experimental evolution

with microbes in laboratory conditions, two commonly continuous culturing strategies including chemostats and turbidostats (Figure 9) are performed. In both of chemostat and turbidostat, fresh medium is continuously added to the growing culture. In a chemostat model, the main characteristic is the use of a defined medium in which a single nutrient is present at a growth limiting concentration [71]. The low concentration of the growth-limiting nutrient defines the selection imposed on cells. The advantage of a chemostat environment evolution is improving the capabilities in the acquisition or utilization of the growth-limiting nutrient.

In contrast to a chemostat, the culture in a turbidostat is diluted by the addition of fresh medium, by which the nutrient limitation during cells cultivation is avoided. The cell density is maintained at a defined level, the difference from chemostat is that all nutrients are present in richness and the dilution rate is set near the maximal growth rate of the cells. Constant monitoring and automated media addition are essential for keeping the cell density under the specified value. It results in a steady-state environment that is similar to a batch culture during the mid-logarithmic phase of growth. Based on the inherent property of turbidostat, the growth ability of cells is not restricted by the abundance of nutrient. The limitation factors for cells rapid replication are nutrient uptake rate, biogenesis rate of macromolecular and organelle, and the complex molecular processes such as DNA replication, transcription, translation, and various metabolism pathways. In principle, the turbidostat model of continuous directed evolution might lead to an increase in the rate of any of these processes [72, 73, 74].

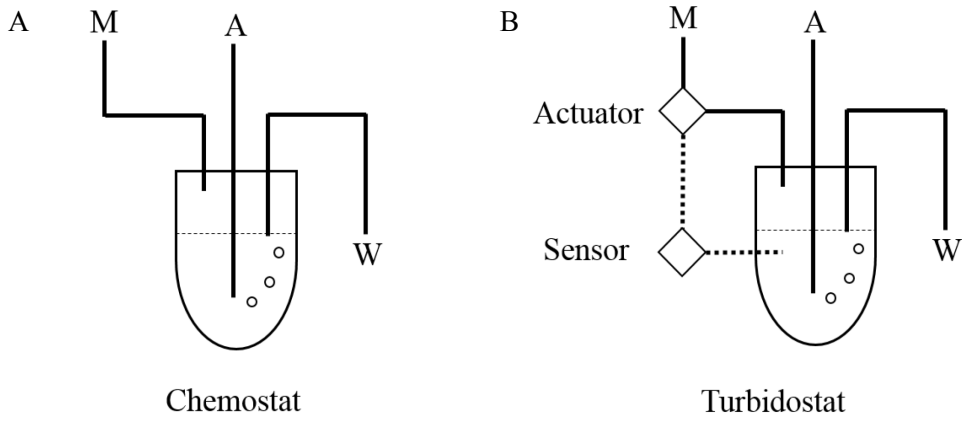

Figure 9. Schemas represent chemostat (A) and turbidostat (B) models continuous cultivation [75]. The letters A, M, and W represent air, medium, and waste, respectively. In turbidostat model, the sensor is a turbidity meter.

An issue for a long time continuous evolution culture is the formation of biofilm, by which bacterial cells attach to the inner wall of the culture vessels, as a result some cells would escape selections. A two growth chambers evolution system GM3 ameliorates the issue of selection escape through cyclical culture transferring and chemical sterilization [69]. Additionally, considering the purpose of our research, to improve the growth robustness of *E. coli* for further study about lanthipeptides heterologous expression and ncAAs incorporation, and to reveal the corresponding machinery at proteome level, a

turbidostat model GM3 (Figure 10) was applied in our investigation. In the GM3 cultivation device, the bacterial cell culture initially carries out in the first chamber and it is supplemented with fresh medium, the flow rate of the medium is regulated by the actuator connected to a turbidity meter monitoring the cell density. After a defined culture time, the whole culture is transferred to the second chamber to avoid selection escape caused by the biofilm formed in the first chamber. Subsequently, the first chamber is cleaned and sterilized with 5M NaOH. After another defined period of cultivation in the second chamber, the culture is transferred back to the first chamber, and this cycle is repeated.

B

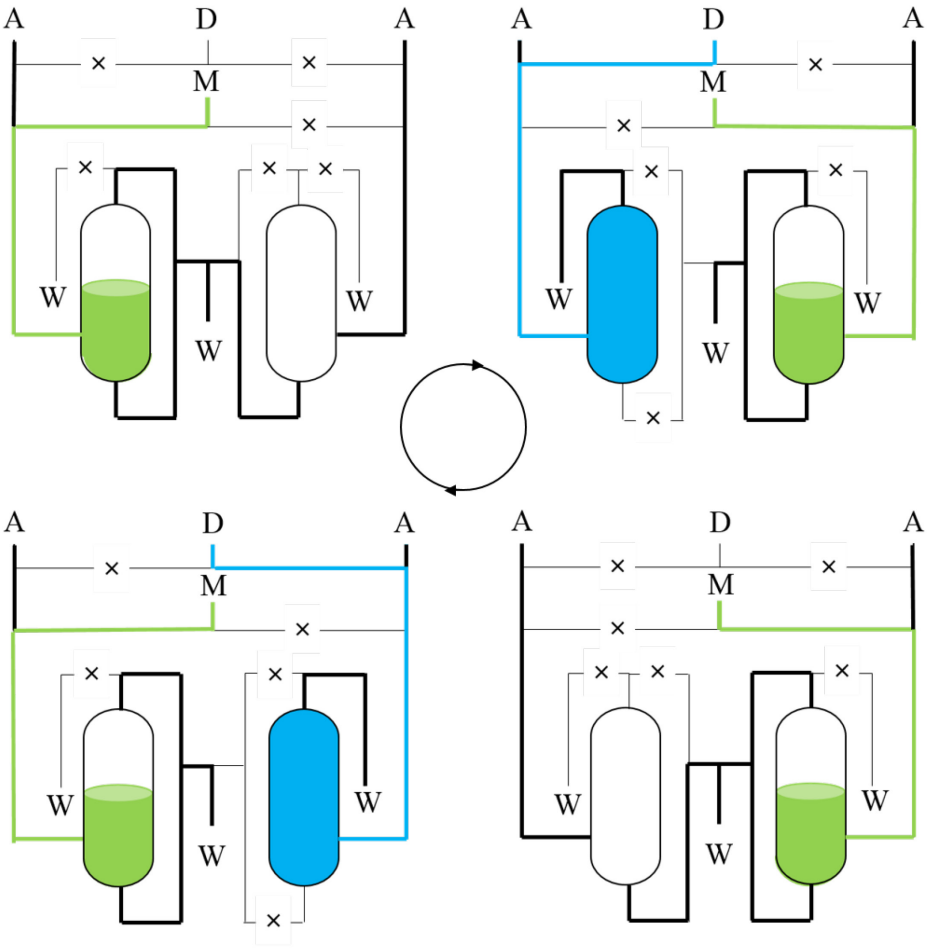

Figure 10. The cultivation cycle in twin chambers of the GM3 device [76]. It shows the fluids flow of the medium (green), the chambers are sterilized by 5M NaOH (blue). The letters A, D, M, and W represent air, 5M NaOH, medium, and waste, respectively. The × indicate the closed valves. The paths are indicated by thick and thin lines for open and closed, respectively.

1.5 Stable isotope labeling by amino acids in cell culture

To reveal the machinery at the proteome level of *E. coli*, which is needed to achieve robust growth to overcome the absence of EF-P, we employed an evolution process generated by turbidostat continuous directed evolution device GM3. Herein, we use a stable isotope labeling by amino acids in cell culture (SILAC) approach for mass spectrometric (MS) quantitation of protein levels contained in the different strains.

The traditional approach of quantitative proteomics mainly relied on two-dimensional (2D) gel electrophoresis to identify, quantify, and compare changes in relative protein abundance among multiple samples [77]. However, this method has many drawbacks, such as the huge amount of sample handling, low reproducibility, and the low abundance of very large or very small proteins. [78, 79]. On the other hand, SILAC is a high-throughput approach in MS-based quantitative proteomics, which can be used to examine proteome changes in various state and compare the discrepancy between different cells. In the method of SILAC, the non-radioactive, stable isotope-containing amino acids are incorporated into the freshly synthesized proteins and labeling the proteomes of cells through normal metabolic pathways. The cells are cultivated in the mediums contains "light" (L), "medium" (M), and "heavy" (H) SILAC amino acids, respectively. The labeled amino acids in the medium replace their equivalent unlabeled amino acids while the cells grow as normal for a sufficient period of time (typically, seven cell divisions) to ensure at least 95% of amino acid labeling [80]. The most widely labeled amino acids are arginine (Arg) and lysine (Lys), the reason is that the polypeptide chains are digested by trypsin at the carboxyl terminal of Arg and Lys as part of the normal sample preparation protocol for MS. Commonly, medium-labeled medium contains ^{13}C-labeled Arg and ^{2}D-labeled Lys, and the heavy-medium contains ^{13}C and ^{15}N-labeled Arg and Lys. Herein, we used L-[$^{13}C_6$] arginine (Arg-6) and L-[$^{2}H_4$] lysine (Lys-4) for medium labeled (M) medium, and L-[$^{13}C_6$, $^{15}N_4$] arginine (Arg-10) and L-[$^{13}C_6$, $^{15}N_2$] lysine (Lys-8) for heavy labeled (H) medium. The normal arginine (Arg-0) and lysine (Lys-0) are used for the light labeled (L) medium. MS can distinguish such medium- and heavy-labeled peptides from their light counterparts due to their known mass differences. The ratio of peak intensities of the peptide pairs accurately reflects their relative changes in the abundance of the corresponding peptides (Figure 11). The most compelling advantage of SILAC is the high accuracy, it is more accurate than either label-free quantification or chemical-labelling methodologies. Due to the particularly advantageous of higher accuracy, SILAC can be further used for analysis of PTMs, especially for phosphoproteomics. Furthermore, the dynamic SILAC can quantify protein turnover and pulsed SILAC can be used for the measurement of protein synthesis changes at proteome level [81, 82, 83].

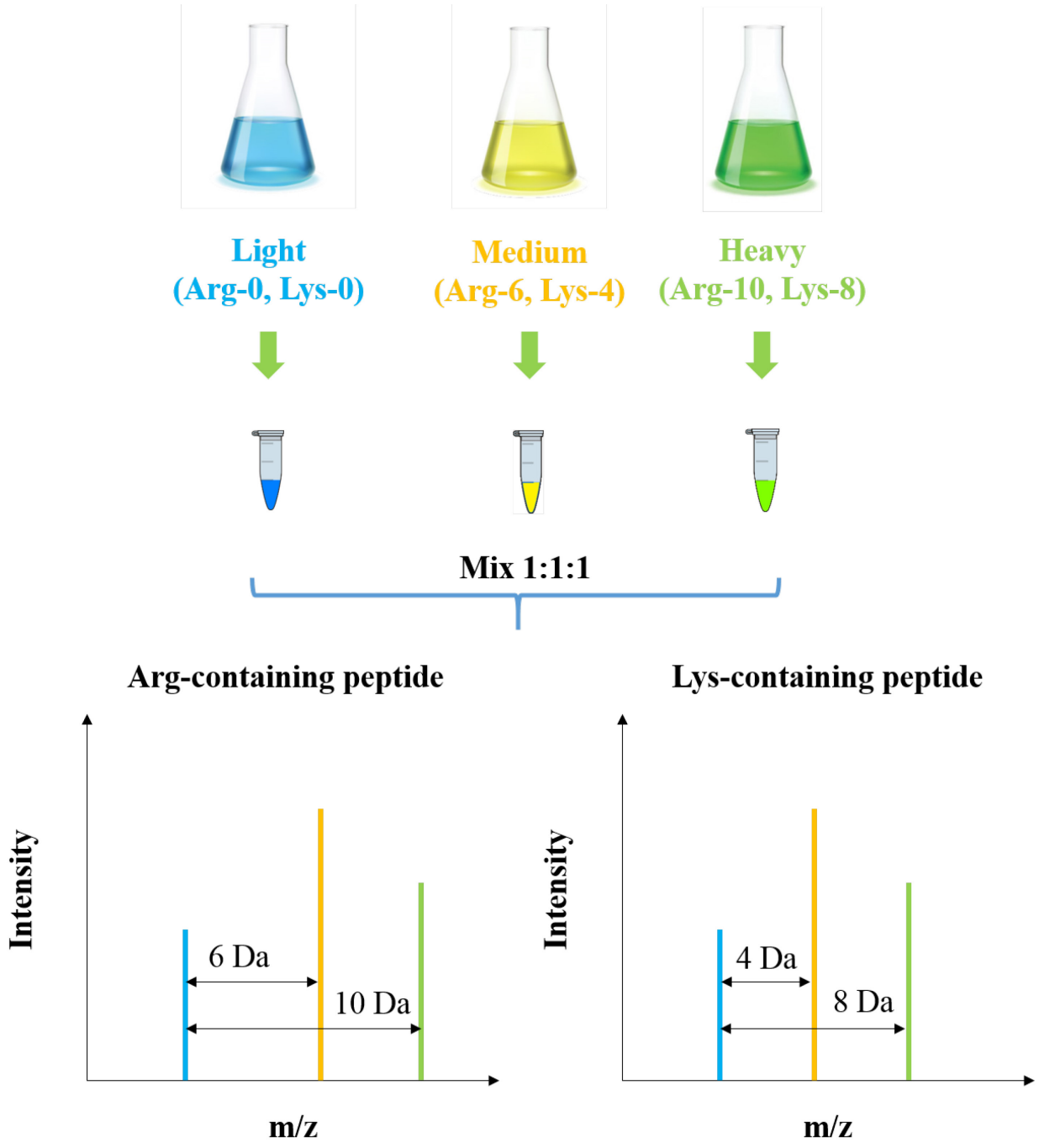

Figure 11. The experimental phase of SILAC. The different cell populations are cultured in different stable isotope labeled amino acids containing mediums, which resulted in the three different labeled proteomes. The proteomes are mixed the total amount of protein with the ratio of 1:1:1, the mixture will be digested into peptides, and then the protein identification and quantification will be performed by the following MS analysis.

1.6 Aim of this study

In previous work, our lab has adapted *E. coli* strains to robustly grow through the continuously directed evolution by GM3 cultivation system. The first aim of this study is to reveal the mechanism of the fast adaptation to robust growth at the proteome level via SILAC. An important prerequisite for the SILAC experiments of *E. coli* is the auxotrophic construction for arginine and lysine.

The second aim of this study is to investigate the role of EF-P in the translation of *E. coli* proteome, especially on the oligo-proline stretches. Towards this goal, the *efp* KO strain has been constructed and cultivated. Expectedly, the growth of the *efp* KO strain is significantly slower than the wildtype (WT) strain. However, upon long time cultivation in GM3 devices, the growth rate of the adapted *efp* KO strains could reach the level of the growth of adapted WT strain (i.e. WT-strain adapted to the cultivation regime in the GM3 devices). In this context, the third aim of this study is to reveal the reasons of the adaptation of *E. coli* robust growth when *efp* gene is absent from bacterial genome.

It is believed that YeiP is the paralog of EF-P. To test this hypothesis, we set out (the fourth aim) experiments to investigate possible role of YeiP in *E. coli*, i.e. to test whether YeiP could serve as the functional replacement of EF-P in this bacterium. By suitably designed SILAC-experiment, it should be possible to find out whether the absence of YeiP leads to the similar effects as EF-P in *E. coli.*

Long-term goal is not only to elucidate mechanisms of adaptation for robust growth in the absence of EF-P but also to provide adapted bacterial expression hosts suitable for incorporation of various proline analogs in single proteins and proteomes. Modified proline analogs are especially valuable building blocks for the design and large scale efficient production high-value protein or peptide based products such as RiPPs.

2 Results and Discussion

2.1 Auxotrophic strains construction for SILAC experiments

In the SILAC experiments, the proteins were labeled by incorporation of stable isotopes of Arg and Lys. To avoid the unlabeled amino acids or other nutrients convert to Arg or Lys, thereby affecting the accuracy of the results, the first step is knocking out the key genes in the biosynthesis pathway of Arg and Lys. Two genes *argA* and *lysA* were selected to be knocked out. The method of genes deletion will be described in the section focused on methodology (See Section 5.1).

In previous work, my colleague Christian Schipp cultured the *E. coli* K12 MG1655 WT strain in two parallel GM3 (machine number is GM117) devices at turbidostat model, each GM3 device contains two cultivation chambers (See section 1.4), the chambers of the first GM3 device were numbered as C1 and C2, and the chambers in the second GM3 device were numbered as C3 and C4, the final evolved strains were harvested in C1 and C3, therefore the two evolved strains were named as GM117C1 and GM117C3. The whole automated continuously cultivation lasted 40 days. During the automated cultivation, at the time about 20 days, the generation time (doubling time) has reduced about 40% from the initial and stayed at a plateau in the following 20 days (Figure 12). In order to characterize the changes led by the evolution process at proteome level via SILAC experiments, first of all, the *argA* and *lysA* genes should be deleted.

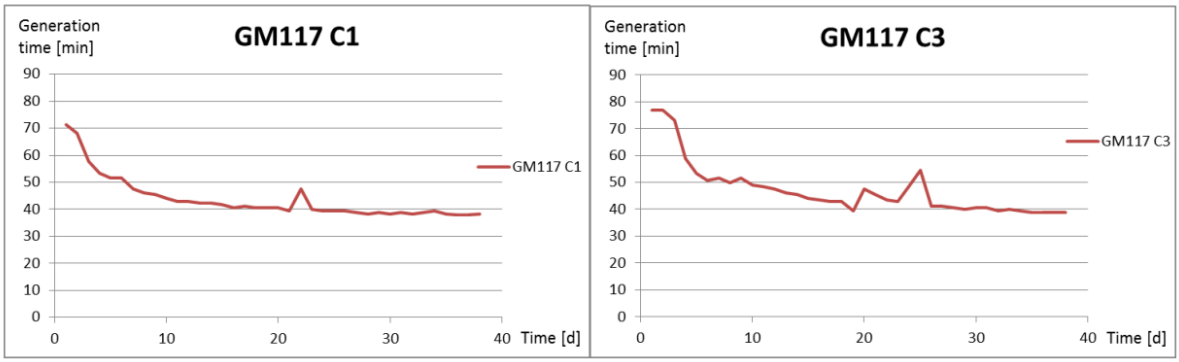

Figure 12. Cultivation of the *Escherichia coli* K12 MG1655 WT strain in two parallel GM3 turbidostat evolution devices at OD_{600} 0.8 E. Left: Generation time of the culture in chamber C1. Right: Generation time of the culture in chamber C3. Sharp peaks down are a sign for bottle changes and sharp peaks up for occurring biofilm in the cultivation chambers. (Reference: Christian Schipp has done, but not published yet)

2.1.1 Preparation of the control *Escherichia coli* strain for SILAC experiment

In order to meet the requirements of SILAC experiment for *E. coli*, it is necessary to construct a control strain without *argA* and *lysA* genes from the wild type strain.

Replacement of *argA* gene with the FRT-kanR-FRT cassette in wildtype *E. coli* strain: Transduction of *ΔargA*-phage (*argA* has been replaced by FRT-kanR-FRT cassette, constructed by Nina

Bohlke) was performed to WT strain (Figure 13). In the negative controls, the WT strain (Figure 13. 3) and *ΔargA*-phage (Figure 13. 4) were separately streaked on LB-agar plates with kanamycin (kan), nothing grown on the plates shows that both of the WT strain and *ΔargA*-phage were not contaminated and are thus reliable for the following use. The two reaction mixtures of WT strain with different amount of *ΔargA*-phage (Figure 13.1 and 2) yielded positive transduction colonies.

One single colony was picked from the test plate (reaction mixture of *ΔargA*-phage with *E. coli* WT strain) and streaked three rounds on LB-agar plates with kanamycin. After three rounds cultures on LB-agar plates with kanamycin, the FRT-kanR-FRT cassette has stably replaced the *argA* gene.

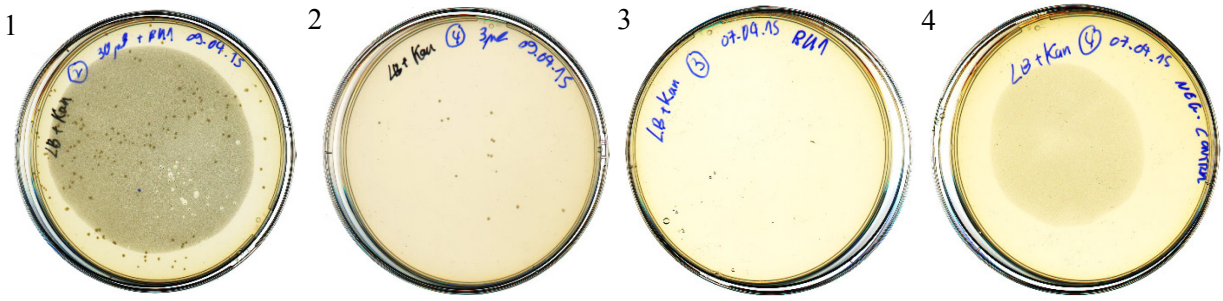

Figure 13. Transduction of *ΔargA*-phage with *E. coli* WT strain and screening on LB plates with kan. 1) The reaction mixture of WT strain with 30ul phage. 2) WT strain with 3µl phage. 3) Negative control: WT strain without phages. 4) Negative control: 10 µl phage without bacterial cells.

Removal of the *kanR* marker by flippase recombination: In order to eliminate the *kanR* gene from the genome of *argA* deletion strain and to prepare for the next deletion of *lysA* gene, the ampicillin (amp) resistance gene and flippase (Flp) coding gene contains plasmid pCP20 were employed. The pCP20 plasmid was transformed into the above-screened *argA* deleted strain through electroporation, the following step is an overnight (O/N) incubation on LB plate with amp at 30 °C.

Figure 14. Transformation and screening of pCP20 into the *argA* deleted WT strain on amp containing LB plate.

8 single colonies were picked from the transformed LB plate (Figure 14) into 8 different wells of one 24- well-plate and incubated in LB medium without antibiotic at 41 °C O/N to remove the pCP20 plasmid and eliminate the amp resistance. Then I streaked cultures from each well on three selection LB

plates with 8 separated sectors on each plate, the first plate is without antibiotic, the second is with kan, and the third is with amp, respectively. After three rounds of repeatedly incubation at 41 °C in 24-well-plate and following selection on LB plates (Figure 15), both of the resistance to kan and amp were completely removed. The screened strain could be used for next gene deletion of *lysA*, we named this strain as *E. coli* WT *ΔargA*.

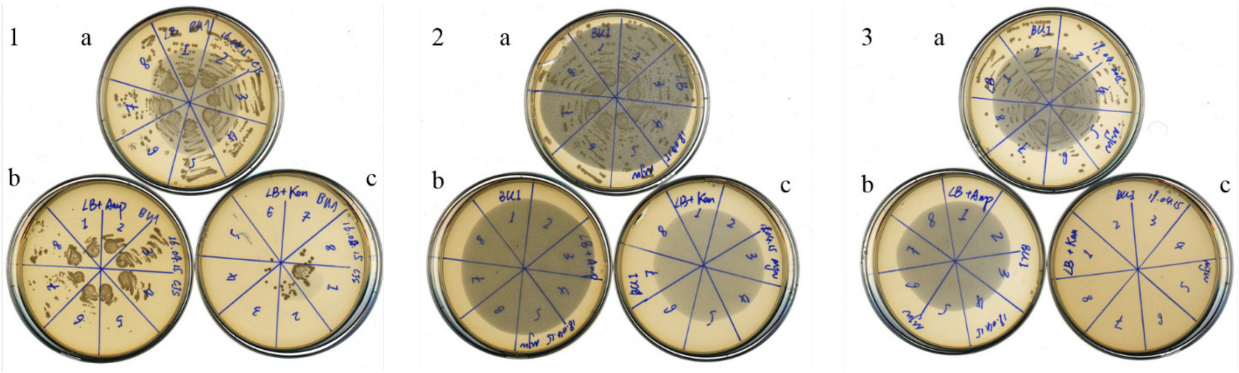

Figure 15. Three-round-selection for *E. coli* WT *ΔargA* strain to remove the kan resistance with the help of the flippase encoding plasmid pCP20. Note that 1, 2, and 3 represent from first to third round selections, respectively. a, b, and c represent three different LB plates of without antibiotic, with amp, and with kan, respectively.

Replacement of *lysA* gene with the FRT-kanR-FRT cassette in *argA* deleted strain: Transduction of *ΔlysA*-phage (*lysA* was replaced by FRT-kanR-FRT cassette) was performed to the *argA* deletion and without antibiotic resistance for kan and amp strain *E. coli* WT *ΔargA*. There was no growth on the negative control (Figure 16.3), which means the WT *ΔargA* strain was reliable to be used for further experiments. The two reaction mixtures of WT *ΔargA* strain with different amount of *ΔlysA*-phage (Figure 16.1 and 2) obtained positive transduction colonies.

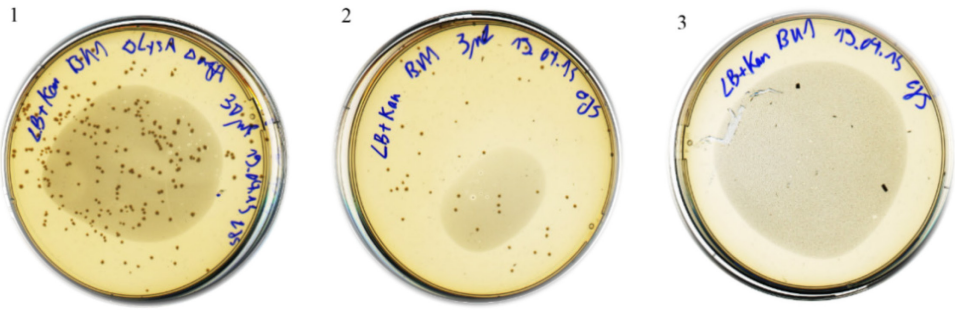

Figure 16. Transduction and screening of *ΔlysA*-phage with *E. coli* WT *ΔargA*. 1) Reaction mixture of WT *ΔargA* with 30 µl *ΔlysA*-phage. 2) Reaction mixture of WT *ΔargA* with 3 µl phage. 3) Negative control: WT *ΔargA* without phage.

Through three rounds selected cultivation for a single colony from the above test plate (reaction mixture of *ΔlysA*-phage with *E. coli* WT *ΔargA*) on LB plates with kan, the *lysA* gene has been stably replaced by the FRT-kanR-FRT cassette.

Verification of transductants via PCR: One single colony was picked from the third-round culture of LB plate with kan and inoculate in liquid LB medium O/N and the strain identity was verified by colony PCR.

Five control primers have been designed to verify the deletion of *argA*, the first (*argA*-C1) and second primer (*argA*-C2) sequences are from upstream and downstream of *argA* recombineering homology, respectively. And the third primer (*argA*-C5) sequence is from the middle of *argA* as reverse primer coupled with *argA*-C1. The fourth (*kanR*-K1) and fifth primer (*kanR*-K2) sequences are inside of kan resistance gene *kanR*. The primers for colony PCR for *lysA* deletion verification are also containing the sequence of upstream and downstream of *lysA* (*lysA*-C1 and *lysA*-C2) and inside sequence (*lysA*-C5), and the *kanR*-K1 and *kanR*-K2 primers are also used (Figure 17). All the information about primer sequences and PCR product length are shown in Section 4.6. In the database of our lab, this verified strain was named as *E. coli* BU173 (*ΔargAΔlysA::kanR*). In this dissertation, it was named as control strain.

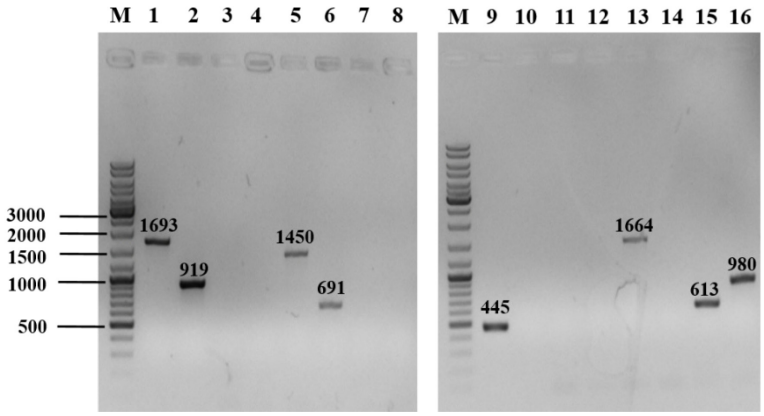

Lane	Forward primer	Reverse primer	Length of PCR product (bps)	Lane	Forward primer	Reverse primer	Length of PCR product (bps)
1	*argA*-C1	*argA*-C2	1693	9	*argA*-C1	*argA*-C2	445
2	*argA*-C1	*argA*-C5	919	10	*argA*-C1	*argA*-C5	-
3	*argA*-C1	*kanR*-K1	-	11	*argA*-C1	*kanR*-K1	-
4	*kanR*-K2	*argA*-C2	-	12	*kanR*-K2	*argA*-C2	-
5	*lysA*-C1	*lysA*-C2	1450	13	*lysA*-C1	*lysA*-C2	1664
6	*lysA*-C1	*lysA*-C5	691	14	*lysA*-C1	*lysA*-C5	-
7	*lysA*-C1	*kanR*-K1	-	15	*lysA*-C1	*kanR*-K1	631
8	*kanR*-K2	*argA*-C2	-	16	*kanR*-K2	*argA*-C2	980

Figure 17. Agarose gel electrophoresis of colony PCR for *argA* and *lysA* KO *E.coli* WT strain. M, 1 kb DNA ladder. Lane 1~8, the template is the WT strain. Lane 9~16, the template is the *argA* and *lysA* KO strain BU173 (*ΔargA ΔlysA::kanR, frt*). The information about the primers' name and length of PCR product listed in the table, "-" represents that no product would be created by the primers with the corresponding template.

2.1.2 Construction of adapted *Escherichia coli* strains for SILAC experiments

The method of *argA* and *lysA* genes deletion in adapted strains is same as in WT strain.

Replacement of *argA* gene with FRT-kanR-FRT cassette in two adapted strains *E. coli* GM117C1 and *E. coli* GM117 C3: The reaction mixtures of *ΔargA*-phage with each adapted strain were streaked on LB plates with kan as testing plates (Figure 18.1 and 2), each strains cultured on LB plates without the mixing of phage as negative control (Figure 18.3 and 4). And all the plates were incubated at 37 °C O/N. As the results, there was nothing grown on the negative control plates which ensured the strains were not contaminated. And the single colonies on the testing plates shown that the adapted strains *E. coli* G117C1 and *E. coli* G117C3 have been successfully transduced with *ΔargA*-phage.

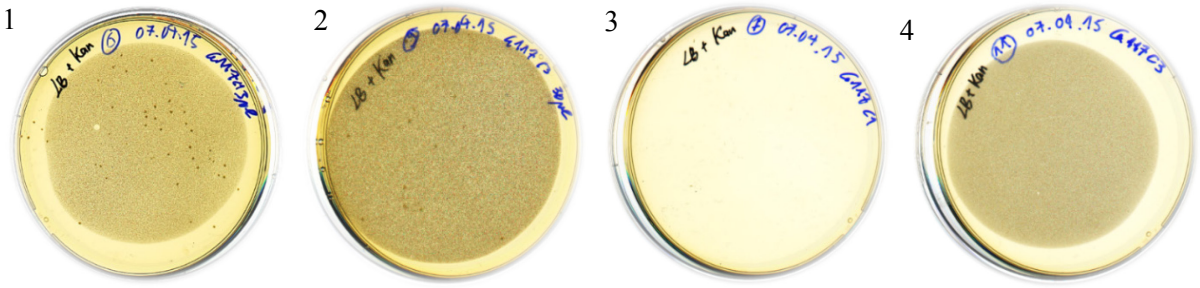

Figure 18. Transduction and screening of *ΔargA*-phage with adapted strains *E. coli* G117C1 and G117C3. 1) Reaction mixture of G117C1 with phage. 2) G117C3 with phage. 3) Negative control: G117C1 without phages. 4) Negative control: G117C3 without bacteria.

Single colonies were picked from the testing plates of each adapted strain mixed with *ΔargA*-phage, and were streaked on kan containing LB plates with three rounds cultivation, by which the FRT-kan-FRT cassette has stably replaced the *argA* gene in both of the adapted strains. The two strains were named as *E. coli* GM117C1-*argA* and *E. coli* GM117C3-*argA*

Removal of *kanR* maker by flippase recombination: The *ampR* and *flp* genes containing plasmid pCP20 was transformed into above *argA* deleted adapted strains by electroporation. And the two transformed strains were incubated on LB plates with amp at 30 °C O/N.

Single colonies were picked from the transformed plates (Figure 19) which were transferred into wells of 24-wells-plate and incubated at 41 °C O/N. The cultures were streaked from each well on three selection LB plates. Through three rounds of repeatedly 24-well-plate incubation at 41 °C and the following selection on LB plates, both resistance for kan and amp were completely removed (Figure 20 and Figure 21). The screened strains *E. coli* G117C1 *ΔargA* and *E. coli* G117C3 *ΔargA* could be used for next *lysA* deletion.

Figure 19. The pCP20 plasmid was transformed into the *argA* deleted adapted strains and screened by the amp containing LB plates. 1) *E. coli* G117C1 (*ΔargA::kanR* / pCP20). 2) *E. coli* G117C3 (*ΔargA::kanR* / pCP20).

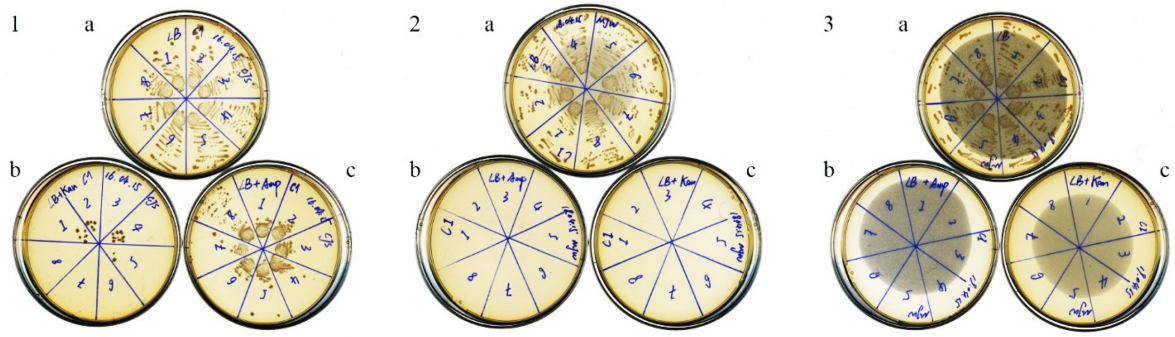

Figure 20. The kan resistance in the *E. coli* G117C1 *ΔargA* strain was removed with the help of the flippase produced by the plasmid pCP20 through a three-round-selection. Note that the numbers of 1, 2, and 3 represent the selection rounds from first to third, respectively. And the alphabets of a, b, and c represent three different LB plates of without antibiotic, with amp, and with kan, respectively.

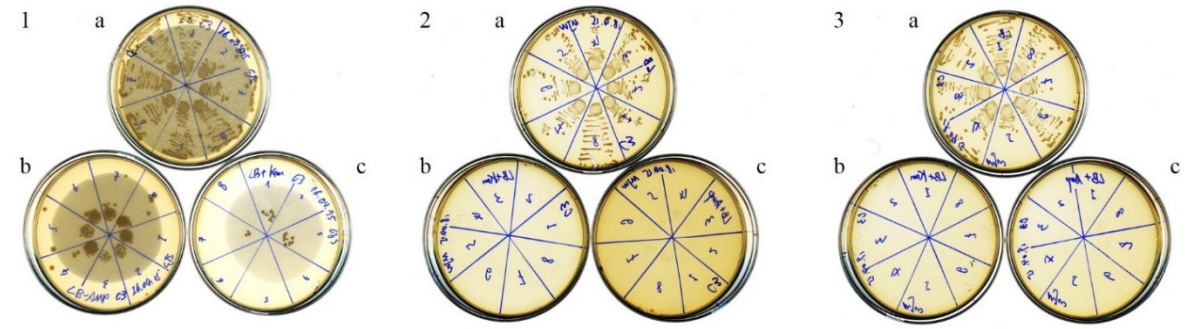

Figure 21. The *E. coli* G117C3 *ΔargA* strain removed its kan resistance with the help of the flippase expression plasmid pCP20 via a three-round-selection. Three rounds of the selection were shown as the number of 1, 2, and 3, respectively. and the letters of a, b, and c separately represent the LB plates without antibiotic, with amp, and with kan.

Replacement of *lysA* gene with the FRT-kanR-FRT cassette in *argA* deleted adapted strains: The above-obtained *argA* deleted adapted strains were transduced with the *ΔlysA*-phage and cultured on the testing LB plates with kan (Figure 22.1 and 2), and incubated at 37 °C O/N. At the same time, the strains were cultured on the LB plates without mixture of phage which as the negative controls (Figure 22.3

and 4). There was nothing grown on the negative control plates, which ensured that the strains were reliable without contamination. The positive colonies on the testing plates were repeatedly picked and culture on the screening LB plates with kan, and as a result, the FRT-kanR-FRT cassette stably replaced the *lysA* gene in the adapted strains.

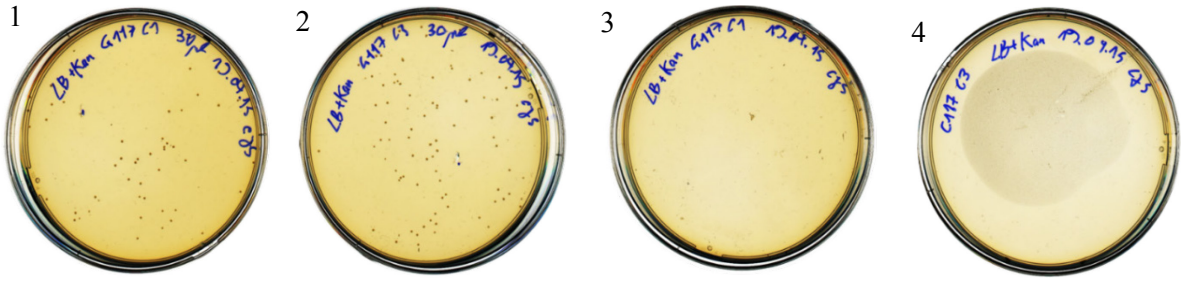

Figure 22. The *argA* deleted adapted strains was transduced by the *ΔlysA*-phage and screened on the kan containing LB plates. 1) Reaction mixture of G117C1 *ΔargA* with phage. 2) Reaction mixture of G117C3 *ΔargA* with phage. 3) Negative control: *E. coli* G117C1 *ΔargA* without phages. 4) Negative control: *E. coli* G117C3 *ΔargA* without phages.

Verification of transductants via PCR: The presence of the genes in the strains with the gene KO should be verified by PCR. One single colony was picked from the third-round culture of LB plate with kan and inoculate in liquid LB medium O/N and then the strain was verified by colony PCR.

The eight primers *argA*-C1, C2, and C5, *kanR*-K1 and K2, *lysA*-C1, C2, and C5 are used for the verification of *argA* and *lysA* deletion in the two adapted *E. coli* strains G117C1 and G117C3. The PCR result (Figure 23) indicated that the deletion of *argA* and *lysA* genes in both of the two adapted strains are already successful. The sequence of the control primers and length of the PCR product fragments are listed in section 4.6.

In our lab database, these verified strains were named as *E. coli* BU171 (Evo, *ΔargAΔlysA*::*kanR*, *frt*+) and *E. coli* BU172 (Evo, *ΔargAΔlysA*::*kanR*, *frt*+). In the following experiments of this dissertation, they were named as Evo-1 and Evo-2, respectively.

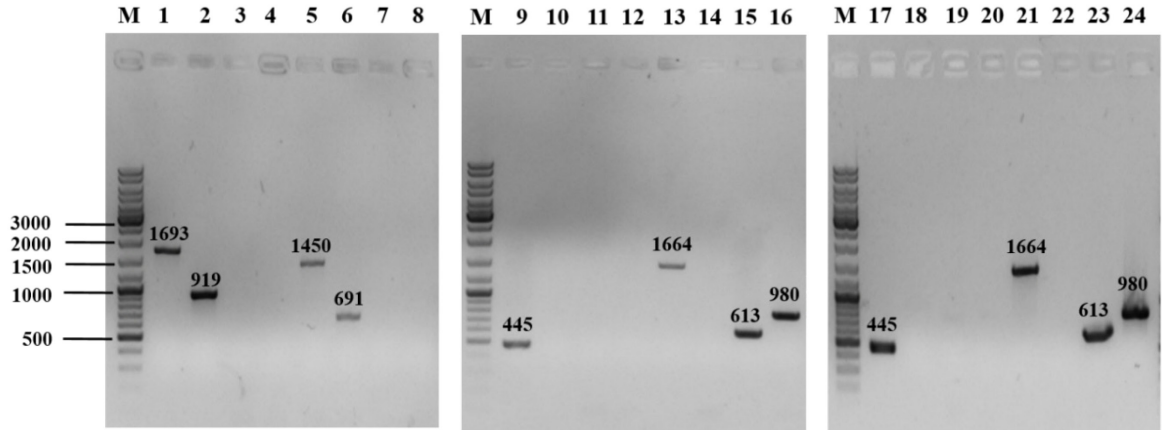

Lane	Forward primer	Reverse primer	Length of PCR product (bps)	Lane	Forward primer	Reverse primer	Length of PCR product (bps)
1	*argA*-C1	*argA*-C2	1693	9, 17	*argA*-C1	*argA*-C2	445
2	*argA*-C1	*argA*-C5	919	10,18	*argA*-C1	*argA*-C5	-
3	*argA*-C1	*kanR*-K1	-	11, 19	*argA*-C1	*kanR*-K1	-
4	*kanR*-K2	*argA*-C2	-	12, 20	*kanR*-K2	*argA*-C2	-
5	*lysA*-C1	*lysA*-C2	1450	13, 21	*lysA*-C1	*lysA*-C2	1664
6	*lysA*-C1	*lysA*-C5	691	14, 22	*lysA*-C1	*lysA*-C5	-
7	*lysA*-C1	*kanR*-K1	-	15, 23	*lysA*-C1	*kanR*-K1	631
8	*kanR*-K2	*argA*-C2	-	16, 24	*kanR*-K2	*argA*-C2	980

Figure 23. Agarose gel electrophoresis of colony PCR for *argA* and *lysA* KO adapted strains *E.coli* G117C1 and G117C3. M, 1 kb DNA ladder. Lane 1~8, the template is the control strain. Line 9~16, the template is the *argA* and *lysA* KO strain BU171. Line 17~24, the template is the *argA* and *lysA* KO strain BU172. The information about the primers' name and length of PCR product list in the above table, "-" represents that no product would be created by the primers with the corresponding template.

2.2 Proteome profile based on SILAC experiments

To study the proteome dynamics of the different *E. coli* strains, we have used an SILAC approach specifically adapted to this type of strains. For the labeling of amino acids with stable isotopes, it is important that the medium has a defined known composition to avoid the presence of non-labeled amino acids. Therefore, the M9 minimal medium was chosen to which the SILAC amino acids were supplemented in the different labels.

The first step in the characterization of *E. coli* strains by SILAC based proteomics was to evaluate the effect that the M9 minimal medium has on the bacterial proteome, relative to the usual LB medium where the cells are normally cultured.

2.2.1 Comparison of significantly altered proteins of the control strain cultures between M9 minimal medium and LB medium

Control strain has been cultured in SILAC-M9 minimal medium with heavy labeled (Lys-8 and Arg-10), and in LB medium as light labeled (Lys-0 and Arg-0), respectively. In two biological replicates, a total of 1824 proteins were identified, of which 1565 proteins were quantified in both MS measurements, the histograms show the distribution of the protein change ratios in M9 minimal medium relative to in LB medium (Figure 24A), the correlation coefficient of the two replicates is 0.95 (Figure 24B). Among the quantified proteins, 79 of them are significantly up-regulated (as calculated from significance A [84] using a p-value < 0.05) in both replicates. On the other hand, 104 proteins showed to be significantly down-regulated. Here I will represent these two replicates as Exp_1 and Exp_2 in the following of this section (2.2.1). All the regulated ratio represents in the log2 ratio in this dissertation.

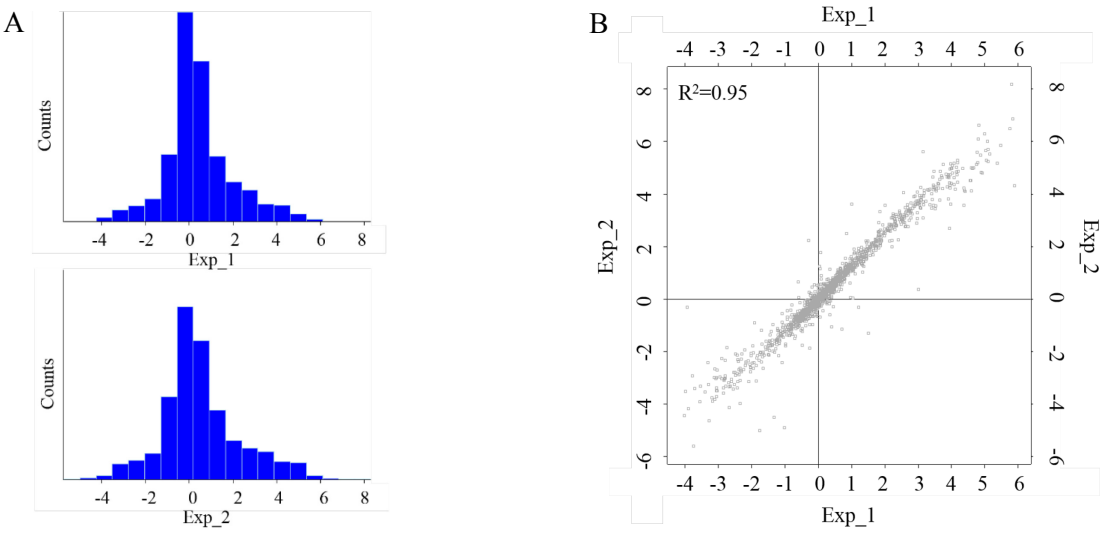

Figure 24. Distribution of the proteome changed ratios (A) and the correlation of two replicates (B) of the control strain cultured in M9 minimal medium compared to in LB medium.

The significantly changed proteins are mainly involved in the transport and metabolisms of nitrogen-containing compounds, carbon sources and energy, and sulfur-containing compounds.

The related nitrogen-containing compounds include peptides, amino acids, and nucleotides. The changes in protein expression are related to different functional systems, which are involved in transport, biosynthesis, and catabolism. Peptides could be capable of sole source of carbon and nitrogen for bacterial growth [85, 86]. Oligopeptide permease (Opp) and dipeptide permease (Dpp) are the major peptide transporters of *E. coli* [87, 88, 89, 90]. Opp also plays an important role in the cell wall peptides recycling [91]. The regulations of these transport systems are responsible for the maintaining of intracellular amino acids pool levels [92]. Expression of Opp and Dpp was activated under the nitrogen limitation [93]. Whereas the biosynthesis of the peptide binding proteins OppA and DppA is repressed in rich medium [94, 95]. In LB medium fermentation, the expression of the *opp* and *dpp* operons was induced when free amino acids and nucleotides are exhausted [96]. In the data of this work, all detected Opp and Dpp relative proteins are increased in M9 minimal medium culture (Table 1), more than half of them are significantly up-regulated. It coincides with the previous finding that Opp and Dpp are increased under the nitrogen limited growth condition, and this result is also correlated with the repression of Opp and Dpp in nutrients rich culture environment of LB medium during the early to the mid-exponential growth phase. Besides the ATP-binding cassette (ABC) transporters of Opp and Dpp, another family of peptide transporter was detected in my experiments. The protein is dipeptide and tripeptide permease A (DtpA) [97, 98], which is belonged to proton-dependent peptide transporter (PTR) family [99, 100]. Unlike other ABC transporters for peptides, DtpA is significantly down-regulated when the control strain was cultured in the M9 minimal medium.

Table 1. Changes of peptide transport system related proteins of control strain from LB medium to M9 minimal medium culture.

Gene name	Exp_1 Fold	Exp_2 Fold	Exp_1 significant	Exp_2 significant	Annotation
dppA	5.10	5.70	+	+	Dipeptide ABC transporter periplasmic binding protein; dipeptide chemotaxis receptor
dppB	4.66	5.00	+	+	Dipeptide ABC transporter permease
dppD	4.41	4.10	+		Dipeptide ABC transporter ATPase
dppF	3.90	3.82	+		Dipeptide ABC transporter ATPase
oppA	5.03	5.66	+	+	Oligopeptide ABC transporter periplasmic binding protein
oppB	3.42	3.80	+		Oligopeptide ABC transporter permease
oppC	2.98	4.09			Oligopeptide ABC transporter permease
oppD	2.75	3.33			Oligopeptide ABC transporter ATP- binding protein
oppF	3.04	3.70			Oligopeptide ABC transporter ATPase
dtpA	-3.04	-3.48	+	+	Dipeptide and tripeptide permease A

Obtained data set revealed that 11 amino acid transport and 24 amino acid biosynthesis related proteins are significantly up-regulated in M9 minimal medium (Table 2). These transports are involved in the transport systems of Arg, Lys, Asp, Gln, Cys, His, Ser, Thr, aromatic amino acids (Phe, Tyr, and Trp), and branched-china amino acids (Leu, Ile, and Val). The biosynthesis pathways are involved in the following 11 individual amino acids: Phe, Tyr, Trp, Gln, His, Leu, Ile, Val, Cys, Met, and Ser. Meanwhile, there are 9 L-amino acids and 2 D-amino acids degradation related proteins are significantly down-regulated (Table 3). The amino acids of these degradation progress are involved in Asn, Asp, Ser, Thr, and Trp.

Table 2. Significantly up-regulated amino acids transports and biosynthesis related proteins of the control strain in M9 minimal medium compared to in LB medium.

Gene name	Exp_1 Fold	Exp_2 Fold	Annotation	Related amino acid
argT	4.59	5.00	Lysine/arginine/ornithine transporter subunit	Arg, Lys
aroP	4.80	6.09	Aromatic amino acid transporter	Phe, Tyr, and Trp
fliY	4.77	5.59	Cystine transporter subunit	Cys
glnH	3.70	4.69	Glutamine transporter subunit	Gln
gltI	4.37	4.23	Glutamate/aspartate periplasmic binding protein	Gln, Asp
hisJ	4.57	4.52	Histidine ABC transporter periplasmic binding protein	His
livG	4.08	5.18	Branched-chain amino acid ABC transporter atpase	Leu
livH	4.82	6.62	Branched-chain amino acid ABC transporter permease	Leu, Ile, Val
livJ	5.10	5.25	Leu/Ile/Val-binding protein	Leu, Ile, Val
livK	4.62	4.98	Leucine transporter subunit	Leu
sstT	4.01	4.98	Sodium: serine/threonine symporter	Ser, Thr
aroL	3.48	4.86	Shikimate kinase II	Phe, Tyr, and Trp
fbaB	3.45	4.33	Fructose-bisphosphate aldolase class I	
gltB	4.03	5.10	Glutamate synthase, large subunit	Gln
gltD	3.84	4.75	Glutamate synthase, 4Fe-4S protein, small subunit	Gln
hisA	3.54	4.18	N-(5'-phospho-L-ribosyl-formimino)-5-amino-1-(5'-phosphoribosyl)-4-imidazolecarboxamide isomerase	His
ilvC	5.14	5.52	Ketol-acid reductoisomerase, NAD(P)-binding	Ile, Van
ilvH	4.18	5.28	Acetolactate synthase 3, small subunit, valine-sensitive	Ile, Van
ilvI	4.57	4.52	Acetolactate synthase isozyme 3 large subunit	Ile, Van
leuA	3.96	4.96	2-isopropylmalate synthase	Leu
leuB	4.92	4.80	3-isopropylmalate dehydrogenase, NAD(+)-dependent	Leu
leuC	5.90	4.32	3-isopropylmalate dehydratase large subunit	Leu
leuD	5.47	5.85	3-isopropylmalate dehydratase small subunit	Leu
cysH	4.17	5.20	Phosphoadenosine phosphosulfate reductase; Paps reductase, thioredoxin dependent	Cys
cysI	3.93	4.44	Sulfite reductase, beta subunit, NAD(P)-binding, heme-binding	Cys
cysJ	4.34	4.98	Sulfite reductase, alpha subunit, flavoprotein	Cys
metA	4.79	5.20	Homoserine O-transsuccinylase	Met
metB	4.08	4.62	Cystathionine gamma-synthase, PLP-dependent	Met
metE	5.83	6.87	5-methyltetrahydropteroyltriglutamate-homocysteine S-methyltransferase	Met

metF	3.59	4.40	5,10-methylenetetrahydrofolate reductase	Met
serA	4.76	5.12	D-3-phosphoglycerate dehydrogenase	Ser
serC	3.36	4.20	3-phosphoserine/phosphohydroxythreonine aminotransferase	Ser
tktB	3.45	4.27	Transketolase 2, thiamine triphosphate-binding	
trpC	3.75	5.14	Indole-3-glycerolphosphate synthetase and N-(5-phosphoribosyl) anthranilate isomerase	Trp
trpE	3.50	4.24	Component I of anthranilate synthase	Trp

Table 3. Significantly down-regulated amino acids degradation related proteins when the control strain cultured in M9 minimal medium compared to in LB medium.

Gene name	Exp_1 Fold	Exp_2 Fold	Annotation	Related amino acid
ansB	-2.94	-2.98	L-asparaginase 2	Asn
aspA	-3.70	-3.41	Aspartate ammonia-lyase	Asp
kbl	-3.05	-3.50	Glycine C-acetyltransferase	Thr
sdaA	-2.50	-2.78	L-serine dehydratase 1	Ser
sdaB	-2.42	-3.13	L-serine dehydratase 2	Ser
sdaC	-2.84	-3.59	Putative serine transporter	Ser
tdcE	-2.43	-2.14	PFL-like enzyme tdce	Thr
tdh	-2.61	-3.05	L-threonine 3-dehydrogenase, NAD(P)-binding	Thr
tnaA	-3.53	-3.31	Tryptophanase/L-cysteine desulfhydrase, PLP-dependent	Trp

Additionally, a group of ammonia assimilation related proteins was significantly down-regulated when control strain cultured in M9 minimal medium (Table 4). Ammonia was reduced to nitrite by nitrite reductase (NirB is the NADH-binding large submit of nitrite reductase). Then nitrite could be reduced to nitrate by nitrate reductases (NAPs), such as NapA (periplasmic nitrate reductase), respiratory nitrate reductase (NarG and NarH). A common attribute of these reductases is that Fe-S cluster is the cofactor. These reduction processes belong to nitrogen assimilation [101].

Table 4. Significantly down-regulated ammonia assimilation related proteins of control strain in M9 minimal medium compared to in LB medium.

Gene name	Exp_1 Fold	Exp_2 Fold	Annotation
napA	-2.78	-2.92	Nitrate reductase, periplasmic, large subunit
narG	-3.03	-2.69	Respiratory nitrate reductase 1 alpha chain
narH	-3.06	-3.38	Respiratory nitrate reductase 1 beta chain
nirB	-2.79	-2.34	Nitrite reductase, large subunit, NAD(P)H-binding
nirC	-2.68	-4.12	Nitrite transporter

In addition to the sulfur amino acids (Met and Cys) biosynthesis related proteins, there are also other five significantly up-regulated proteins are involved in sulfur metabolism (Table 5). These proteins are involved in the transporters of sulfate/thiosulfate, conversion of sulfate into sulfite which is an important raw material for biosynthesis of Cys and *de novo* biosynthesis pathway of Met [102].

Table 5. Significantly up-regulated sulfur metabolism related proteins of control strain in M9 minimal medium compared to in LB medium.

Gene neme	Exp_1 Fold	Exp_2 Fold	Annotation
cysA	3.96	4.24	Sulfate/thiosulfate transporter subunit
cysC	3.91	4.72	Adenosine 5'-phosphosulfate kinase
cysH	4.17	5.20	Phosphoadenosine phosphosulfate reductase; Paps reductase, thioredoxin dependent
cysI	3.93	4.44	Sulfite reductase, beta subunit, NAD(P)-binding, heme-binding
cysJ	4.34	4.98	Sulfite reductase, alpha subunit, flavoprotein
cysN	5.04	5.29	Sulfate adenylyltransferase, subunit 1
cysU	3.92	4.62	Sulfate/thiosulfate ABC transporter permease
metA	4.79	5.20	Homoserine O-transsuccinylase
metB	4.08	4.62	Cystathionine gamma-synthase, PLP-dependent
sbp	4.89	4.83	Sulfate transporter subunit

Another group of significantly up-regulated proteins is involved in biosynthesis and transport of nucleotides (Table 6). These proteins include 10 purine and 5 pyrimidine metabolism related proteins, and one pyrimidine transporter. 8 of the 10 purine metabolism related proteins are involved in the "*de novo* pathway" of inosine monophosphate (IMP) biosynthesis. IMP is the precursor of guanylate and adenylate. 4 of the 5 pyrimidine metabolism related proteins are involved in the "*de novo* pathway" of uridine monophosphate (UMP) biosynthesis. The remaining one proteins (*codA*) is a cofactor in the salvage pathway of pyrimidine nucleotides biosynthesis. *De novo* and salvage are two synthetic pathways in cells. The *de novo* pathways involve synthesizing nucleotides or amino acids from simple molecules such as bicarbonate and amino acids, which consume a lot of energy. On the other hand, the salvage pathways include synthesis of nucleotides from the intermediates of the degradation of RNA and DNA, which could save a large quantity of energy [103, 104, 105]. However, in M9 medium such macromolecules are not available for cells which are in constant growth.

Table 6. Significantly up-regulated nucleotides biosynthesis and transport related proteins of control strain in M9 minimal medium compared to in LB medium.

Gene name	Exp_1 Fold	Exp_2 Fold	Annotation
carA	3.61	4.38	Carbamoyl phosphate synthetase small subunit, Glutamine amidotransferase
carB	3.65	4.56	Carbamoyl-phosphate synthase large subunit

codA	3.67	4.88	Cytosine/isoguanine deaminase
codB	5.00	6.28	Cytosine transporter
purC	3.98	5.15	Phosphoribosylaminoimidazole-succinocarboxamide synthetase
purD	3.87	4.28	Phosphoribosylglycinamide synthetase phosphoribosylamine-glycine ligase
purE	3.84	4.75	N5-carboxyaminoimidazole ribonucleotide mutase
purF	3.72	4.63	Amidophosphoribosyltransferase
purH	3.95	4.74	IMP cyclohydrolase and phosphoribosylaminoimidazolecarboxamide formyltransferase
purL	3.99	4.98	Phosphoribosylformylglycinamidine synthase
purM	4.11	4.19	Phosphoribosylaminoimidazole synthetase
purT	4.15	5.02	Phosphoribosylglycinamide formyltransferase 2
pyrB	5.38	5.18	Aspartate carbamoyltransferase, catalytic subunit
pyrI	5.75	6.49	Aspartate carbamoyltransferase, regulatory subunit
cysC	3.91	4.72	Adenosine 5'-phosphosulfate kinase
cysN	5.04	5.29	Sulfate adenylyltransferase, subunit 1

On the contrary, there are 8 nucleoside catabolism related enzymes were significantly down-regulated when the control strain was cultured in M9 minimal medium (Table 7). Under the action of these enzymes, various nucleosides would be degraded to respective intermediates (such as inosine) or bases [106, 107]. Among these proteins, adenosine deaminase (Add) is involved in the salvage pathway for purine base and nucleosides biosynthesis [108], cytidine/deoxycytidine deaminase (Cdd) and uridine phosphorylase (Udp) are involved in pyrimidine salvage synthesis pathways [109, 110, 111]. These salvage pathways consume adenosine, cytidine, and uridine as raw materials.

Table 7. Significantly down-regulated nucleoside catabolism related proteins of control strain in M9 minimal medium compared to in LB medium.

Gene name	Exp_1 Fold	Exp_2 Fold	Annotation
add	-2.04	-2.49	Adenosine deaminase
cdd	-3.11	-2.98	Cytidine/deoxycytidine deaminase
deoA	-2.17	-2.40	Thymidine phosphorylase
deoD	-1.56	-1.91	Purine nucleoside phosphorylase 1; nicotinamide 1-beta-D-riboside phosphorylase
nrdD	-1.86	-2.53	Anaerobic ribonucleoside-triphosphate reductase
rihA	-1.77	-2.33	Ribonucleoside hydrolase 1
rihC	-2.01	-2.07	Ribonucleoside hydrolase 3
udp	-2.02	-2.59	Uridine phosphorylase

In M9 minimal medium, a large amount of significantly down-regulated proteins are involved in various metabolic pathways of carbon and energy, and related transport systems of different carbon sources (Table 8). These pathways are including the metabolism of amino-sugar and nucleotide-sugar, trehalose,

galactose, D-ribose, fructose, mannose, glycerol, methane, and pyruvate, and the pathways of acetyl-CoA biosynthesis, gluconeogenesis, amino acids degradation, oxidative phosphorylation, sugar phosphotransferase system (PTS). The transporters are involved in glycine betaine (ProU transporter), maltose, and D-ribose.

Table 8. Significantly down-regulated carbon and energy metabolism and transport system related proteins of control strain in M9 minimal medium compared to in LB medium.

Gene name	Exp_1 Fold	Exp_2 Fold	Annotation
ackA	-2.30	-2.77	Acetate kinase A and propionate kinase 2
dctA	-2.38	-2.87	C4-dicarboxylic acid, orotate and citrate transporter
dmsA	-1.66	-2.63	Dimethyl sulfoxide reductase dmsa
fdoG	-3.55	-3.92	Formate dehydrogenase-O, large subunit
fdoH	-4.02	-4.43	Formate dehydrogenase-O iron-sulfur subunit
fdoI	-3.73	-5.59	Formate dehydrogenase-O, cytochrome b556 subunit
frdA	-2.67	-3.33	Anaerobic fumarate reductase catalytic and NAD/flavoprotein subunit
frdB	-3.11	-3.82	Fumarate reductase iron-sulfur subunit
frdC	-2.90	-3.04	Fumarate reductase subunit C
fruA	-2.60	-3.14	Fused fructose-specific PTS enzymes: iibcomponent/IIC components
fruB	-2.82	-3.10	Fused fructose-specific PTS enzymes: IIA component/hpr component
fruK	-3.05	-3.70	Fructose-1-phosphate kinase
garR	-2.21	-1.93	Tartronate semialdehyde reductase
gatD	-2.79	-3.02	Galactitol-1-phosphate dehydrogenase, Zn-dependent and NAD(P)-binding
glpA	-3.05	-2.98	Anaerobic sn-glycerol-3-phosphate dehydrogenase, large FAD/NAD(P)-binding subunit
glpB	-2.29	-2.09	Anaerobic glycerol-3-phosphate dehydrogenase subunit B
glpC	-3.11	-2.65	Anaerobic glycerol-3-phosphate dehydrogenase subunit C
glpQ	-2.10	-2.36	Periplasmic glycerophosphodiester phosphodiesterase
glpT	-2.54	-2.79	Sn-glycerol-3-phosphate transporter
lamB	-2.18	-2.44	Maltose outer membrane porin (maltoporin)
lldD	-2.33	-2.73	L-lactate dehydrogenase, FMN-linked
lldP	-2.35	-3.97	L-lactate permease
maa	-1.72	-2.04	Maltose O-acetyltransferase
malF	-2.23	-2.69	Maltose transporter subunit
malK	-2.68	-3.19	Maltose ABC transportor atpase
malM	-2.03	-2.77	Maltose regulon periplasmic protein
nanA	-3.18	-3.90	N-acetylneuraminate lyase
nanE	-2.48	-2.90	Putative N-acetylmannosamine-6-phosphate 2-epimerase
nanK	-2.48	-2.08	N-acetylmannosamine kinase
ndh	-1.52	-1.90	Respiratory NADH dehydrogenase 2/cupric reductase
proV	-3.78	-2.92	Glycine betaine/proline ABC transporter periplasmic binding protein
proW	-2.90	-2.26	Glycine betaine/proline ABC transport system permease protein
proX	-2.01	-2.17	Glycine betaine/proline ABC transporter periplasmic binding protein

pta	-1.51	-1.84	Phosphate acetyltransferase
rbsA	-2.19	-2.52	Ribose import ATP-binding protein
rbsC	-2.08	-3.14	Ribose import permease protein
rbsD	-2.42	-2.83	D-ribose pyranase
rbsK	-1.83	-2.15	Ribokinase
srlD	-2.43	-3.39	Sorbitol-6-phosphate dehydrogenase
srlE	-2.55	-3.42	PTS system glucitol/sorbitol-specific EIIB component
treB	-3.06	-3.02	PTS system trehalose-specific EIIBC component
treC	-3.29	-3.26	Trehalose-6-phosphate hydrolase
ucpA	-2.42	-2.32	Furfural resistance protein, putative short-chain oxidoreductase
yqhD	-3.40	-3.54	Aldehyde reductase, NADPH-dependent
deoC	-1.67	-2.19	2-deoxyribose-5-phosphate aldolase, NAD(P)-linked
aphA	-2.38	-2.69	Acid phosphatase/phosphotransferase, class B, non-specific
ansB	-2.94	-2.98	L-asparaginase 2
aspA	-3.70	-3.41	Aspartate ammonia-lyase
dadA	-2.34	-3.10	D-amino acid dehydrogenase
dsdA	-1.94	-2.05	D-serine dehydratase
kbl	-3.05	-3.50	Glycine C-acetyltransferase
sdaA	-2.50	-2.78	L-serine dehydratase 1
sdaB	-2.42	-3.13	L-serine dehydratase 2
sdaC	-2.84	-3.59	Putative serine transporter
tdcE	-2.43	-2.14	PFL-like enzyme tdce
tdh	-2.61	-3.05	L-threonine 3-dehydrogenase, NAD(P)-binding
tnaA	-3.53	-3.31	Tryptophanase/L-cysteine desulfhydrase, PLP-dependent

The significant regulation on the proteome of E. coli control strain cultured in M9 minimal medium compared to LB medium is also evidenced in the transcription, translation and protein folding. In the data, it was found that 13 extremely decreased proteins are related to transcription regulator, tRNA synthesis, ribosomal subunits, translation elongation, and heat shock proteins (Table 9).

Table 9. Significantly down-regulated transcription, translation, and proteins folding related proteins of control strain in M9 minimal medium compared to in LB medium.

Gene name	Exp_1 Fold	Exp_2 Fold	Annotation
epmA	-1.99	-2.43	Elongation factor P--(R)-beta-lysine ligase
htpG	-1.56	-1.92	Protein refolding molecular co-chaperone Hsp90, Hsp70-dependent; Heat-shock protein; atpase
ibpA	-2.77	-3.31	Heat shock chaperone
ibpB	-3.90	-4.17	Heat shock chaperone
lysU	-2.64	-3.32	Lysine tRNA synthetase, inducible
rapA	-1.47	-1.97	RNA polymerase-associated protein
rplV	-1.66	-2.02	50S ribosomal subunit protein L22
rpmA	-1.61	-2.13	50S ribosomal subunit protein L27

rpsL	-1.59	-1.83	30S ribosomal subunit protein S12
rpsQ	-1.92	-2.42	30S ribosomal subunit protein S17
rpsR	-2.03	-2.62	30S ribosomal subunit protein S18
rpsS	-2.52	-3.26	30S ribosomal subunit protein S19
rpsT	-1.74	-2.03	30S ribosomal subunit protein S20

Summary

The M9 minimal medium contains glucose as the only carbon source and NH_4Cl as the only nitrogen source. Comparing with complex medium LB, M9 minimal medium lacks various nutrients, such as various amino acids (except Arg, Lys, and Pro), peptides, peptones, polypeptides, nucleic acids, vitamins, and a variety of carbohydrates. The great difference of composition between M9 minimal medium and complex medium LB leads to great changes in *E. coli* proteome. The differences of protein expression are involved in nutrients uptake, anabolism, and catabolism, and the processes of transcription, translation, and protein folding.

The metabolisms of nutrients are mainly involved in nitrogen-containing compounds, sulfur-containing compounds, and carbon sources. Under the organic nitrogen source limitation environment of M9 minimal medium culture, the ABC transport systems of peptide were significantly up-regulated. The increasing of Opp and Dpp is correlated with previous studies showing that they were induced under nitrogen limitation and inhibited in rich medium [93, 94, 95, 96]. On the contrary, the PTR family transporter DtpA was significantly down-regulated. In terms of amino acids, the transporters and biosynthesis pathways related proteins were significantly up-regulated, in contrast to amino acids degradation related proteins whose levels were significantly down-regulated. Additionally, the proteins related to nucleotides transport and biosynthesis especially de novo pathways were significantly up-regulated, and the nucleosides degradation and salvage biosynthesis pathways related enzymes were down-regulated as well. In minimal medium, bacteria cannot directly obtain amino acids and nucleotides from the medium. In order to protect the basic survival, growth, and division of the cells, they have to enhance the biosynthesis of the raw materials of RNA, DNA, and protein by themselves. At the same time, the degradation should be repressed. Moreover, under the nutrients limitation environment, the control strain prefers the *de novo* pathways rather than salvage pathways of biosynthesis, due to the lacking of intermediates degraded from RNA, DNA, proteins, and their degradation products.

As a complex medium, LB medium is composed of tryptone peptone, yeast extract, and NaCl. Peptone and yeast extract contain not only amino acids, vitamins, and metal ions, but also a variety of carbohydrates, such as maltose, trehalose, D-mannose, melibiose, D-galactose, L-fucose, L-rhamnose, D-mannitol, amino sugars, and L-arabinose. It has been verified with transcriptional microarray that *E. coli* could use these different carbohydrates of LB medium at different culture time with different utilization rates. Maltose is the most favorite carbohydrate among the substrates in LB medium [112], trehalose [113], D-ribose, and glycerol are also highly utilized by *E. coli* when it grows in LB medium,

otherwise other sugars could be used, whereas arabinose is the lowest employed substrate [114]. The results of this research correlate well with these published conclusions. In M9 minimal medium, glucose is the only carbohydrate, the proteins related to transport and catabolism of maltose, trehalose, D-ribose, glycerol, and some other carbohydrates are much less expressed than in LB medium. Glycine betaine plays an important role in the adaptation of osmotic stress [115]. ProU is the corresponding transport system of glycine betaine [116, 117, 118]. The proteins involved ProU are also found to be decreased in M9 minimal medium.

In addition, down-regulations of transcription, translation, and protein folding related proteins correspond to the low growth rate of *E. coli* in M9 minimal medium.

2.2.2 Proteome comparisons of the adapted strains and the control strain

After nearly 40 days evolution in the GM3 device, the generation time of *E. coli* WT strain was reduced from almost 80 minutes to less than 40 minutes. To study the proteome changes between the adapted strains and WT strain by SILAC based MS measurement, I have constructed Arg and Lys auxotrophic control strain, Evo-1 and Evo-2 strains from WT strain, and the adapted strains, GM117C1 and GM117C3, respectively (in section 2.1).

However, since the construction of the Arg and Lys auxotrophic strains needs two weeks, period of time in which the adapted strains could revert the proteome changes achieved in the process, my colleague Christian Schipp used for a second approach to the evolution culture two strains directly based on the control strain already containing the *argA* and *lysA* KO. These two strains were named as *E. coli* BU174 and *E. coli* BU175 in our lab database. For the purpose of easy reading and understanding, they were named as Evo-3 and Evo-4 in this dissertation.

To characterize the proteome changes of the adapted strains, I performed SILAC experiments of each adapted strains compared with control strain. Each comparison has been done two biological replicates where the SILAC labels have been swapped to avoid any source of artifacts due to the technique.

In a total of the comparisons of Evo-1, Evo-2, Evo-3, and Evo-4 strains to control strain, 1535 proteins were quantified in all experiments. If an average of the two replicates is considered, there are 1152 proteins which could be quantified for each adapted strain relative to the control counterpart. The nomenclature Evo1, Evo2, Evo3, and Evo4, refers to the respective comparisons of the Evo-1, Evo-2, Evo-3, and Evo-4 adapted strains to the control strain. Figure 25A-D displays the distribution of the protein ratios in histograms. The regulated ratio is between -7.67 and 3.27. Notable, strains Evo-2 and Evo-4 show a different behavior as Evo-1 and Evo-3. This first observation would suggest that bacteria adapted in biological replicates can lead to different proteome changes. The correlation coefficient between the two biological replicates for each comparison of adapted strains to control ranged between 0.49 and 0.84 (Figure 25E-H).

When we take the four comparisons together (Figure 26A), there is no one common protein was significantly up-regulated in all the adapted strains. However, there are three proteins extremely increased in three of the adapted strains (Figure 26B). They are the agmatinase (SpeB), the hydrogen peroxide and cadmium resistance periplasmic protein (YgiW), and the peroxiredoxin (OsmC). In addition, 30 proteins are significantly up-regulated in at least one adapted strain. These proteins are involved in the biosynthesis of putrescine, glycolysis, RNA degradation regulators, and some of them are the components of ribosome (Table S1).

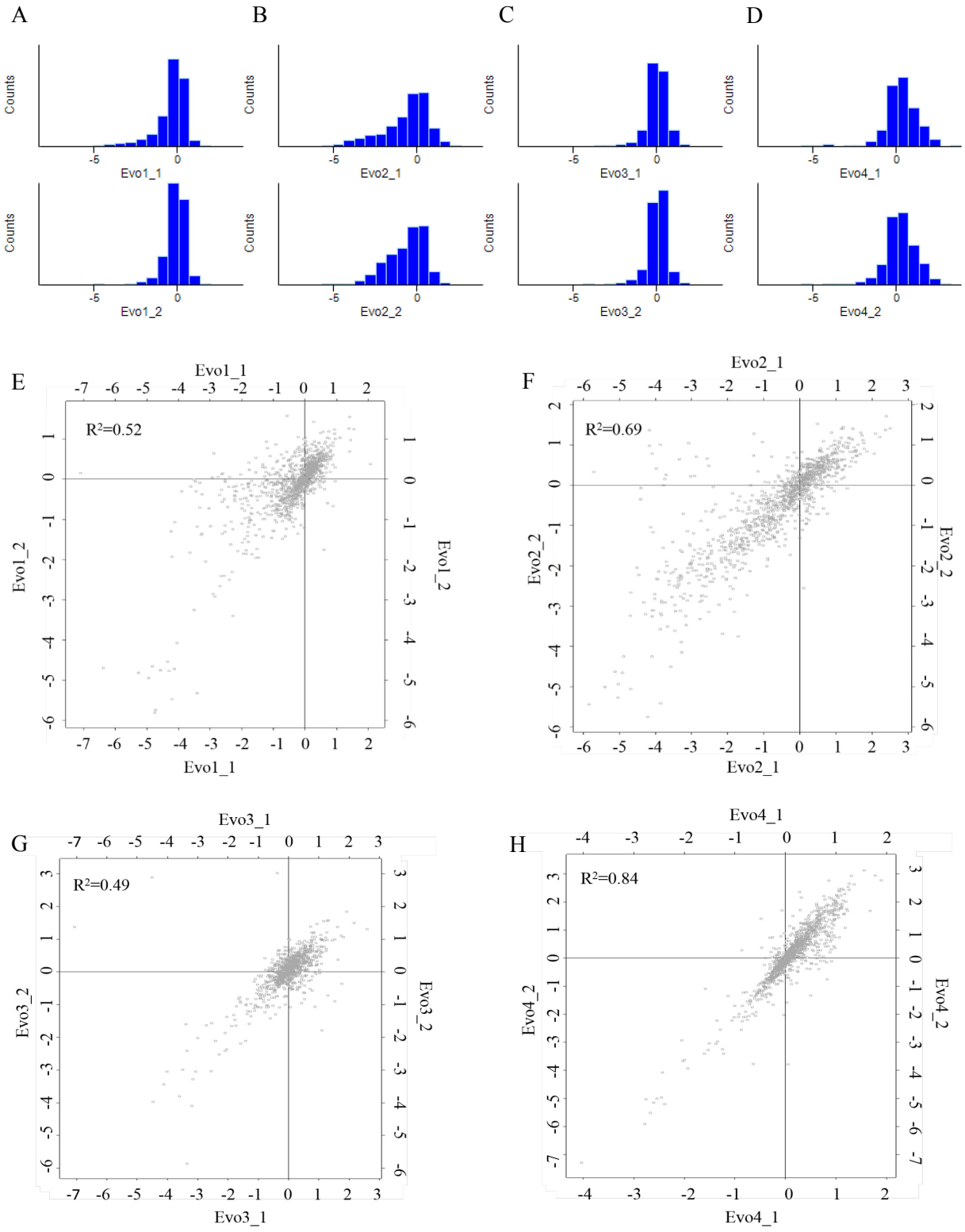

Figure 25. The proteome changed ratios of each adapted strains compared to the control strain that are shown in the histograms (A. Evo1, B. Evo2, C. Evo3, and D. Evo4). And the correlations of two replicates for each comparison are shown in the Scatter plot graphs (E. Evo1, F. Evo2, G. Evo3, and H. Evo4).

A

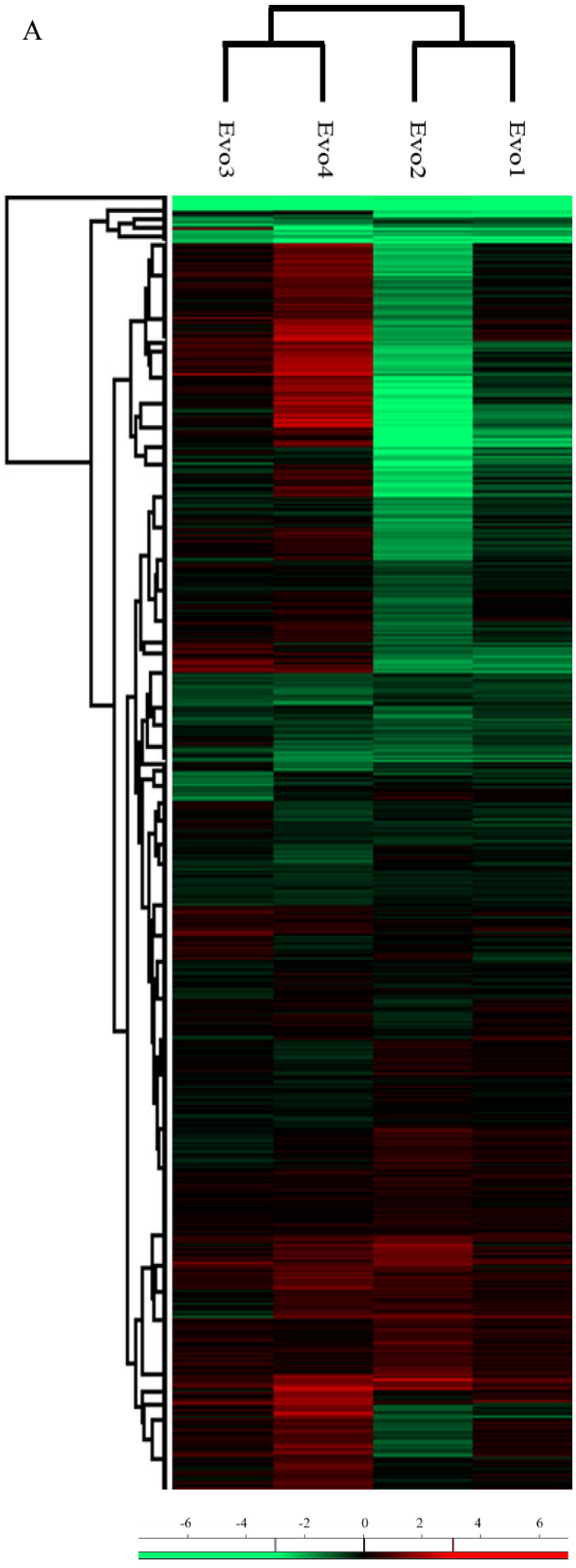

B

Gene name	Evo1 Fold	Evo2 Fold	Evo3 Fold	Evo4 Fold
speB	1.09	1.31	1.42	0.61
ygiW	1.04	1.96	0.36	2.59
osmC	0.86	2.05	1.35	1.82

C

Gene name	Evo1 Fold	Evo2 Fold	Evo3 Fold	Evo4 Fold
flgE	-4.55	-4.37	-2.98	-4.94
ycgR	-4.37	-4.98	-2.88	-4.34
cheY	-5.04	-5.20	-3.70	-5.27
cheZ	-4.54	-4.57	-3.05	-4.47
cheW	-5.53	-5.64	-4.61	-5.73
pyrI	-4.67	-4.78	-0.81	-5.43
pyrB	-4.44	-4.18	-3.53	-5.18
cheA	-4.84	-4.64	-3.65	-3.52
tar	-4.74	-4.87	-3.23	-3.90
tsr	-5.23	-4.88	-3.77	-5.05
fliC	-5.29	-5.16	-4.22	-4.98
gatY	-2.88	-3.72	-2.18	-3.30
gatA	-2.67	-4.04	-2.27	-1.98
gntR	-3.47	-2.69	-2.84	-7.67
pykF	-4.95	-4.98	-0.78	-1.19
ridA	-1.68	-1.30	-1.98	-1.70
modA	-1.63	-1.57	-2.05	-2.07
fliN	-1.76	-1.78	-2.51	-2.93
aroF	-1.90	-2.09	-1.95	-2.83
gdhA	-1.48	-1.08	-1.27	-2.18
pyrD	-1.82	-2.02	-1.88	-1.91
codA	-1.95	-1.74	-2.21	-2.57
tap	-4.43	-2.99	-1.77	-2.13
fliL	-1.71	-3.54	-3.24	-1.86
carA	-2.45	-2.32	-2.25	-3.17
carB	-2.48	-2.04	-2.41	-3.02
pyrC	-1.61	-1.92	-0.88	-1.46

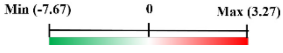

Figure 26. The hierarchical clustering for the complete proteomics data (A), the significantly up-regulated (B) and down-regulated proteins (C) of the comparisons between the adapted strains and the control strain that are shown by the heat maps.

There are 42 proteins down-regulated in all four adapted strains relative to control counterpart, which in addition show significant values in at least two of the strains. 27 of these proteins are significantly down-regulated in at least three of the four adapted strains (Figure 26C). The majority of down-regulated protein in the adapted strains are involved in bacterial chemotaxis and flagellar assembly, while the rest participate in the biosynthetic pathway of amino acids and pyrimidine, and in the tricarboxylic acid cycle (TCA-cycle).

SpeB is involved in the biosynthesis of putrescine (1, 4-diaminobutane). As an important polyamine in *E. coli*, it is essential for the cells proliferation and growth [119, 120]. In *E. coli*, the biosynthesis of putrescine is started from arginine, which was converted to agmatine under the action of arginine decarboxylase (SpeA), and sequentially converted to ornithine by SpeB, then putrescine could be synthesized from ornithine by two forms of ornithine decarboxylase (ODC), SpeC and SpeF. Putrescine could be further converted to another polyamine spermidine by putrescine aminopropyltransferase (spermidine synthase, SpeE) [121, 122]. In the data, except SpeF which was not identified in my experiments, the remaining relative proteins mentioned above were quantified in all experiments. For putrescine synthesis, the up-regulation is not only is evident in SpeB but also happens in SpeA and SpeC, although to different levels. On the contrary, the spermidine synthesis related proteins were down-regulated (Figure 27).

Gene name	Evo1 Fold	Evo2 Fold	Evo3 Fold	Evo4 Fold	Evo1 significant	Evo2 significant	Evo3 significant	Evo4 significant
speA	0.56	0.34	0.61	1.26				
speB	1.09	1.31	1.42	0.61	+	+	+	
speC	0.75	1.09	0.74	0.42	+			
speD	-0.78	-0.99	-0.32	-1.26				+
speE	-0.53	-0.59	-0.38	-1.12				+
speG	-0.01	0.26	-0.37	0.22				

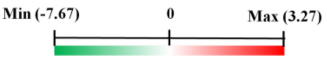

Figure 27. The putrescine and spermidine biosynthesis related proteins in the adapted strains are changed as the heat map shows.

In addition, the evolution leads to great regulation of the central carbon metabolism. In here presented experiments, the enzymes of each step of glycolysis and TCA-cycle were quantified (Table 10). Careful inspection of the data indicates, that the majority of enzymes are involved in the conversion from glucose-1-phosphate (G1P) to phosphoenolpyruvate (PEP) were up-regulated to varying degrees. However, start from the synthesis of pyruvate from PEP and the subsequent reactions of TCA-cycle related enzymes were decreased to different levels (Figure 28). The majority of these down-regulations are involved in the synthesis of ATP.

Table 10. The quantified central carbon metabolism related proteins in the comparisons between the adapted strains and control strain.

Gene name	Annotation	Carbon Metabolic Pathway
pgm	Phosphoglucomutase	Glycolysis / Gluconeogenesis; Pentose phosphate pathway
pgi	Glucosephosphate isomerase	Glycolysis / Gluconeogenesis; Pentose phosphate pathway
pfkA	6-phosphofructokinase I	Glycolysis / Gluconeogenesis; Pentose phosphate pathway
pfkB	6-phosphofructokinase II	Glycolysis / Gluconeogenesis; Pentose phosphate pathway
fbaA	Fructose-bisphosphate aldolase, class II	Glycolysis / Gluconeogenesis; Pentose phosphate pathway
tpiA	Triosephosphate isomerase	Glycolysis / Gluconeogenesis
gapA	Glyceraldehyde-3-phosphate dehydrogenase A	Glycolysis / Gluconeogenesis
pgk	Phosphoglycerate kinase	Glycolysis / Gluconeogenesis
gpmA	Phosphoglyceromutase 1	Glycolysis / Gluconeogenesis
gpmB	Phosphatase	Glycolysis / Gluconeogenesis
gpmI	Phosphoglycero mutase III, cofactor-independent	Glycolysis / Gluconeogenesis
eno	Enolase	Glycolysis / Gluconeogenesis; RNA degradation
pykA	Pyruvate kinase II	Glycolysis / Gluconeogenesis; Pyruvate metabolism
pykF	Pyruvate kinase I	Glycolysis / Gluconeogenesis; Pyruvate metabolism
aceE	Pyruvate dehydrogenase, decarboxylase component E1, thiamine triphosphate-binding	TCA cycle; Glycolysis / Gluconeogenesis; Pyruvate metabolism
aceF	Pyruvate dehydrogenase, dihydrolipoyltransacetylase component E2	TCA cycle; Glycolysis / Gluconeogenesis; Pyruvate metabolism
gltA	Citrate synthase	TCA cycle
acnA	Aconitate hydratase 1; aconitase A	TCA cycle
acnB	Aconitate hydratase 2; aconitase B; 2-methyl-cis-aconitate hydratase	TCA cycle
icd	Isocitrate dehydrogenase; e14 prophage attachment site; tellurite reductase	TCA cycle
sucA	2-oxoglutarate decarboxylase, thiamine triphosphate-binding	TCA cycle
sucB	Dihydrolipoyltranssuccinase	TCA cycle
sucC	Succinyl-coa synthetase, beta subunit	TCA cycle
sucD	Succinyl-coa synthetase, NAD(P)-binding, alpha subunit	TCA cycle
sdhA	Succinate dehydrogenase, flavoprotein subunit	TCA cycle
sdhB	Succinate dehydrogenase, fes subunit	TCA cycle
sdhD	Succinate dehydrogenase, membrane subunit, binds cytochrome b556	TCA cycle
fumA	Fumarate hydratase (fumarase A), aerobic Class I	TCA cycle
mdh	Malate dehydrogenase, NAD(P)-binding	TCA cycle

A

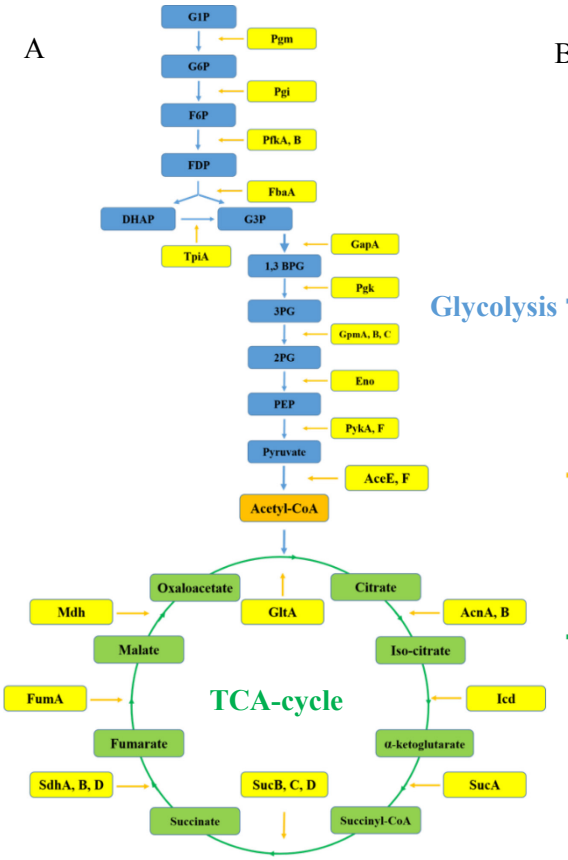

B

Gene names	Evo1	Evo2	Evo3	Evo4	Evo1 significant	Evo2 significant	Evo3 significant	Evo4 significant
pgm	0.27	0.46	0.37	0.34				
pgi	0.83	1.10	0.21	0.34	+			
pfkA	0.98	1.27	-0.03	0.62	+	+		
pfkB	0.55	1.15	0.97	1.98			+	
fbaA	0.17	-1.57	0.03	0.61				
tpiA	0.02	-0.03	0.14	-0.24				
gapA	0.08	0.14	-0.55	-0.04				
pgk	0.27	0.43	-0.14	0.03				
gpmA	0.90	1.01	0.20	0.74	+			
gpmB	-0.19	-0.93	-0.06	0.13				
gpmI	0.77	-0.15	-0.38	0.47	+			
eno	0.87	1.28	0.29	0.39	+	+		
pykA	-0.40	-0.46	-0.24	-0.31				
pykF	-4.95	-4.98	-0.78	-1.19	+	+		+
aceE	-0.08	-0.21	-0.62	0.00				
aceF	-0.25	-0.14	-0.45	0.24				
gltA	-0.09	0.18	-0.27	-0.93				
acnA	-0.20	-0.04	0.30	-0.40				
acnB	-1.42	-3.97	-0.41	0.49	+	+		
icd	-0.14	-0.97	-0.32	-0.42				
sucA	-1.35	-3.36	-1.00	1.07			+	
sucB	-0.54	-0.56	-0.87	-1.02			+	
sucC	-0.52	-2.31	-1.05	-0.86			+	
sucD	-0.55	-2.35	-0.85	-0.75			+	
sdhA	-0.42	-0.59	-1.45	-1.53			+	+
sdhB	-0.66	-1.10	-1.33	-1.47			+	+
sdhD	-0.81	-0.65	-1.76	-1.44			+	+
fumA	-0.59	-2.18	-0.46	-0.46				
mdh	-0.06	0.09	-0.34	0.02				

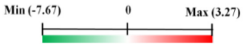

Figure 28. A. Pathway of glycolysis (blue) and TCA-cycle (green), and the enzymes (yellow) examined in this thesis. B. Heat map shows the up- (red) and down- (green) regulations of central carbon metabolism relative proteins in adapted strains compared to control strain.

Gene name	Evo1 Fold	Evo2 Fold	Evo3 Fold	Evo4 Fold	Evo1 significant	Evo2 significant	Evo3 significant	Evo4 significant	Biosynthetic Pathway
glnA	-0.79	-0.45	-1.30	-1.25			+	+	Gln
gltB	-0.91	-0.23	-1.00	-1.35			+	+	Glu
aroF	-1.90	-2.09	-1.95	-2.83	+		+	+	Phe, Tyr, and Trp
trpE	-1.57	-2.60	-0.83	-0.27	+		+		Phe, Tyr, and Trp
pyrI	-4.67	-4.78	-0.81	-5.43	+	+	+	+	UMP via de novo
pyrB	-4.44	-4.18	-3.53	-5.18	+	+	+	+	UMP via de novo
carA	-2.45	-2.32	-2.25	-3.17	+		+	+	UMP via de novo
carB	-2.48	-2.04	-2.41	-3.02	+		+	+	UMP via de novo
pyrD	-1.82	-2.02	-1.88	-1.91	+		+	+	UMP via de novo
pyrC	-1.61	-1.92	-0.88	-1.46	+		+	+	UMP via de novo

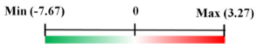

Figure 29. The significantly down-regulated amino acids and pyrimidine biosynthesis related proteins in the adapted strains compared to the control strain are shown in the Heat map.

The level of the proteins involved in biosynthetic pathways of some amino acids and pyrimidine are also extremely decreased after the evolution in *E. coli*. The significant down-regulations have involved in

the synthesis of Glu, Gln, and aromatic amino acids (Phe, Tyr, and Trp), and the *de novo* pathway for UMP (Figure 29 and Table S2).

The most stably and significantly down-regulated proteins in the adapted strains are the chemotaxis and the flagellar assembly related proteins (Figure 31 and Table S2). In a variety of motile cells, chemotaxis protein plays an essential role in response to the stimulus of attractant and repellent chemicals from the environment. The movement of *E. coli* cells is achieved by flagella that drove by a rotary motor powered by proton-motive force. The cell swims forward (runs) when the motor rotates counter-clockwise (CCW). On the contrary, the cell's swimming action changes to the random direction (tumbles) by the clockwise (CW) rotating motor. The direction of flagella motor rotation is controlled by a ternary receptor signaling complex (Figure 30A), which is formed by a transmembrane chemoreceptor with kinase CheA and receptor coupling protein CheW [123]. This kind of transmembrane chemoreceptors is methyl-accepting chemotaxis proteins (MCPs), by which the motile bacterial cells sense and track chemical gradients [124, 125]. In *E. coli* cells, five MCPs have been identified, of which Tar and Tsr are the two most abundant members, in addition, Tap, Trg, and Aer are three low-abundance members. The receptor signaling complexes emerge two output states, kinase-ON and kinase-OFF (Figure 30B). Under the stimulation of attractant (ATT), the receptors shift to the OFF state. Accompanied by the reduction of stimulation, the phosphoryl groups of CheA transfer to two response regulators, CheB and CheY. Phospho-CheY (CheY~P) triggers flagella motor to an ephemeral CW rotation, subsequent dephosphorylation is performed by CheZ. Phospho-CheB (CheB~P) is part of a sensory adaptation system that regulates the receptor signaling complexes to its pre-stimulus state. The sensory adaptation system adjusts receptor output state through the cytoplasmic portion of MCPs covalent modification by glutamyl residues. The chemotaxis protein methyltransferase (CheR) shifts the Off-state to On-state through catalyzing the glutamyl residues methylation. On the contrary, the methylesterase CheB shifts the On-state MCPs to Off-state through hydrolyzes glutamyl methyl group to glutamate [126].

In my data, the sensory adaptation system proteins (CheB and CheR) were not identified, the proteins related to receptor signaling, flagellar motor controlling, and flagellar assembling were quantified (Figure 31). It is clear that all of these quantified chemotaxis related proteins were significantly down-regulated in all of the four adapted strain.

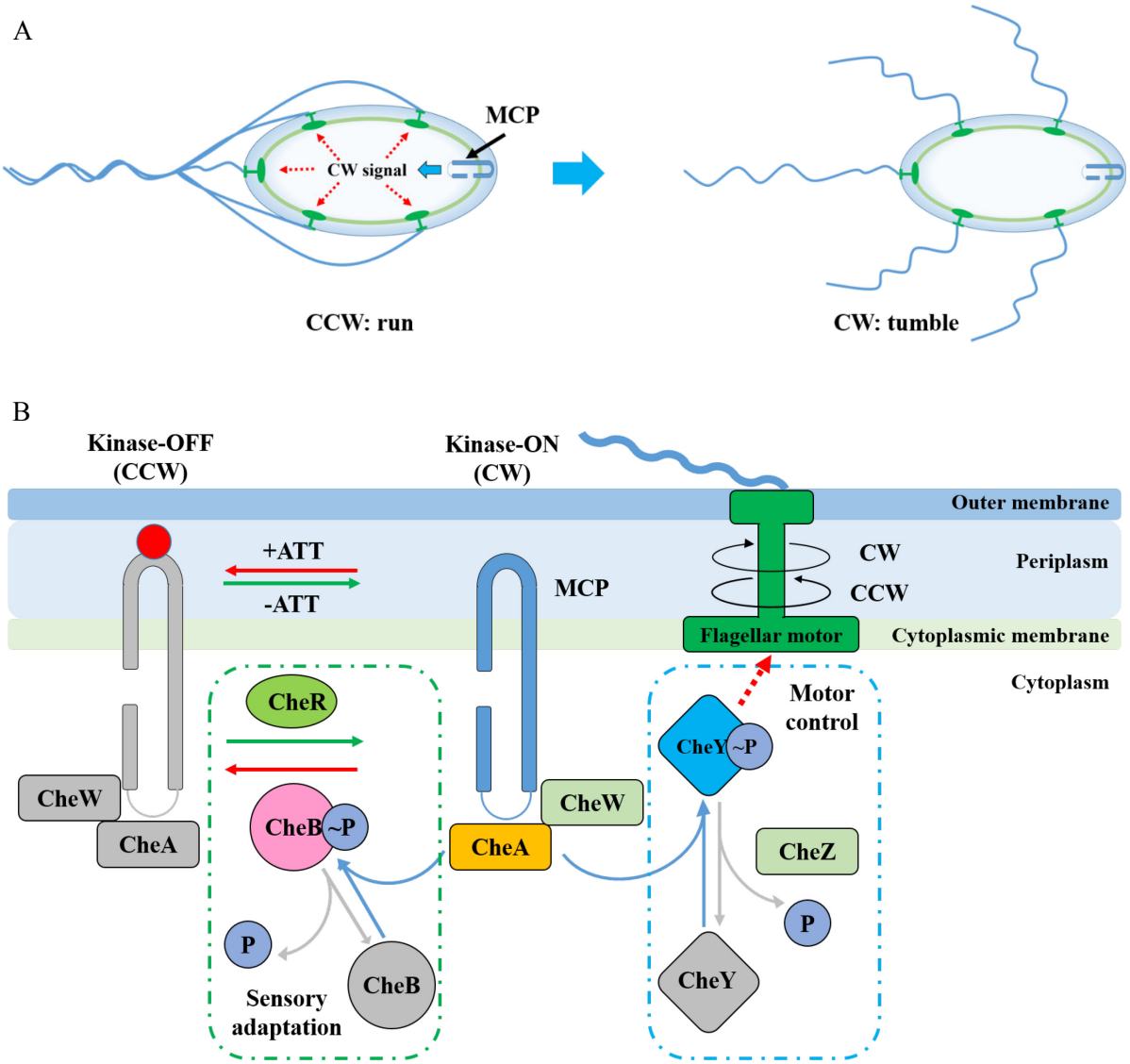

Figure 30. Transduction mechanism of *E. coli* chemotaxis pathway, modified based on the publications [127, 123, 126, 125]. A. Cell swimming behavior is controlled by the receptor signaling complex (MCP/CheA/CheW). The default rotary direction of flagellar is CCW. A short-lived CW rotation is caused by the signal generated by the receptor. B. OFF- and ON-state of receptor signaling complexes. Gray components are inactive forms.

Gene name	Evo1 Fold	Evo2 Fold	Evo3 Fold	Evo4 Fold	Evo1 significant	Evo2 significant	Evo3 significant	Evo4 significant
cheA	-4.84	-4.64	-3.65	-3.52	+	+	+	+
cheW	-5.53	-5.64	-4.61	-5.73	+	+	+	+
cheY	-5.04	-5.20	-3.70	-5.27	+	+	+	+
cheZ	-4.54	-4.57	-3.05	-4.47	+	+	+	+
flgE	-4.55	-4.37	-2.98	-4.94	+	+	+	+
flgH	-1.25	-1.26	-2.49	-1.88			+	+
fliC	-5.29	-5.16	-4.22	-4.98	+	+	+	+
fliF	-1.38	-1.43	-0.93	-4.26			+	+
fliL	-1.71	-3.54	-3.24	-1.86	+		+	+
fliN	-1.76	-1.78	-2.51	-2.93	+		+	+
tap	-4.43	-2.99	-1.77	-2.13	+		+	+
tar	-4.74	-4.87	-3.23	-3.90	+	+	+	+
tsr	-5.23	-4.88	-3.77	-5.05	+	+	+	+
ycgR	-4.37	-4.98	-2.88	-4.34	+	+	+	+

Figure 31. The significantly down-regulated chemotaxis and the flagellar assembly related proteins in the adapted strains are shown in the heat map.

Summary

The evolution performed by GM3 device resulted in great improvement in the growth rate of *E. coli* control strain. The corresponding proteomics regulations have been identified by the data that shown above. The changes at proteome level involve biological pathways of polyamine synthesis, central carbon metabolism, amino acids and pyrimidine synthesis, and chemotaxis and flagellar assembly.

It has been manifested by a large number of research that polyamines are very important growth factors for various organisms. Putrescine and spermidine are two main polyamines in *E. coli*. Our data shows that in all of the adapted strains the putrescine synthesis related proteins were up-regulated, in contrast, the proteins involved in spermidine synthesis from putrescine were decreased. It indicates that during the adaptation process *E. coli* strains selectively enhanced the biosynthetic pathway of putrescine but dismissed the pathway of spermidine synthesis.

In terms of central carbon metabolism, the data shows that the proteins related to glycolysis steps before pyruvate synthesis were increased, however, start from the conversion of PEP to pyruvate, the following conversion to acetyl-CoA, and all the TCA-cycle were down-regulated. These changes indicated that the evolution process strengthened a part of glycolysis but repressed a lot of ATC synthetic reactions.

The down-regulations of amino acids and pyrimidine biosynthesis related proteins are mainly involved in Glu, Gln, and aromatic amino acids, and the *de novo* pathway for UMP. These pathways consume a large amount of energy. These changes reveal that the evolution inhibits some energy utilization pathways.

The most obvious down-regulation happened on the chemotaxis and flagellar assembly related proteins. Considering the culture environment is turbidostat always supplemented with fresh medium, in which the adapted strains do not need as much movement as normal culture condition to forage. In addition, since the movement of *E. coli* cells is an energy consuming process, the evolution of *E. coli* in a GM3 device reduces the ATP consumption in bacteria by the decreasing the levels of proteins involved in chemotaxis pathways.

2.2.3 Proteome comparison between the *efp* knock-out strain and the control strain

To study the effects of EF-P KO on the proteome of *E. coli* via SILAC-based MS measurement, my colleague Christian Schipp has constructed the auxotrophic strain of which the *efp* and *argA* genes have been deleted and the *lysA* gene has been replaced by kan resistance gene *kanR*. The strain was named as *E. coli* BU62 (*ΔefpΔargAΔlysA::kanR, frt+*), here we will refer to it as *Δefp* strain.

When the control and *Δefp* strains were cultured in M9 minimal medium, the growth rate of *Δefp* strain is lower than control strain (Figure 32) at the early-exponential growth phase (OD_{600} is between 0.3 and 0.5), and the maximal cells amount of *Δefp* is only two third (the OD_{600} is around 1.2 compared to 1.8) of the control strain's. It is clear that the absence of EF-P greatly inhibits the growth of *E. coli*.

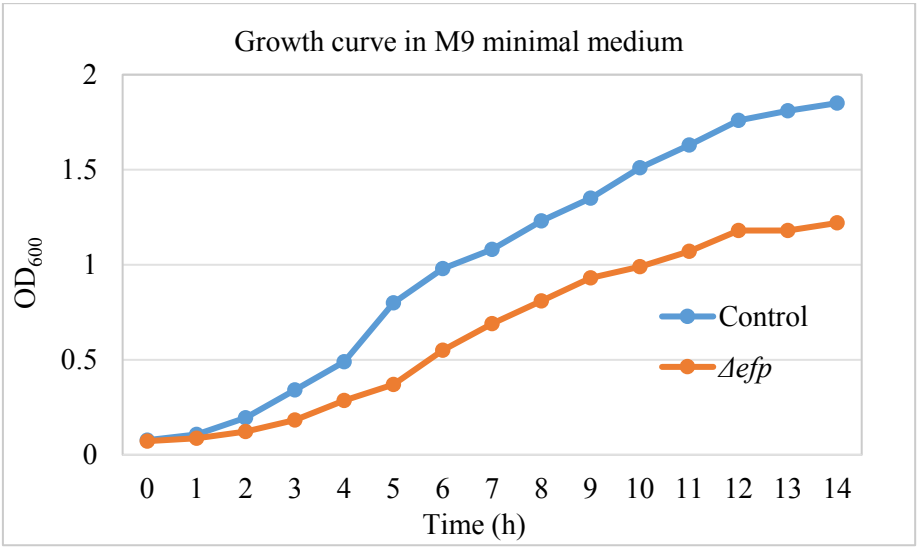

Figure 32. Growth curves of the control strain and *Δefp* strain cultured in M9 minimal medium.

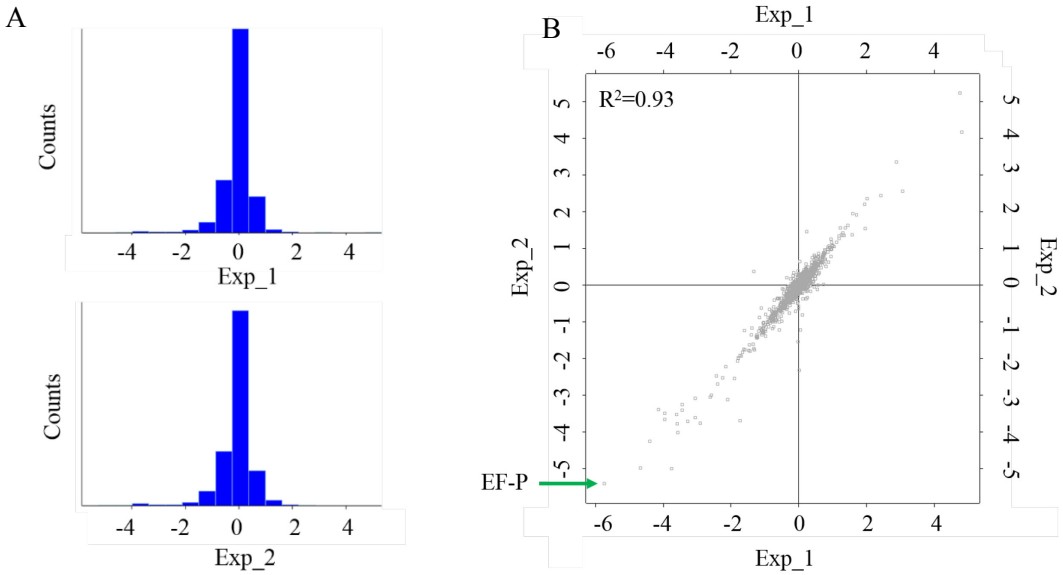

Figure 33. A. Histograms show changes of proteome from control strain to *Δefp* strains. B. Scatter plot shows the correlation of two replicate measurements.

An SILAC-based proteomics study was performed by growing the control strain in M9 minimal medium with light labeled (Lys-0, Arg-0), and the *Δefp* strain in M9 minimal medium with medium labeled (Lys-4, Arg-6). Two biological replicates of this experiment were performed. In the following of this section (2.2.3), the two replicates will be presented as Exp_1 and Exp_2. In a total of 1756 proteins were identified, of which 1345 proteins were quantified in both replicate MS measurements. The contribution of the proteins changed ratios (Figure 33A) shows that there are more proteins are down-regulated than up-regulated. The two replicates are correlated with a high coefficient of 0.93 (Figure 33B). Among these quantified proteins, 143 of them were significantly changed, of which 56 proteins were up-regulated, and the remaining 87 proteins were down-regulated.

Expectedly, measured EF-P protein levels were much lower in *Δefp* strain than control strain (Table 11 and Figure 33B). These results verified at protein level that the *efp* gene has been successfully knocked out from the genome of the *Δefp* strain.

Table 11. Changes of EF-P expression from control to *Δefp* strain.

Gene name	Exp_1 Fold	Exp_2 Fold	Exp_1 significant	Exp_2 significant	Annotation
efp	-5.74	-5.40	+	+	translation elongation factor EF-P

The most significantly up-regulated group of proteins is involved in transport and catabolism of galactitol. Galactitol (also was named dulcitol) together with D-sorbitol and D-mannitol are three naturally occurring hexitols. Galactitol could not be utilized as a sole source of carbon and energy, but it could be adapted during the culture of *E. coli* [128, 129]. The transport of galactitol is based on the PEP-dependent PTS. During the PTS transport of a carbohydrate, the phosphoryl group is transferred from PEP sequentially through the two general cytosolic proteins, enzyme I (EI, codified by *ptsI*) and histidine carrier protein (HPr, codified by *ptsH*) to a substrate-specific Enzyme II (EII) complex. The galactitol-specific transporter of *E. coli* (EII^{gat} complex) consists of two cytoplasmic polypeptide chains, GatA (IIA^{gat}) and GatB (IIB^{gat}), and a transmembrane protein GatC (IIC^{gat}) [130, 131]. Galactitol is generated to galactitol 1-phosphate (Gat1P) during the transport by EII^{gat} and converted into D-tagatose 6-phosphate (Tag6P) by GatD. In further metabolism, Tag6P is converted to D-tagatose 1, 6-bisphosphate (TagBP) by the phosphofructokinase I (PfkA), and then the TagBP is degraded by the TagBP aldolases GatYZ and KbaYZ [132, 133, 134, 135]. In presented data, the general proteins as EI, HPr, and PfkA were not significantly changed, however, five of the six quantified galactitol-specific PTS and degradation related proteins were significantly up-regulated in *Δefp* strain (Table 12). The Kba proteins were not identified in these experiments.

Table 12. Changes in galactitol transport and catabolism related proteins from control to *Δefp* strain.

Gene name	Exp_1 Fold	Exp_2 Fold	Exp_1 significant	Exp_2 significant	Annotation
gatA	0.57	0.65			Galactitol-specific enzyme IIA component of PTS
gatB	1.45	1.63	+	+	Galactitol-specific enzyme IIB component of PTS
gatC	4.74	5.24	+	+	Galactitol-specific enzyme IIC component of PTS
gatD	2.87	3.36	+	+	Galactitol-1-phosphate dehydrogenase, Zn-dependent and NAD(P)-binding
gatY	0.71	0.84	+	+	D-tagatose 1,6-bisphosphate aldolase 2, catalytic subunit
gatZ	1.37	1.57	+	+	D-tagatose 1,6-bisphosphate aldolase 2, subunit
pfkA	-0.16	-0.28			ATP-dependent 6-phosphofructokinase isozyme 1
ptsH	0.01	0.05			Phosphohistidinoprotein-hexose phosphotransferase component of PTS system (Hpr)
ptsI	-0.19	-0.26			PEP-protein phosphotransferase of PTS system (enzyme I)

Other significantly up-regulated proteins (Table S1) are involved in amino acids biosynthesis (mainly related to Asn), carbon and energy metabolism (related to the pathways of NAD biosynthesis, glycerol degradation, D-amino acids degradation, and oxidative phosphorylation), sulfur-containing compounds transport and metabolism.

The significantly down-regulated proteins are involved in amino acids biosynthesis, protein synthesis, iron uptake, and Fe-S cluster assembly.

The biosynthetic pathways related amino acids include His, aromatic amino acids (Phe, Tyr, and Trp), and branched-china amino acids (Leu, Ile, and Val) (Table 13).

Table 13. Significantly down-regulated amino acids biosynthesis related proteins in *Δefp* strain *vs.* control strain.

Gene name	Exp_1 Fold	Exp_2 Fold	Annotation	Related amino acid
hisA	-0.80	-0.90	N-(5'-phospho-L-ribosyl-formimino)-5-amino-1-(5'-phosphoribosyl)-4-imidazolecarboxamide isomerase	His
hisB	-1.47	-1.78	Histidinol-phosphatase and imidazoleglycerol-phosphate dehydratase	His
hisH	-1.22	-1.41	Imidazole glycerol phosphate synthase, glutamine amidotransferase subunit	His
aroC	-0.85	-1.03	Chorismate synthase	Phe, Tyr, and Trp
aroF	-1.79	-2.00	3-deoxy-D-arabino-heptulosonate-7-phosphate synthase, tyrosine-repressible	Phe, Tyr, and Trp
trpA	-0.96	-1.14	Tryptophan synthase, alpha subunit	Phe, Tyr, and Trp
trpE	-1.18	-1.26	Component I of anthranilate synthase	Phe, Tyr, and Trp
trpGD	-0.82	-0.97	Fused glutamine amidotransferase (component II) of anthranilate synthase/anthranilate phosphoribosyl transferase	Phe, Tyr, and Trp

tyrA	-1.31	-1.76	Fused chorismate mutase T/prephenate dehydrogenase	Phe, Tyr, and Trp
ilvC	-1.11	-1.30	Ketol-acid reductoisomerase (NADP(+))	Val, Leu, and Ile
ilvN	-1.06	-1.17	Acetolactate synthase isozyme 1 small subunit	Val, Leu, and Ile

The extremely decreased levels of proteins involved in protein synthesis include transcription factors, translation factors, proteins related to mRNA degradation and aminoacyl-tRNA biosynthesis, and ribosome (Table 14).

Table 14. Significantly down-regulated protein synthesis related proteins in *Δefp* strain *vs.* control strain.

Gene name	Exp_1 Fold	Exp_2 Fold	Annotation
fnr	-2.09	-3.11	Oxygen-sensing anaerobic growth regulon transcriptional regulator
ettA	-2.61	-3.05	Energy-dependent translational throttle protein A
lepA	-1.24	-1.43	Back-translocating elongation factor EF4, gtpase
rnb	-1.70	-1.92	Ribonuclease II
rpsQ	-0.79	-0.94	30S ribosomal subunit protein S17
rpsR	-1.00	-1.08	30S ribosomal subunit protein S18
valS	-1.25	-1.41	Valyl-tRNA synthetase

Nearly a quarter of the significantly down-regulated proteins in *Δefp* strain compared to the control strain is involved in iron uptake, transport, and Fe-S cluster assembly (Table 15).

In the data, a number of independent iron uptake systems related proteins were quantified. These proteins are involved in ferrous (Fe^{2+}) permeases [136] such as the GTP-binding transporter FeoB [137], broad substrate specificity divalent cations transporter MntH [138]. The transport of ferric iron (Fe^{3+}) utilizes siderophore, which is a kind of high-affinity extracellular ferric-chelators [139]. Ferri-siderophore complexes are taken up by specific outer-membrane receptors, the known siderophore receptors of *E. coli* are six proteins, such as Cir, FecA, FepA, FhuA, FhuE, and Fiu. Except for FecA, other five proteins were quantified in my experiments, and all of these five proteins were repressed in *Δefp* strain, and four of them were significantly down-regulated (Table 16). The up taking processes of ferri-siderophore are mediated by the energy transducing system of TonB-ExbB-ExbD [140, 141]. All of the three components of TonB-ExbB-ExbD system were significantly down-regulated in *Δefp* strain (Table 17). The transport of ferri-siderophore performed by three periplasmic-binding protein dependent ABC-transporter systems, FecBCDF, FepBCDG, and FhuBCD [142]. FepBCDG is the only quantified system in my experiments, only the two components FepB and FepD are detected, and both of these two proteins were extremely repressed in *Δefp* strain. All of FepA and FepBCDG are involved in the ferri-enterobactin transport system.

Enterobactin is known as one of the most efficient ferric iron chelating compounds. Enterobactin is biosynthesized from the precursor chorismate by the enzymes encoded by six genes of *entA* to *–F*, and secreted by the cells. The complex of ferri-enterobactin is transported back into the cells by the transport system encoded by *fepABCDG* [143, 144, 145]. Five of the biosynthetic enzymes and three of the transporter related proteins were quantified and all of them were significantly down-regulated in *Δefp* strain (Table 15). In addition, the EntH plays a proofreading role during enterobactin biosynthesis in vivo [146]. The expression of EntH was also decreased in *Δefp* strain (Table 15).

Table 15. Significantly down-regulated iron uptake, transport, and storage related proteins in *Δefp* strain compared to control strain.

Gene name	Exp_1 Fold	Exp_2 Fold	Annotation
cirA	-3.58	-4.02	Colicin IA outer membrane receptor and translocator; Ferric iron-catecholate transporter
entA	-2.16	-2.21	2,3-dihydro-2,3-dihydroxybenzoate dehydrogenase
entB	-2.57	-3.00	Enterobactin synthase multienzyme complex component B
entC	-2.25	-2.53	Isochorismate synthase
entE	-1.89	-2.53	Enterobactin synthase multienzyme complex component E
entF	-3.06	-3.61	Enterobactin synthase multienzyme complex component F, ATP-dependent
entH	-2.61	-3.05	Proofreading thioesterase
exbB	-1.03	-1.30	Membrane spanning protein in tonb-exbb-exbd complex
exbD	-1.24	-1.36	Membrane spanning protein in tonb-exbb-exbd complex
fecR	-2.39	-2.69	Anti-sigma transmembrane signal transducer for ferric citrate transport; Periplasmic feca-bound ferric citrate sensor and cytoplasmic feci ECF sigma factor activator
feoB	-1.78	-1.98	Ferrous iron transporter protein B and GTP-binding protein; membrane protein
fepA	-3.45	-3.25	Ferrienterobactin outer membrane transporter
fepB	-1.38	-1.16	Ferrienterobactin-binding periplasmic protein
fepD	-1.04	-1.25	Ferric enterobactin transport system permease protein
fhuE	-3.44	-3.40	Ferric-rhodotorulic acid outer membrane transporter
fiu	-4.41	-4.25	Catecholate siderophore receptor
mntH	-2.90	-3.77	Divalent metal cation transporter
iscR	-1.11	-1.16	Isc operon transcriptional repressor; Suf operon transcriptional activator; Oxidative stress- and iron starvation-inducible; autorepressor
sufA	-1.43	-1.78	Fe-S cluster assembly protein
sufC	-1.32	-1.73	Sufbcd Fe-S cluster assembly scaffold protein, ATP-binding protein
sufD	-1.34	-1.61	Component of sufbcd Fe-S cluster assembly scaffold
sufE	-1.59	-1.76	Sulfur acceptor protein
sufS	-2.43	-2.47	Cysteine desulfurase, stimulated by sufe; Selenocysteine lyase, PLP-dependent

As a transition metal, iron plays an essential role as a cofactor for multiple biochemical reactions. Iron-sulfur (Fe-S) clusters are widely present in various organisms. Fe-S clusters play roles as electron transfer and gene regulator for both of transcription and translation. And Fe-S clusters are also required for many cellular redox and non-redox catalytic processes [147]. In *E. coli*, the iron-sulfur cluster (ISC) system and the sulfur mobilization (SUF) system are two major identified coordinate assembly pathways of Fe-S cluster. IscS and SufS are core components of these two systems, respectively. IscS is a housekeeping L-Cys desulfurase. With the interaction of IscS and its scaffold proteins IscU and IscA, the iron and sulfur are assembled to form [2Fe-2S] or [4Fe-4S] clusters [148]. The SUF pathway is encoded by the *sufABCDSE* operon [149]. The transcriptional regulator IscR plays a role as a repressor in ISC, but plays an activator role in SUF system [150]. ISC and SUF are both overlapped and divergent in function. Both systems are induced by oxidative stress and iron starvation. ISC is mainly regulated by the IscR repressor [151], but SUF is regulated by OxyR and Fur under the stress of hydrogen peroxide and iron starvation, respectively. The roles of ISC and SUF system are differed under iron starvation. SUF system is more sensitive for the limitation of iron [152, 153, 154]. In addition, there is a third Fe-S assembly system, CSD, which consists of CsdA and CsdE (formerly named YgdK) [155].

In the data of comparison between *Δefp* and control strain, the ISC and CSD systems related proteins and the SUF related regulator OxyR and Fur were not significantly changed, however, the SUF system proteins and IscR are significantly suppressed in *Δefp* strain (Table 18).

Table 16. Changes of ferri-siderophore outer-membrane receptors from control to *Δefp* strain.

Gene name	Exp_1 Fold	Exp_2 Fold	Exp_1 significant	Exp_2 significant	Annotation
cirA	-3.58	-4.02	+	+	Colicin IA outer membrane receptor and translocator; ferric iron-catecholate transporter
fepA	-3.45	-3.25	+	+	Ferrienterobactin outer membrane transporter
fhuA	-0.72	-0.76			Ferrichrome outer membrane transporter
fhuE	-3.44	-3.40	+	+	Ferric-rhodotorulic acid outer membrane transporter
fiu	-4.41	-4.25	+	+	Catecholate siderophore receptor

Table 17. Changes of TonB-ExbB-ExbD system expression from control to Δefp strain.

Gene name	Exp_1 Fold	Exp_2 Fold	Exp_1 significant	Exp_2 significant	Annotation
tonB	-0.70	-0.96		+	Membrane spanning protein in tonb-exbb-exbd complex
exbB	-1.03	-1.30	+	+	Membrane spanning protein in tonb-exbb-exbd complex
exbD	-1.24	-1.36	+	+	Membrane spanning protein in tonb-exbb-exbd complex

Table 18. Changes of Fe-S assembly systems related proteins from control to *Δefp* strain.

Gene name	Exp1 Fold	Exp2 Fold	Exp1 significant	Exp2 significant	Annotation
CSD pathway					
csdE	0.11	0.15			Csda-binding activator; Fe-S protein
ISC pathway					
iscA	0.64	0.66	+		Fes cluster assembly protein
iscS	0.39	0.30			Cysteine desulfurase (trna sulfurtransferase), PLP-dependent
iscU	0.24	0.32			Iron-sulfur cluster assembly scaffold protein
fdx	0.31	0.34			[2Fe-2S] ferredoxin
hscA	-0.08	0.30			Dnak-like molecular chaperone specific for iscu
ISC repressor, SUF activator					
iscR	-1.11	-1.16	+	+	Isc operon transcriptional repressor; Suf operon transcriptional activator; Oxidative stress- and iron starvation-inducible; Auto-repressor
SUF pathway					
sufA	-1.43	-1.78	+	+	Fe-S cluster assembly protein
sufC	-1.32	-1.73	+	+	Sufbcd Fe-S cluster assembly scaffold protein, ATP-binding protein
sufD	-1.34	-1.61	+	+	Component of sufbcd Fe-S cluster assembly scaffold
sufE	-1.59	-1.76	+	+	Sulfur acceptor protein
sufS	-2.43	-2.47	+	+	Cysteine desulfurase, stimulated by sufe; Selenocysteine lyase, PLP-dependent
fur	0.10	0.02			Ferric uptake regulation protein
oxyR	0.19	0.02			Oxidative and nitrosative stress transcriptional regulator

The majority of previous reports [29, 30, 32] about EF-P are focused on the rescuing of translation stalling caused by consecutive Pro stretches. In this study, our focus on the global effects of *efp* KO on the expression of consecutive Pro containing proteins. There are 452 two or more consecutive Pro (PP) containing proteins were detected in two biological replicates of the experiments. Among all these PP containing proteins, 43 of them were significantly down-regulated, and 20 proteins were significantly up-regulated, the remaining 86% PP containing proteins were not significantly changed. There are 94 possible polyproline (PPP)-containing proteins in *E. coli* K12 MG1566 strain, 26 of them were quantified in both replicates. In these quantified PPP-containing proteins, seven of them were significantly down-regulated, the remaining proteins were not significantly changed (Figure 34). The functions of these PPP containing proteins could refer to Table S3.

Gene name	Exp1 Fold	Exp2 Fold	Exp1 significant	Exp2 significant
entF	-3.06	-3.61	+	+
valS	-1.25	-1.41	+	+
rnb	-1.70	-1.92	+	+
lepA	-1.24	-1.43	+	+
ycgR	-1.73	-1.91	+	+
qorA	-1.39	-1.35	+	+
tonB	-0.70	-0.96		+
ftsK	-0.29	-0.41		
gltB	-0.15	-0.09		
katE	0.05	0.03		
mrcA	0.51	0.46		
ppc	-0.27	-0.40		
nuoC	0.37	0.31		
uvrB	-0.73	-0.59		
nlpD	0.25	0.33		
cyoB	0.11	0.11		
agp	0.06	0.10		
dppF	-0.62	-0.82		
hisD	-0.25	-0.26		
clsA	-0.07	-0.06		
rsmA	0.24	0.20		
yhbW	0.06	0.30		
ydiK	0.06	0.23		
sdaC	-0.08	-0.34		
nudC	-0.16	-0.18		
ycgL	0.37	0.43		

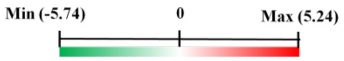

Figure 34. Heat map shows the up (red) and down-regulations (green) of PPP-containing proteins from control strain to *Δefp* strain.

The significantly down-regulated proteins include valyl-tRNA synthetase (ValS), ribonuclease II (Rnb), back-translocating elongation factor EF4 (LepA), and flagellar velocity braking protein (YcgR). The regulation of these four proteins agrees with the previous report of Lauri Peil, et al [32]. Apart from these four proteins, the down-regulation of PPP-containing proteins is also involved in the quinone oxidoreductase (QorA), and the two mentioned above iron metabolism related EntF and TonB.

Summary

The absence of EF-P greatly slows down the growth and reduces the maximal cells number of *E. coli*, correspondingly leading to significant changes at the proteome level.

The highlight regulations include the increase of the pathways of galactitol transport and catabolism, repression of biosynthesis of amino acids and proteins, and the decrease of iron metabolism. As a non-major carbon and energy source, the effect that is caused by changes of galactitol metabolism is unknown. The remarkable down-regulation of amino acids and proteins synthesis coincides with the low growth rate of *Δefp* strain. The tremendous repression of enterobactin biosynthesis, ferri-enterobactin transport, and SUF Fe-S assembly pathway related proteins demonstrates that the lack of EF-P critically impacts on the iron take-up and storage in *E. coli*. And considering the important roles iron plays in various intracellular biochemical reactions as cofactors, the deletion of *efp* indirectly affects a large number of biological processes.

The data about PP-containing proteins reveals that the expression of majority these proteins were not affected by the lack of EF-P. Only approximately 10% of the quantified PP-containing proteins were obviously repressed, and there are even around 5% of them were significantly increased.

A part of the data on PPP-containing proteins is agreement with the previous publication by Lauri Peil, et al. [32]. However, it is worth noting that Lauri Peil's experiments employed MOPS medium, which contains normal doses of iron. On the contrary, I used the M9 minimal medium without additional iron. These results indicate that independently of the used medium (M9 or MOPS) four PPP-containing proteins, ValS, Rnb, LepA, and YcgR are stably inhibited by the lack of EF-P. In addition, EntF was not mentioned in Lauri Peil's work, while my results demonstrate that EntF as a PPP-containing protein was significantly down-regulated in the absence of EF-P in the iron limited M9 medium.

2.2.4 Proteome comparisons of the adapted *Δefp* strains and the *Δefp* strain

Two strains have been adapted from an EF-P KO strain in two parallel experiments by means of a GM3 device (see method 5.2). After about 40 days continuous cultivation, the initial generation time of EF-P KO strain reduced approximately 40% and stayed at a plateau in the following 60 days (Figure 35). The evolution of EF-P KO strain is taken twice the time than the wild type strain (~20 days). To study the proteome changes of the adapted strains from the EF-P KO strain by SILAC-based MS measurement, two auxotrophic strains for Arg and Lys have been constructed, they were named as *E. coli* BU165 and *E. coli* BU166 in our lab database, here we will refer to name them as *Δefp* Evo-1 and *Δefp* Evo-2.

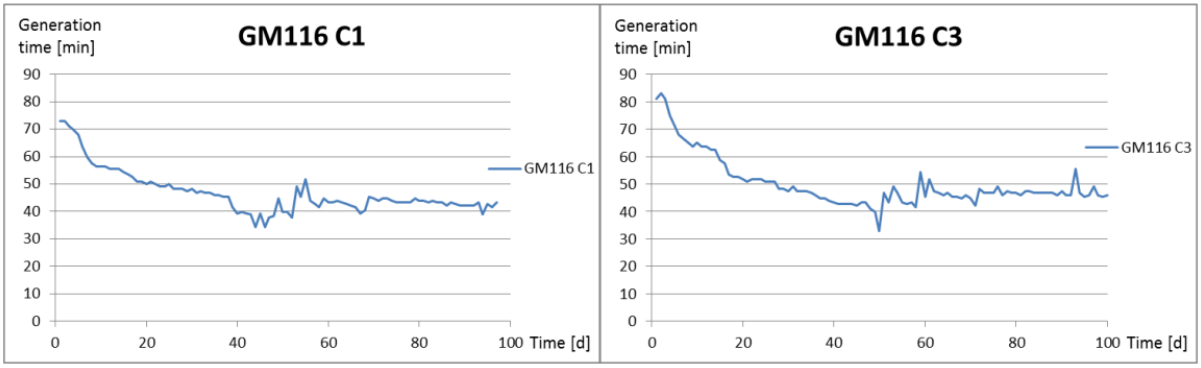

Figure 35. Automated evolution of EF-P KO strain in two parallel GM3 turbidostat evolution devices at OD600 0.8 E. Left: Generation time of the culture in chamber C1. Right: Generation time of the culture in chamber C3. Sharp peaks down are a sign for bottle changes and sharp peaks up for occurring biofilm in the cultivation chambers. (Reference: Christian Schipp has done, but not published yet)

Δefp Evo-1 and *Δefp* Evo-2 were adapted with *argA* and *lysA* deletion. In order to see how the genes deletion influences the proteome dynamics, therefore, other two strains were adapted without the two genes deletion. These two adapted strains were named as *E. coli* BU167 and *E. coli* BU168 in our lab database, and sequentially referred as *Δefp* Evo-3 and *Δefp* Evo-4 in the following.

To characterize the proteome changes of the adapted EF-P KO strains, SILAC-based mass spectrometry experiments were performed. The comparisons between the four adapted *Δefp* strains to the *Δefp* strain will be represented as *Δefp* Evo1, *Δefp* Evo2, *Δefp* Evo3, and *Δefp* Evo4 below. Each comparison has been done two biological replicates where the SILAC labels have been swapped to avoid any source of artifacts due to the technique.

In the total of the four comparisons, 1683 proteins were quantified in all experiments. If an average of the two replicates is considered, there are then 1198 proteins which could be quantified for each adapted *Δefp* strain relative to the *Δefp* counterpart. Figure 36A-D displays observed protein ratios in histograms depicting the expected normal distribution of these values. Notably, strain *Δefp* Evo-1 shows a similar behavior as *Δefp* Evo-3 and *Δefp* Evo-4 strains, while the distribution of *Δefp* Evo-2 seems to be broader with a clear shift to the negative values. The correlation coefficient between the two biological replicates

for each comparison of adapted *Δefp* strains to the *Δefp* strain ranged between 0.62 and 0.76 (Figure 36E-H), suggesting consistent changes of the proteome during the evolution process in all biological replicates.

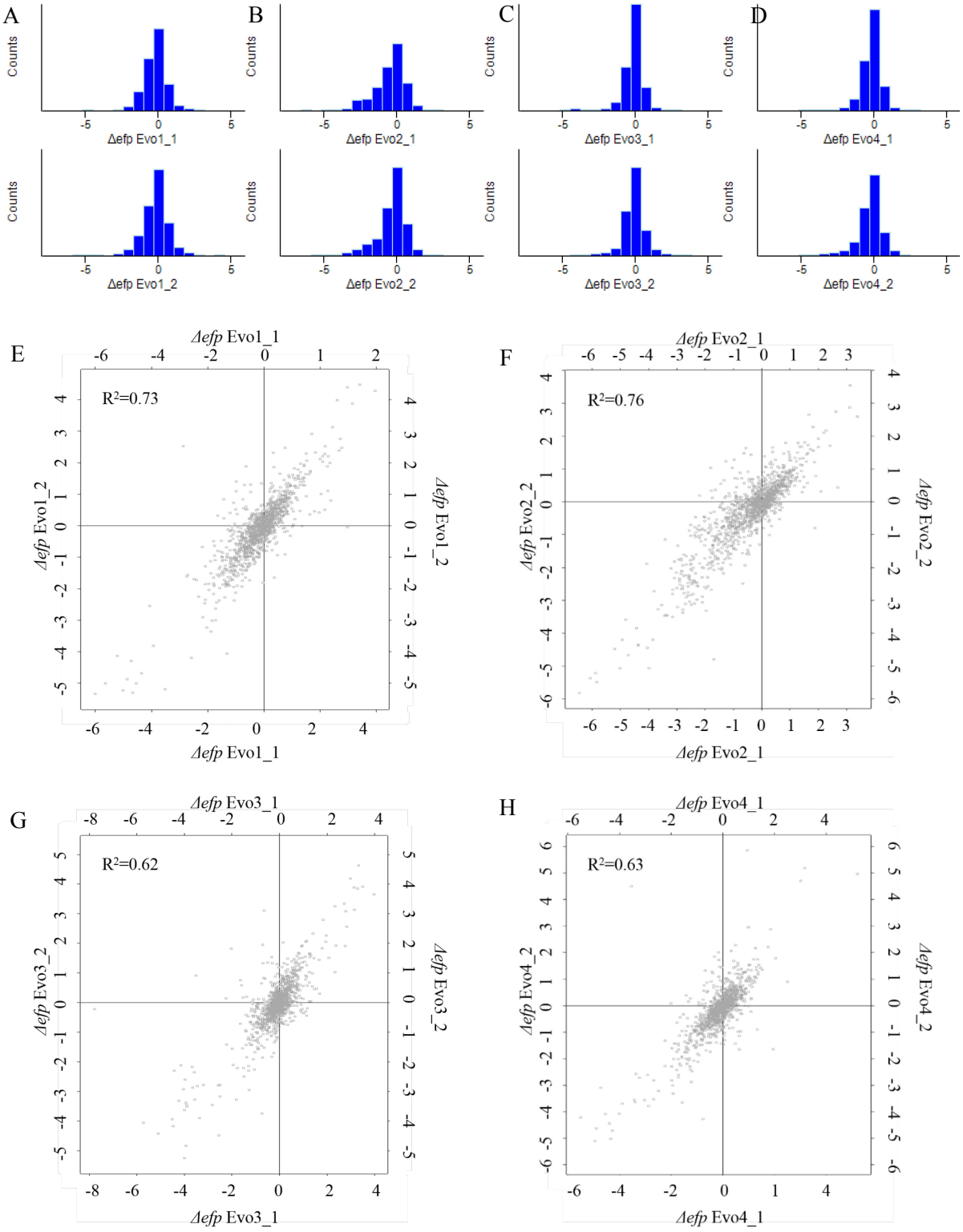

Figure 36. The proteome changed ratios of each adapted *Δefp* strains that distribute as the histograms (A. *Δefp* Evo1, B. *Δefp* Evo2, C. *Δefp* Evo3, and D. *Δefp* Evo4). And the two replicates for each comparisons correlate as the Scatter plot graphs shown (E. *Δefp* Evo1, F. *Δefp* Evo2, G. *Δefp* Evo3, and H. *Δefp* Evo4).

A

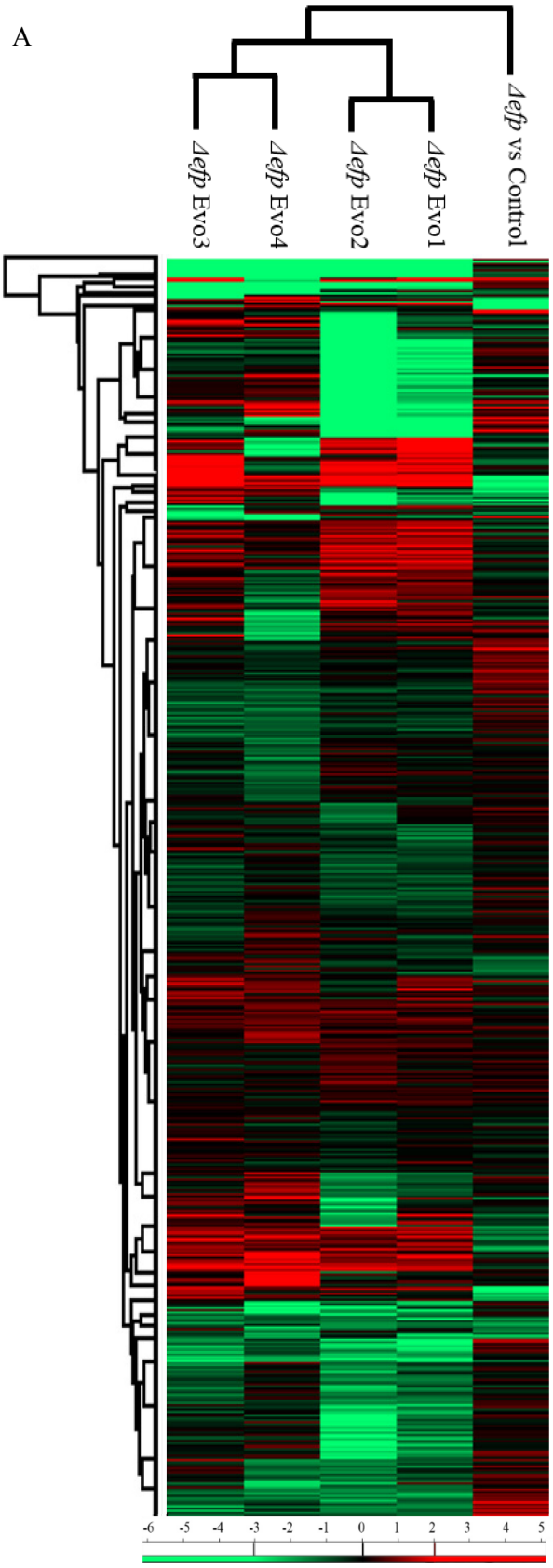

B

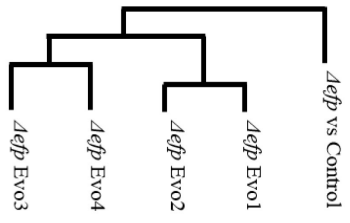

Gene name	*Δefp* Evo3 Fold	*Δefp* Evo4 Fold	*Δefp* Evo1 Fold	*Δefp* Evo2 Fold	*Δefp* vs Control
nanA	0.05	0.44	1.09	2.04	0.31
yciF	0.07	-1.20	1.66	1.13	
yghA	0.36	0.15	1.80	1.25	
aroG	-0.06	0.34	-1.58	-2.73	-0.21
aroH	-0.47	-0.22	-2.27	-3.37	-0.47
asnA	-0.20	-0.74	-2.62	-3.24	1.36
cysC	-0.73	-0.34	-2.06	-3.27	0.82
deaD	-0.75	0.32	-1.83	-3.45	-0.18
epd	0.28	0.46	-1.80	-2.71	-1.21
leuC	0.03	0.06	-2.17	-2.74	-0.08
miaB	-0.53	-0.39	-2.43	-2.70	1.03
mreB	-0.49	0.26	-1.97	-3.47	0.28
pepB	-0.38	-0.26	-1.57	-2.74	-0.06
ptsP	-0.67	-0.49	-1.78	-2.66	0.13
rapA	0.18	0.19	-1.60	-2.79	-0.44
rho	-0.49	-0.03	-1.97	-2.65	0.15
sbcC	-0.21	0.24	-1.81	-3.35	1.12
tyrR	-0.05	0.02	-1.59	-3.09	0.22
ubiE	0.15	0.33	-1.64	-2.72	0.34
uvrC	-0.27	0.24	-2.55	-2.80	-0.19
wbbI	-0.52	0.01	-2.70	-3.44	0.12
ybjX	-0.51	0.10	-2.01	-3.66	0.24
yeaK	-0.45	-0.50	-2.10	-2.58	0.25

C

Gene name	*Δefp* Evo3 Fold	*Δefp* Evo4 Fold	*Δefp* Evo1 Fold	*Δefp* Evo2 Fold	*Δefp* vs Control
fiu	1.23	1.97	0.81	0.52	-4.33
hslU	0.98	1.44	0.85	0.96	-0.44
hslV	1.06	1.43	0.72	0.69	-0.16
yghJ	1.24	0.92	0.58	0.45	-0.22
flgE	-1.89	-2.11	-0.53	0.53	-0.40
flgH	-3.70	-2.00	-0.08	-0.38	-0.12
fliL	-4.62	-1.75	-0.92	-1.33	-0.59
fliM	-2.92	-2.04	-1.13	-1.95	-0.63
fliN	-4.89	-1.74	0.31	-0.03	-0.61
carA	-1.62	-2.16	-1.14	-0.95	-0.16
carB	-1.86	-2.22	-1.23	-1.02	-0.09
pyrD	-1.21	-1.84	-0.93	-0.94	0.01
pyrF	-1.13	-1.64	-0.92	-0.90	0.17
aceB	-1.08	-1.94	-0.01	-0.06	-0.25
bioA	-1.57	-1.27	-1.54	-2.35	-0.42
codA	-1.99	-2.62	-1.54	-1.49	0.31
hdhA	-1.08	-1.51	-0.21	-1.50	0.11
modA	-2.11	-1.78	-0.45	-1.11	-0.78
pstS	-1.35	-1.69	-0.94	-0.56	0.98
sbp	-2.54	-2.48	-0.96	-1.21	1.23
upp	-1.72	-1.83	-1.36	-1.50	0.40

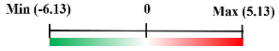

Figure 37. A. Heat map shows the hierarchical clustering of all quantified proteins that are up- (red) and down- (green) regulated in the comparisons of *Δefp* vs control, *Δefp* Evo1, *Δefp* Evo2, *Δefp* Evo3, and *Δefp* Evo4. B. The proteins that are only significantly changed in *Δefp* Evo1 and *Δefp* Evo2. C, Proteins that are only significantly changed in *Δefp* Evo3 and *Δefp* Evo4. The gray squares represent the unidentified value.

In the overall proteomics data, it is noteworthy that a large number of proteins were significantly down-regulated in the adapted *Δefp* strains, while only a few of proteins were significantly up-regulated after the evolution of the culture (Figure 37A). There are a certain number of different regulations between the evolution with (*Δefp* Evo1 and *Δefp* Evo2) and without (*Δefp* Evo3 and *Δefp* Evo4) *argA* and *lysA* genes. Among of these differences, 23 proteins are only significantly regulated in *Δefp* Evo1 and *Δefp* Evo2 (Figure 37B), three of these proteins are up-regulated, and the remaining 20 proteins are down-regulated, these proteins are mainly involved in amino acids biosynthesis and transcription, but no clear interaction between each other. On the other side, 21 proteins are only significantly regulated in *Δefp* Evo3 and *Δefp* Evo4 (Figure 37C), the regulation of these proteins in *Δefp* Evo1 and *Δefp* Evo2 show similar trend but in lower extent, these proteins are adapted in flagellar assembly and pyrimidine biosynthesis via *de novo* pathway, and show clear interactions (Figure 38). It is indicated that the down-regulations of these two groups of proteins reverted at a certain extent during the deletion of *argA* and *lysA* after the evolution.

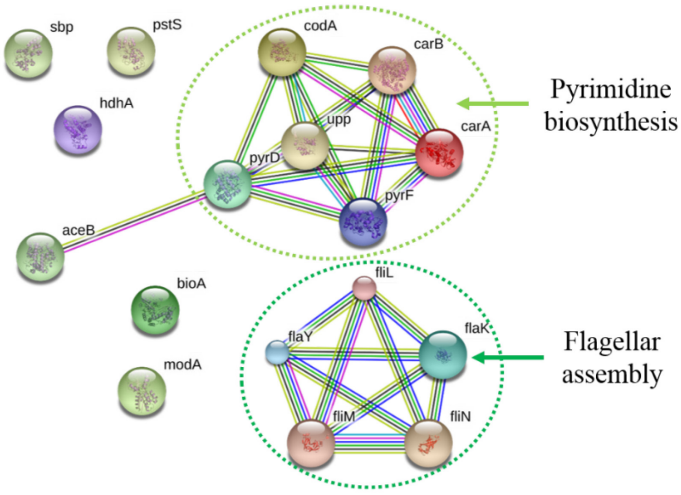

Figure 38. Interaction of the only significantly down-regulated proteins in *Δefp* Evo3 and *Δefp* Evo4.

From the proteomics data analysis, it became apparent that there are five proteins significantly up-regulated in all of the four adapted *Δefp* strains. A conserved protein encoded by the *yeeN* gene which belongs to some uncharacterized proteins family UPF0082 and probably functions as a transcriptional regulator [156], the 3'(2'),5'-bisphosphate nucleotidase CysQ by which the 3'(2')-phosphoadenosine 5'-phosphate (PAP) is converted to AMP, the oligopeptidase PrlC, *de novo* biosynthesis of UMP protein PyrE, and a Fe-S cluster assembly protein SufA. CysQ and SufA were significantly down-regulated in the *Δefp* strain compared to control strain (see section 2.2.3). In addition, 18 proteins were significantly up-regulated in at least two of the four adapted *Δefp* strains (Figure 39), the functions of these proteins were described in Table S4. The major of these proteins are involved in the iron metabolism, but also include an ATP-dependent protease complex HslVU [157], and several uncharacterized proteins. The HslVU protease is known to plays an important role in the regulation of *E. coli* cells division through

degrading the cell division inhibitor SulA [158, 159, 160, 161]. These proteins showed to be significantly up-regulated in the adapted *Δefp* strains relative to the *Δefp* strain.

Gene name	*Δefp* vs Control Fold	*Δefp* Evo1 Fold	*Δefp* Evo2 Fold	*Δefp* Evo3 Fold	*Δefp* Evo4 Fold	*Δefp* vs Control significant	*Δefp* Evo1 significant	*Δefp* Evo2 significant	*Δefp* Evo3 significant	*Δefp* Evo4 significant
cysQ	-1.82	2.74	2.23	1.79	1.07	+	+	+	+	+
prlC	-0.36	1.56	1.14	2.32	0.97		+	+	+	+
pyrE		2.62	2.68	3.51	1.39		+	+	+	+
sufA	-1.73	1.48	1.53	1.41	1.19	+	+	+	+	+
yeeN		2.53	2.15	3.98	2.36		+	+	+	+
argB		1.41	1.06	0.03	1.84		+	+		+
ghrB	-0.10	1.34	1.24	1.87	0.26		+	+	+	
grcA	-4.83	1.09	1.40	1.81	0.56	+	+	+	+	
malE	0.37	1.52	1.51	2.06	0.15		+	+	+	
qorA	-1.38	2.14	1.96	1.56	0.06	+	+	+	+	
sufS	-2.45	2.25	2.06	1.46	0.75	+	+	+	+	
valS	-1.32	1.61	1.65	1.47	0.64	+	+	+	+	
yhjJ	0.26	1.29	1.39	1.61	0.31		+	+	+	
argH	-0.26	1.36	1.13	0.69	0.70		+	+		
bcsG	-0.63	1.34	0.49	2.11	0.11		+		+	
fiu	-4.33	0.81	0.52	1.23	1.97	+			+	+
hslU	-0.44	0.85	0.96	0.98	1.44				+	+
hslV	-0.16	0.72	0.69	1.06	1.43				+	+
malP	-0.39	1.34	0.81	1.40	0.31		+		+	
nanA	0.31	1.09	2.04	0.05	0.44		+	+		
yghA		1.80	1.25	0.36	0.15		+	+		
yghJ	-0.22	0.58	0.45	1.24	0.92				+	+
yjjU		1.32	0.74	3.04	0.59		+		+	

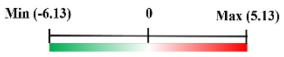

Figure 39. Heat map shows the proteins that are significantly up-regulated in at least two adapted *Δefp* strains. The gray squares represent the unidentified value.

Among the significantly changed proteins, 50 proteins are significantly down-regulated in at least two adapted *Δefp* strains (Figure 40). These proteins are mainly involved in pyrimidine biosynthesis (Figure 41) and chemotaxis and flagellar assembly machinery (Figure 42). Among the chemotaxis and cell movement related proteins, both the quantified receptor signaling complex and flagellar motor controller are significantly down-regulated in all adapted *Δefp* strains. However, as it has been mentioned above that the proteins related to flagellar assembly and the pyrimidine biosynthesis primarily for the *de novo* route of UMP are not down-regulated in *Δefp* Evo-1 and -2 as significantly as in *Δefp* Evo-3 and -4 strains (Figure 37C). It should be recollected that *Δefp* Evo-1 and -2 strains are adapted without deletions of *argA* and *lysA*. These results suggest that the switching off intracellular biosynthesis of Arg and Lys has an impact on flagellar assembly and *de novo* synthesis of UMP pathway during the evolution.

Gene name	*Δefp* vs Control Fold	*Δefp* Evo1 Fold	*Δefp* Evo2 Fold	*Δefp* Evo3 Fold	*Δefp* Evo4 Fold	*Δefp* vs Control significant	*Δefp* Evo1 significant	*Δefp* Evo2 significant	*Δefp* Evo3 significant	*Δefp* Evo4 significant
cheA	-0.57	-3.88	-4.38	-2.99	-3.48		+	+	+	+
cheW	-0.26	-5.67	-6.13	-4.38	-4.76		+	+	+	+
cheY	-0.02	-4.87	-4.25	-3.26	-5.03		+	+	+	+
cheZ	-0.39	-3.39	-3.42	-3.14	-5.78		+	+	+	+
dcyD	0.35	-4.44	-4.33	-2.97	-3.10		+	+	+	+
fliA	0.56	-4.36	-4.53	-3.28	-1.97		+	+	+	+
fliC	-0.45	-4.98	-5.55	-3.77	-4.86		+	+	+	+
fliY	0.34	-5.33	-5.72	-4.22	-4.41		+	+	+	+
mgtA	0.83	-3.15	-3.60	-3.68	-2.14	+	+	+	+	+
pyrB	0.31	-4.77	-5.05	-4.32	-4.49		+	+	+	+
pyrI	0.31	-5.13	-5.66	-4.75	-4.68		+	+	+	+
tap	0.08	-4.51	-4.69	-3.13	-3.91		+	+	+	+
tar	-0.39	-4.68	-4.36	-3.42	-4.05		+	+	+	+
tsr	-0.65	-4.53	-4.84	-3.49	-4.31		+	+	+	+
ycgR	-1.81	-3.31	-4.20	-2.68	-3.29	+	+	+	+	+
yecC	0.35	-2.46	-4.39	-3.37	-2.71		+	+	+	+
aceA	-0.15	-0.79	-2.59	-1.23	-2.11			+	+	+
bfr	1.29	-1.70	-2.45	-1.79	-2.61	+	+		+	+
bioD1	0.41	-1.72	-2.97	-0.45	-1.30		+	+		+
cysD	0.43	-2.28	-3.40	-1.11	-0.47		+	+	+	
cysN	0.56	-2.55	-4.03	-1.12	-0.71		+	+	+	
fimC	0.95	-1.67	-1.86	-1.18	-1.40	+	+		+	+
ridA	0.36	-2.00	-1.88	-2.02	-2.86		+		+	+
uspG	1.04	-2.22	-3.33	-0.62	-1.78	+	+	+		+
aceB	-0.25	-0.01	-0.06	-1.08	-1.94				+	+
aroH	-0.47	-2.27	-3.37	-0.47	-0.22		+	+		
asnA	1.36	-2.62	-3.24	-0.20	-0.74	+	+	+		
bioA	-0.42	-1.54	-2.35	-1.57	-1.27				+	+
carA	-0.16	-1.14	-0.95	-1.62	-2.16				+	+
carB	-0.09	-1.23	-1.02	-1.86	-2.22				+	+
codA	0.31	-1.54	-1.49	-1.99	-2.62				+	+
cysC	0.82	-2.06	-3.27	-0.73	-0.34	+	+	+		
fis	-0.11	-1.57	-1.25	-1.32	-0.09		+		+	
flgH	-0.12	-0.08	-0.38	-3.70	-2.00				+	+
fliL	-0.59	-0.92	-1.33	-4.62	-1.75				+	+
fliM	-0.63	-1.13	-1.95	-2.92	-2.04				+	+
hdhA	0.11	-0.21	-1.50	-1.08	-1.51				+	+
lipA	2.01	-2.18	-2.28	-1.30	-0.62	+	+		+	
miaB	1.03	-2.43	-2.70	-0.53	-0.39	+	+	+		
modA	-0.78	-0.45	-1.11	-2.11	-1.78				+	+
ompF	-0.75	-2.14	-1.00	-1.77	-1.12		+		+	
pepB	-0.06	-1.57	-2.74	-0.38	-0.26		+	+		
pstS	0.98	-0.94	-0.56	-1.35	-1.69	+			+	+
ptsP	0.13	-1.78	-2.66	-0.67	-0.49		+	+		
pyrD	0.01	-0.93	-0.94	-1.21	-1.84				+	+
pyrF	0.17	-0.92	-0.90	-1.13	-1.64				+	+
rho	0.15	-1.97	-2.65	-0.49	-0.03		+	+		
sbp	1.23	-0.96	-1.21	-2.54	-2.48	+			+	+
upp	0.40	-1.36	-1.50	-1.72	-1.83				+	+
yeaK	0.25	-2.10	-2.58	-0.45	-0.50		+	+		

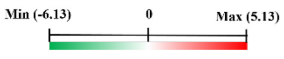

Figure 40. Heat map with comparison of four adapted strains. Note the significantly down-regulated proteins in at least two adapted *Δefp* strains.

Gene name	*Δefp* vs Control Fold	*Δefp* Evo1 Fold	*Δefp* Evo2 Fold	*Δefp* Evo3 Fold	*Δefp* Evo4 Fold	*Δefp* vs Control significant	*Δefp* Evo1 significant	*Δefp* Evo2 significant	*Δefp* Evo3 significant	*Δefp* Evo4 significant
carA	-0.16	-1.14	-0.95	-1.62	-2.16				+	+
carB	-0.09	-1.23	-1.02	-1.86	-2.22				+	+
pyrB	0.31	-4.77	-5.05	-4.32	-4.49		+	+	+	+
pyrC	-1.00	-0.67	-0.86	-0.49	-0.09	+				
pyrD	0.01	-0.93	-0.94	-1.21	-1.84				+	+
pyrE		2.62	2.68	3.51	1.39		+	+	+	+
pyrF	0.17	-0.92	-0.90	-1.13	-1.64				+	+

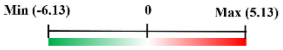

Figure 41. The changes of *de novo* UMP biosynthetic pathway in adapted *Δefp* strains shown in the heat map. Note that the gray squares represent the not identified values.

Gene name	*Δefp* vs Control	*Δefp* Evo1 Fold	*Δefp* Evo2 Fold	*Δefp* Evo3 Fold	*Δefp* Evo4 Fold	*Δefp* vs Control significant	*Δefp* Evo1 significant	*Δefp* Evo2 significant	*Δefp* Evo3 significant	*Δefp* Evo4 significant
cheA	-0.57	-3.88	-4.38	-2.99	-3.48		+	+	+	+
cheW	-0.26	-5.67	-6.13	-4.38	-4.76		+	+	+	+
cheY	-0.02	-4.87	-4.25	-3.26	-5.03		+	+	+	+
cheZ	-0.39	-3.39	-3.42	-3.14	-5.78		+	+	+	+
flgE	-0.40	-0.53	0.53	-1.89	-2.11				+	+
flgH	-0.12	-0.08	-0.38	-3.70	-2.00				+	+
fliC	-0.45	-4.98	-5.55	-3.77	-4.86		+	+	+	+
fliL	-0.59	-0.92	-1.33	-4.62	-1.75				+	+
fliM	-0.63	-1.13	-1.95	-2.92	-2.04				+	+
fliN	-0.61	0.31	-0.03	-4.89	-1.74				+	+
tap	0.08	-4.51	-4.69	-3.13	-3.91		+	+	+	+
tar	-0.39	-4.68	-4.36	-3.42	-4.05		+	+	+	+
tsr	-0.65	-4.53	-4.84	-3.49	-4.31		+	+	+	+
ycgR	-1.81	-3.31	-4.20	-2.68	-3.29	+	+	+	+	+

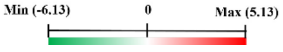

Figure 42. The chemotaxis and flagellar assembly related proteins in adapted *Δefp* strains changed as the heat map shown.

In addition, the iron metabolism related proteins, Fiu, SufA, and SufS are significantly up regulated in the adapted *Δefp* strains, which were significantly down-regulated when *Δefp* strain compared to the control strain. Careful inspection of iron metabolism related proteins as shown in (Figure 43) reveals that the enterobactin biosynthesis and related transport system were not significantly changed after the evolution of the cultures. On the other hand, the iron transport related energy system proteins TonB-ExbB-ExbD increased to a certain extent, but not significant. Finally, for Fe-S cluster assembly, nether the CSD nor the ISC pathways are significantly changed. However, the most interesting observation is

that the SUF system and its activator IscR are significantly up-regulated in the adapted *Δefp* strains compared to the EF-P KO strain.

Gene name	*Δefp* vs Control Fold	*Δefp* Evo1 Fold	*Δefp* Evo2 Fold	*Δefp* Evo3 Fold	*Δefp* Evo4 Fold	*Δefp* vs Control significant	*Δefp* Evo1 significant	*Δefp* Evo2 significant	*Δefp* Evo3 significant	*Δefp* Evo4 significant
Enterobactin biosynthesis										
entA	-2.16	0.44	0.60	0.42	-0.06	+				
entB	-2.76	-1.19	-2.30	0.52	-0.01	+				
entC	-2.35	-0.93	-0.88	0.60	0.32	+				
entE	-2.27	-0.13	-0.10	0.65	-0.09	+				
entF	-3.31	0.53	-0.14	1.05	0.47	+			+	
entH	-2.88	-0.09	-0.37	0.57	0.21	+				
Iron transport system										
fepA	-3.34	-0.18	0.06	-1.04	0.74	+			+	
fepB	-0.99	-0.50	0.03	0.52	0.17	+				
cirA	-3.80	-1.19	-1.30	-0.10	0.91	+				+
fhuA	-0.77	0.06	0.15	0.09	0.50					
fhuE	-3.43	-0.02	-0.21	-0.44	1.06	+				+
fecR	-2.40	-1.03	-1.52	0.60	0.76	+				
feoB	-1.89	-1.16	-2.06	-0.09	0.12	+				
fhuF	-1.31	-1.16	-0.42	0.62	1.72	+				+
fiu	-4.33	0.81	0.52	1.23	1.97	+			+	+
TonB-ExbB-ExbD system										
tonB	-0.85	0.79	0.50	-0.05	0.91	+				+
exbB	-1.17	0.98	1.56	0.16	0.24	+		+		
exbD	-1.27	-0.04	0.04	0.36	0.43	+				
Fe-S assembly systems										
CSD pathway										
csdE	0.11	0.47	0.74	0.27	-0.41					
ISC pathway										
iscA	0.66	-0.64	-0.10	-0.25	0.50	+				
iscS	0.34	-0.99	-0.92	-0.38	-0.06					
iscU	0.28	-0.21	0.03	-0.03	0.39					
fdx	0.36	0.00	0.08	-0.18	-0.06					
hscA	0.36	-1.38	-1.38	-0.23	-0.12					
ISC repressor, SUF activator										
iscR	-1.12	0.99	0.98	0.67	0.97	+				+
SUF pathway										
sufA	-1.73	1.48	1.53	1.41	1.19	+	+	+	+	+
sufB	-1.59	0.81	0.99	0.74	0.52	+				
sufC	-1.63	0.49	0.18	0.83	0.44	+				
sufD	-1.49	0.76	0.83	0.80	0.56	+				
sufE	-1.75	1.17	1.04	0.58	-0.27	+	+	+		
sufS	-2.45	2.25	2.06	1.46	0.75	+	+	+	+	
fur	0.08	-1.11	-0.72	-0.60	0.34					
oxyR	0.11	-0.04	0.15	0.00	-0.37					

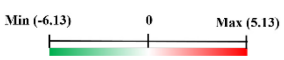

Figure 43. Hat map with some major players of iron physiology in *E. coli*. Note that iron metabolism related proteins in the adapted *Δefp* strains are changed.

Furthermore, the evolution cultures lead to some changes on the levels of proteins containing oligo-proline stretches to different extents. As the Figure 44 shown, 22 PPP-containing proteins were quantified in all the four adapted *Δefp* strains. However, the majority of these proteins are not significantly changed. Nonetheless, we have observed an interesting phenomenon when focusing on the seven significantly down-regulated proteins in the comparison between *Δefp* strain and control strain. First, Rnb and the iron metabolism related proteins, EntF and TonB have increased in the majority of data but at a limited level or even no change in certain individual comparisons of adapted *Δefp* strain relative to *Δefp* strain. Second, among the four proteins ValS, Rnb, LepA, and YcgR, which are consistent and significantly down-regulated when EF-P is absent, YcgR as a flagellar regulator that is significantly down-regulated accompanied with the chemotaxis and bacterial movement system. Third, the LepA remains almost unchanged during the evolution of culture. Fourth, the expression of ValS and QorA are significantly enhanced after the cultivation period, and the up-regulated ratios are closer to their down-regulated ratios in *Δefp* strain.

Gene name	*Δefp* vs Control Fold	*Δefp* Evo1 Fold	*Δefp* Evo2 Fold	*Δefp* Evo3 Fold	*Δefp* Evo4 Fold	*Δefp* vs Control significant	*Δefp* Evo1 significant	*Δefp* Evo2 significant	*Δefp* Evo3 significant	*Δefp* Evo4 significant
entF	-3.31	0.53	-0.14	1.05	0.47	+			+	
ycgR	-1.81	-3.31	-4.20	-2.68	-3.29	+	+	+	+	+
rnb	-1.80	0.77	0.70	0.83	0.32	+				
qorA	-1.38	2.14	1.96	1.56	0.06	+	+	+	+	
lepA	-1.33	-0.07	-0.68	0.56	0.83	+				
valS	-1.32	1.61	1.65	1.47	0.64	+	+	+	+	
tonB	-0.85	0.79	0.50	-0.05	0.91	+				+
dppF	-0.71	-0.78	-0.22	0.24	-0.66					
ppc	-0.33	-0.11	-0.33	-0.09	0.20					
ftsK	-0.30	-0.47	-0.81	0.10	0.17					
hisD	-0.25	0.64	0.69	0.39	0.28					
gltB	-0.12	0.19	0.50	-0.14	-1.05					
clsA	-0.07	-0.75	-1.64	-0.05	-0.30					
katE	0.07	-0.26	-0.77	0.33	-0.50					
cyoB	0.12	-0.70	-1.47	-0.74	-0.08					
yhbW	0.14	0.58	0.48	0.69	1.99					+
agp	0.16	1.01	0.61	0.34	-0.01					
rsmA	0.22	-0.77	-0.93	-0.33	-0.32					
nlpD	0.25	-0.09	0.04	-0.08	-0.55					
nuoC	0.30	-0.44	-0.38	0.15	-0.51					
ycgL	0.40	0.06	0.19	-0.13	0.49					
mrcA	0.43	-0.74	-1.72	-0.13	-0.15					
amiB		0.82	1.13	0.17	-0.14			+		

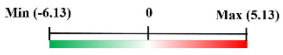

Figure 44. Heat map showing the dynamics of change of PPP-containing proteins in the adapted *Δefp* strains. Note that the gray squares represent the unidentified value.

Summary

After the cell adaptation during the cultivation experiment, the growth rate of *Δefp* strain has been tremendously improved.

The proteomics data reveals the following conclusions:

When the *Δefp* strain adapted without the deletions of *argA* and *lysA* genes (*Δefp* Evo-1 and *Δefp* Evo-2), the down-regulation of the proteins related to flagellar assembly and UMP *de novo* biosynthetic pathway that is less than when the evolution accompanied with the genes deletions (*Δefp* Evo-3 and *Δefp* Evo-4).

Significantly up-regulated proteins belong to the iron metabolism, the HslVU protease complex, as well as to some uncharacterized proteins. HslVU has been proven that plays an important role in suppression of bacterial cells division inhibitor SulA. The up-regulation of HslVU coincides the higher growth rate of adapted strains. Our data suggest that the uncharacterized proteins, such as YeeN, YghA, YghJ, and YjjU, could be involved in bacterial cells growth as well.

Down-regulation of *de novo* pathway of UMP biosynthesis and chemotaxis related proteins in the adapted *Δefp* strains is in good agreement with the comparisons between the adapted strains relative to control strains (section 2.2.2). Since these two pathways are energetically demanding their down-regulation is a logical step in order to economize the utilization of energy for vital cellular processed under the selective pressure conditions.

It is interesting that iron metabolism related proteins, enterobactin biosynthesis and iron transport systems, and those two Fe-S assembly system, CSD and ISC, are almost not significantly changed after the adaptation. On the other hand, the energy supply system TonB-ExbB-ExbD complex is up-regulated to a limited extent. Finally, the SUF system for Fe-S assembly is clearly up-regulated by the evolution process, which was significantly down-regulated in the *Δefp* strain. The results indicate that the adaptation restored the SUF system.

The repertoire of adaptation changes included also the stretches of PPP-containing proteins. Those significantly down-regulated PPP-containing proteins in *Δefp* strain, which are changed in different directions. The expression level of QorA and ValS have been restored with the similar ratios of which were down-regulated in *Δefp* strain. At the same time, RnB, EntF, and TonB are merely up-regulated at a limited level. On the other side, the flagellar regulator, YcgR is furtherly down-regulated. Other PPP-containing proteins are almost not significantly changed in the adapted *Δefp* strains.

2.2.5 Proteome comparisons of the *yeiP* knock-out strain, the *efp* and *yeiP* double knock-out strains to the control strain

The EF-P paralog in *E. coli* is encoded by the *yeiP* gene. YeiP shears a 27 amino acids homology block with EF-P. The match percentage of the homology block is 66% (Figure 45). In order to investigate the function of YeiP whether distinct or redundant with EF-P, a *yeiP* KO strain and *an efp* and *yeiP* double KO strain have been constructed based on the control strain by Dr. Ying Ma (Biocatalysis, TU Berlin). The *yeiP* KO strain was named as *E. coli* BU193 in our lab database, here we will refer to it as *ΔyeiP* strain. The *efp* and *yeiP* double KO strain will be referred to DK strain. Herein, we performed the proteome comparisons of the *yeiP* KO and DK strain to the control strain through SILAC.

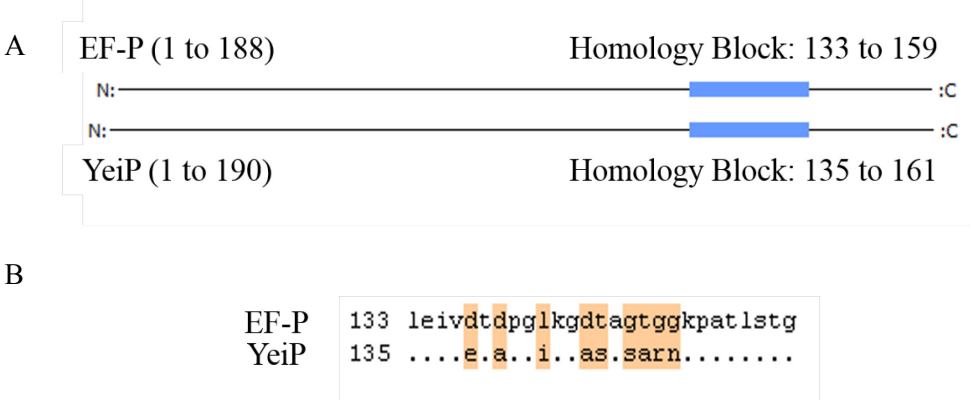

Figure 45. Homolog block of EF-P and YeiP sequence at amino acid level. A. The length of EF-P and YeiP amino acid sequence and the position of the homolog block at each protein. B. Sequence view of the homology block, the color highlights the non-matches.

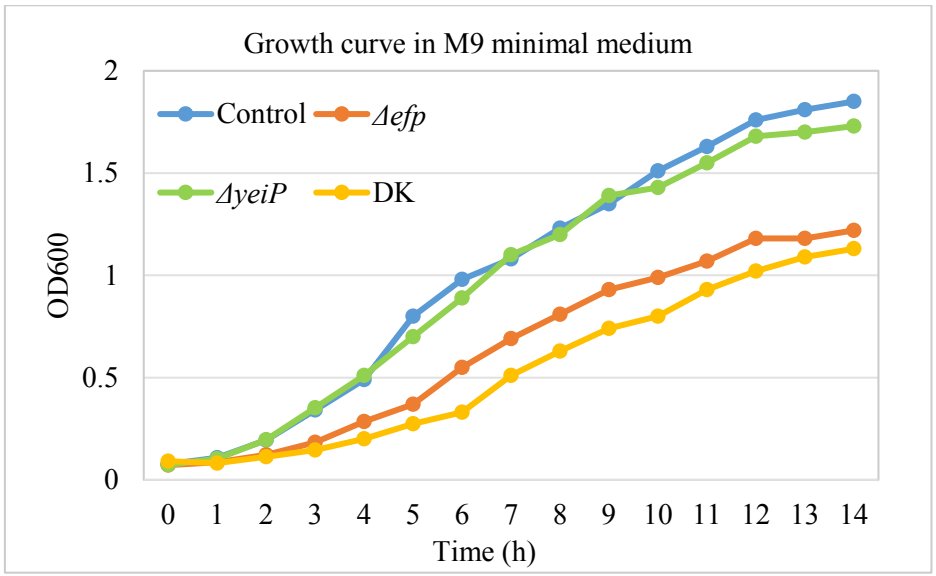

Figure 46. Growth curves of the control, *Δefp*, *ΔyeiP*, and DK strains cultured in M9 minimal medium.

The growth curves (Figure 46) of the strains cultured in M9 minimal medium show that the *ΔyeiP* strain grown with a similar growth rate and behavior as the control strain, it is displaying a minor difference after 10 hours culture, and the maximum number of bacteria is less than the control strain, not more than 6.5%. On the other side, the growth rate of *Δefp* strain is clearly lower than *ΔyeiP* and the control strains, and its maximum number of cell is about 66% of the control strain. In addition, the DK strain grew more slowly than *Δefp* strain, and its maximum bacteria number is only about 60% of the control strain. It appears that the absence of YeiP decreases the growth rate and maximum cell number of *E. coli* to a certain limited extent, but does not affect as much as the absence of EF-P.

In order to characterize the proteome changes from the control strain to *ΔyeiP* and DK strains, I performed two biological replicates SILAC experiments for each comparison. In the comparison between *ΔyeiP* and the control strains where *ΔyeiP* strain was labeled with heavy amino acids (Lys-8, Arg-10) and the control strain with light (Lys-0, Arg-0). In the biological replicate, SILAC labels where *ΔyeiP* strain was labeled with light (Lys-0, Arg-0), while the control strain was labeled with medium (Lys-4, Arg-6). Both replicates of the experiments where the *ΔyeiP* strain was compared to the control one will be referred as *ΔyeiP*_1 and *ΔyeiP*_2. Proteomics data on both biological replicates showed a total of 1326 proteins which could be quantified in both. The majority of protein levels did not change beyond the value of 1 (log2 fold), suggesting only minor alterations in the proteome of the *ΔyeiP* strain relative to the control strain (Figure 47A). The correlation coefficient between replicates was 0.60 (Figure 47B).

Two biological replicates of the comparison between DK strain and the control strain were set as: In the first experiment, the DK and the control strains were labeled with heavy (Lys-8, Arg-10) and light (Lys-0, Arg-0) amino acids, respectively. And in the replicate, the labeling was swapped. The two replicates of the proteome comparison are presented as DK_1 and DK_2 here. There is a total of 1406 proteins were quantified in both. The histograms (Figure 47A) show the distribution of the proteins changed ratios (log2). And the two replicates correlated with a high coefficient of 0.83 (Figure 47B).

In the proteomics data, it is clear that the YeiP was significantly down-regulated in the *ΔyeiP* strain, and both of EF-P and YeiP were significantly down-regulated in the DK strain. These down-regulations verified that the deletion of *efp* or *yeiP* genes in each corresponding strains of *Δefp, ΔyeiP,* and DK strains (Table 19). In the following data analysis of this chapter, the results of *Δefp*_1 and *Δefp*_2 (Chapter 2.2.3) will be combined with *ΔyeiP*_1 and *ΔyeiP*_2, DK_1 and DK_2.

In the proteomics data of comparison between *ΔyeiP* and the control strains, among the proteins which showed the stronger alterations, 39 proteins are significantly up-regulated in both replicates, but only MgtA (magnesium-transporting ATPase) is up-regulated more than the value (log2) of 1 (Figure 48A). There are about one-third of these proteins are significantly up-regulated in DK strain, and the ratios are higher than in *ΔyeiP* stain. Additionally, among of them, only MgtA and FimC are significantly down-regulated in both two replicates of *Δefp* stain.

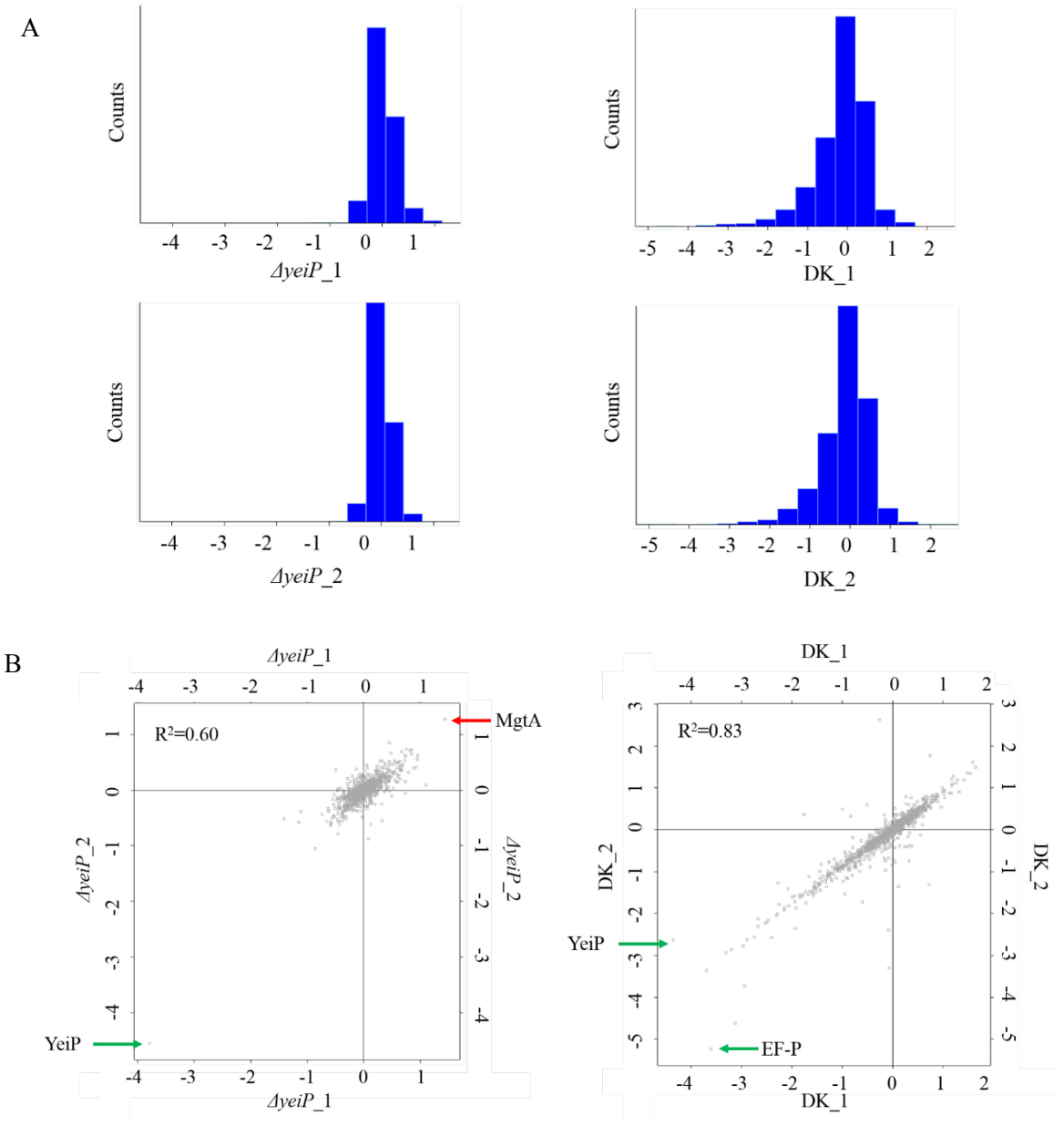

Figure 47. Distributions (A) and correlations (B) of protein changed ratios in two replicates of the *ΔyeiP and* DK strains compared to the control strain.

Table 19. Changes of EF-P and YeiP from the control strain to *Δefp*, *ΔyeiP*, and DK strains.

Gene name	*Δefp*_1 Fold	*Δefp*_2 Fold	*ΔyeiP*_1 Fold	*ΔyeiP*_2 Fold	DK_1 Fold	DK_2 Fold
efp	-5.74	-5.40	0.22	0.28	-3.61	-5.23
yeiP	0.10	-0.21	-3.79	-4.55	-4.36	-2.63

Gene name	*Δefp*_1 significant	*Δefp*_2 significant	*ΔyeiP*_1 significant	*ΔyeiP*_2 significant	DK_1 significant	DK_2 significant
efp	+	+			+	+
yeiP			+	+	+	+

On the other side, except for YeiP, 34 proteins are significantly down-regulated in both replicates of *ΔyeiP* strain compared to the control strain, but the majority of the regulation ratios are not more than 1 log2 value (Figure 48B). Among of these proteins, two-thirds are also down-regulated in *Δefp* and DK stain.

A

Gene name	*ΔyeiP*_1 Fold	*ΔyeiP*_2 Fold	DK_1 Fold	DK_2 Fold	*Δefp*_1 Fold	*Δefp*_2 Fold
mgtA	1.44	1.27	1.29	1.19	0.77	0.84
fliS	0.66	0.39	1.21	1.28	-0.12	-0.08
fimC	0.73	0.63	1.13	0.88	0.94	0.97
fhuA	0.95	0.62	1.02	0.94	-0.72	-0.76
ompC	0.82	0.71	1.00	0.91	-0.08	-0.27
borD	0.62	0.52	0.96	0.54	0.65	0.48
lptD	0.61	0.48	0.89	0.84	-0.05	0.07
slyB	0.64	0.37	0.88	0.75	-0.09	-0.17
cyoA	0.52	0.46	0.85	0.74	0.24	0.13
dcuA	0.65	0.52	0.81	0.66	0.58	0.67
yajC	0.62	0.40	0.79	0.81	-0.05	-0.08
yqhA	0.89	0.39	0.75	0.52	0.06	-0.01
btuB	0.58	0.49	0.70	0.77	-0.24	-0.40
cyoB	0.69	0.46	0.67	0.64	0.11	0.11
yhjH	0.72	0.53	0.53	0.33	-0.30	-0.40
sstT	0.48	0.66	0.43	0.37	0.57	0.65
tonB	0.79	0.32	0.31	0.09	-0.70	-0.96
murJ	0.52	0.31	0.27	0.16	0.12	0.34
ompF	0.94	0.55	0.22	0.25	-0.69	-0.80
ompX	0.45	0.51	0.22	0.17	-0.43	-0.57
wzzB	0.42	0.40	0.19	0.18	0.05	-0.19
mipC	0.65	0.35	0.19	0.27	-0.29	-0.33
lnt	0.46	0.34	0.13	0.17	-0.45	-0.41
adeP	0.85	0.66	0.12	0.19	0.22	-0.17
fliC	0.67	0.69	-0.25	-0.20	-0.42	-0.50
yedE	0.45	0.36	-0.29	-0.23	-0.45	-0.22
rpsL	0.64	0.44	-0.34	-0.27	-0.26	-0.33
trg	0.54	0.52	-0.38	-0.61	-0.31	-0.42
glnK	0.85	0.73	-0.46	-0.32	0.09	0.12
ompA	0.73	0.61	-0.46	-0.39	-0.78	-1.00
fhuE	0.42	0.30	-0.47	-0.28	-3.44	-3.40
rplN	0.67	0.43	-0.50	-0.45	-0.48	-0.52
cstA	0.50	0.32	-0.65	-0.54	-0.34	-0.36
ptsG	0.75	0.74	-0.66	-0.66	-0.08	-0.07
acrB	0.59	0.41	-0.66	-0.56	-0.92	-0.99
rplO	0.57	0.30	-0.93	-0.86	-0.11	-0.10
rplP	0.54	0.34	-0.99	-0.86	-0.27	-0.33
rnpA	0.45	0.85	-1.79	-1.59	-0.49	-0.10
malE	0.46	0.46	-3.70	-3.36	0.32	0.35

B

Gene name	*ΔyeiP*_1 Fold	*ΔyeiP*_2 Fold	DK_1 Fold	DK_2 Fold	*Δefp*_1 Fold	*Δefp*_2 Fold
yeiP	-3.79	-4.55	-4.36	-2.63	0.10	-0.21
raiA	-1.42	-0.52	-0.08	-3.30	4.81	4.18
mtlD	-1.12	-0.38	0.50	0.36	1.12	1.18
ubiE	-0.86	-1.05	-0.42	-0.43	0.36	0.34
sufA	-0.74	-0.44	-0.69	-0.55	-1.43	-1.78
iscR	-0.65	-0.56	-0.33	-0.28	-1.11	-1.16
ybiX	-0.63	-0.33	-1.58	-1.57	-3.06	-3.08
sufE	-0.63	-0.39	-0.93	-0.74	-1.59	-1.76
slp	-0.62	-0.37	0.15	0.04	0.38	0.56
rpsR	-0.59	-0.61	-2.15	-1.86	-1.00	-1.08
ygaM	-0.59	-0.63	-1.39	-1.11	-0.25	-0.18
poxB	-0.58	-0.58	-1.84	-1.56	-1.03	-1.28
yegP	-0.56	-0.50	-0.34	-0.27	-0.07	-0.14
rpoZ	-0.54	-0.46	0.74	1.76	-0.34	-0.09
galE	-0.52	-0.48	-1.56	-1.38	-0.85	-1.03
ynhG	-0.50	-0.33	-0.69	-0.49	-0.36	-0.66
galK	-0.46	-0.53	-2.07	-1.82	-0.99	-1.19
yigI	-0.46	-0.42	0.39	0.28	-0.23	-0.23
yahK	-0.46	-0.79	-1.52	-1.38	-0.49	-0.74
ihfA	-0.45	-0.36	0.22	0.21	-0.01	0.15
ftnA	-0.45	-0.56	-0.36	-0.29	0.63	0.67
acs	-0.44	-0.56	-1.83	-1.62	-0.72	-0.78
wrbA	-0.44	-0.32	-0.16	-0.13	0.15	0.17
qorA	-0.44	-0.29	-2.67	-2.30	-1.39	-1.35
fadE	-0.43	-0.61	-1.02	-0.94	-0.78	-0.75
yagU	-0.42	-0.31	-0.83	-0.73	-0.76	-0.96
ecnB	-0.42	-0.34	-0.32	-0.29	-0.32	-0.22
galT	-0.40	-0.48	-1.78	-1.54	-1.14	-1.16
talA	-0.39	-0.41	-1.56	-1.35	-0.73	-0.84
bfr	-0.38	-0.56	0.31	0.20	1.19	1.34
elaB	-0.38	-0.41	-0.50	-0.49	-0.09	-0.14
pspA	-0.38	-0.44	-0.01	-0.16	0.21	0.37
osmC	-0.37	-0.41	-0.28	-0.33	0.04	0.04
tktB	-0.37	-0.45	-1.14	-0.93	-0.45	-0.63
ybaY	-0.36	-0.38	-0.14	-0.36	-0.07	-0.25

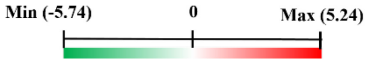

Figure 48. Significantly up-regulated (A) and down-regulated (B) proteins in both replicates of *ΔyeiP* stain compared to the control strain, and the corresponding changes of these proteins in DK and *Δefp* strain compared to the control strain.

In the data of DK strain compared to the control strain, 27 proteins are significantly up-regulated in both replicates, among of them, about one third are also significantly up-regulated in *ΔyeiP* strain, and about two thirds are extremely increased in *Δefp* strain (Figure 49A). On the other hand, there are 60 proteins are significantly down-regulated in DK strain, of which almost no proteins down-regulated such high ratios in *ΔyeiP* strain, and two-thirds are significantly down-regulated in *Δefp* strain (Figure 49B).

A

Gene name	*ΔyeiP*_1 Fold	*ΔyeiP*_2 Fold	DK_1 Fold	DK_2 Fold	*Δefp*_1 Fold	*Δefp*_2 Fold
mgtA	1.44	1.27	1.29	1.19	0.77	0.84
fimC	0.73	0.63	1.13	0.88	0.94	0.97
fluA	0.95	0.62	1.02	0.94	-0.72	-0.76
ompC	0.82	0.71	1.00	0.91	-0.08	-0.27
fliS	0.66	0.39	1.21	1.28	-0.12	-0.08
slyB	0.64	0.37	0.88	0.75	-0.09	-0.17
lptD	0.61	0.48	0.89	0.84	-0.05	0.07
fliA	0.52	0.03	1.65	1.50	0.58	0.54
ilvD	0.08	0.13	1.48	1.35	0.86	0.91
pstS	-0.24	-0.21	1.54	1.34	0.92	1.05
speC	0.10	0.14	1.17	1.20	0.86	1.04
purC	0.08	0.02	1.32	0.90	0.77	0.93
lipA	0.28	0.21	1.59	1.60	1.96	1.55
dadA	-0.19	-0.06	1.41	1.20	0.76	0.96
pdxY	-0.05	0.01	0.90	0.79	0.71	0.68
degP	-0.18	-0.04	0.85	0.77	0.70	0.74
yjbR	-0.10	-0.15	0.84	0.74	0.50	0.67
iscA	-0.02	-0.12	1.01	0.86	0.64	0.66
erpA	-0.10	-0.10	0.84	0.82	0.63	0.55
ilvA	0.14	0.13	1.18	1.06	0.51	0.52
ppsA	-0.09	-0.16	0.98	1.00	0.48	0.54
rcsF	0.10	0.16	1.26	1.12	0.45	0.40
tolB	-0.14	-0.01	1.03	0.94	0.44	0.42
rsmH	-0.20	0.02	1.04	0.76	0.10	0.14
tap	0.33	0.27	0.89	0.83	0.10	0.06
ilvB	0.18	0.03	1.18	1.10	-0.18	-0.17
flgH	0.23	-0.07	1.17	0.87	-0.11	-0.13

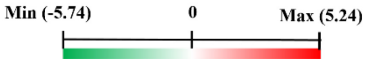

B

Gene name	*ΔyeiP*_1 Fold	*ΔyeiP*_2 Fold	DK_1 Fold	DK_2 Fold	*Δefp*_1 Fold	*Δefp*_2 Fold
efp	0.22	0.28	-3.61	-5.23	-5.74	-5.40
yeiP	-3.79	-4.55	-4.36	-2.63	0.10	-0.21
hrpA	0.04	0.08	-3.12	-4.61	-3.28	-3.71
grxA	-0.20	0.25	-2.95	-3.73	-1.74	-3.69
malE	0.46	0.46	-3.70	-3.36	0.32	0.35
rnb	-0.02	0.00	-3.31	-2.94	-1.70	-1.92
fiu	0.33	0.22	-3.21	-2.87	-4.41	-4.25
rplQ	0.41	0.27	-2.96	-2.77	-0.37	-0.41
aroF	-0.50	0.37	-2.90	-2.62	-1.79	-2.00
cysQ	-0.14	-0.11	-2.40	-2.57	-1.66	-1.82
ycgR	0.18	0.17	-2.75	-2.56	-1.73	-1.91
gatD	-0.15	-0.21	-1.94	-2.36	2.87	3.36
qorA	-0.44	-0.29	-2.67	-2.30	-1.39	-1.35
glpT	0.19	0.25	-2.52	-2.23	-4.15	-3.39
hisB	-0.20	-0.03	-2.50	-2.21	-1.47	-1.78
lepA	0.06	0.00	-2.47	-2.16	-1.24	-1.43
rpsT	0.11	-0.16	-2.67	-2.14	-0.56	-0.58
valS	-0.04	-0.02	-2.30	-2.04	-1.25	-1.41
tyrA	-0.29	0.12	-2.28	-2.01	-1.31	-1.76
tamB	0.08	0.26	-2.15	-1.92	-1.05	-1.21
hisH	-0.18	-0.01	-1.92	-1.87	-1.22	-1.41
rpsR	-0.59	-0.61	-2.15	-1.86	-1.00	-1.08
galK	-0.46	-0.53	-2.07	-1.82	-0.99	-1.19
fruA	-0.03	0.29	-2.26	-1.78	0.44	0.49
bamD	-0.01	-0.03	-1.73	-1.75	-1.45	-1.62
entF	-0.49	-0.19	-1.94	-1.72	-3.06	-3.61
acs	-0.44	-0.56	-1.83	-1.62	-0.72	-0.78
mglB	-0.07	-0.08	-1.99	-1.60	-0.92	-1.01
rnpA	0.45	0.85	-1.79	-1.59	-0.49	-0.10
malP	0.13	0.14	-1.94	-1.58	-0.38	-0.42

Gene name	*ΔyeiP*_1 Fold	*ΔyeiP*_2 Fold	DK_1 Fold	DK_2 Fold	*Δefp*_1 Fold	*Δefp*_2 Fold
cysJ	0.15	0.12	-1.85	-1.58	-0.95	-1.13
ybiX	-0.63	-0.33	-1.58	-1.57	-3.06	-3.08
poxB	-0.58	-0.58	-1.84	-1.56	-1.03	-1.28
ilvC	-0.15	-0.09	-1.67	-1.55	-1.11	-1.30
galT	-0.40	-0.48	-1.78	-1.54	-1.14	-1.16
rplT	0.40	0.13	-1.58	-1.50	-0.14	-0.15
gatA	0.14	0.05	-1.60	-1.49	0.57	0.65
atpG	0.22	0.19	-1.53	-1.48	-0.77	-1.18
pyrC	-0.11	0.01	-1.73	-1.48	-0.89	-1.13
atpD	0.20	0.15	-1.65	-1.47	-1.07	-1.27
gatZ	0.45	0.18	-1.45	-1.44	1.37	1.57
hisA	-0.03	0.00	-1.52	-1.43	-0.80	-0.90
artJ	-0.01	-0.14	-1.57	-1.43	-0.38	-0.42
uraA	0.60	0.27	-2.08	-1.42	-0.99	-1.38
aldA	-0.15	-0.19	-1.55	-1.40	-0.51	-0.71
yahK	-0.46	-0.79	-1.52	-1.38	-0.49	-0.74
hisF	-0.20	-0.10	-1.54	-1.38	-0.68	-0.89
galE	-0.52	-0.48	-1.56	-1.38	-0.85	-1.03
putA	-0.15	-0.25	-1.50	-1.38	-0.49	-0.62
talA	-0.39	-0.41	-1.56	-1.35	-0.73	-0.84
ettA	0.08	0.13	-1.32	-1.35	-0.88	-0.97
trpA	-0.22	-0.08	-1.46	-1.32	-0.96	-1.14
rplC	0.45	0.21	-1.45	-1.31	-0.58	-1.22
trpE	-0.05	0.06	-1.54	-1.31	-1.18	-1.26
plaP	0.31	0.10	-1.47	-1.30	-0.75	-0.76
manX	-0.01	0.13	-1.47	-1.28	0.19	0.19
rpsS	-0.26	-0.15	-2.28	-1.26	-0.87	-0.66
cirA	0.06	0.40	-1.55	-1.25	-3.58	-4.02
atpF	0.22	0.35	-1.33	-1.24	-1.03	-1.01
acnB	0.00	-0.17	-1.41	-1.24	-0.45	-0.49

Figure 49. Significantly up- (A) and down-regulated (B) proteins in both replicates of DK stain compared to the control strain, and the corresponding changes of these proteins in *Δefp* and *ΔyeiP* strains compared to the control strain.

In addition, the heat map of the hierarchical clustering (Figure 50) depicts stranger alterations to the control proteome caused by the absence of EF-P than the lack of YeiP. And the alterations in DK strain is closer to *Δefp* strain than *ΔyeiP* strain.

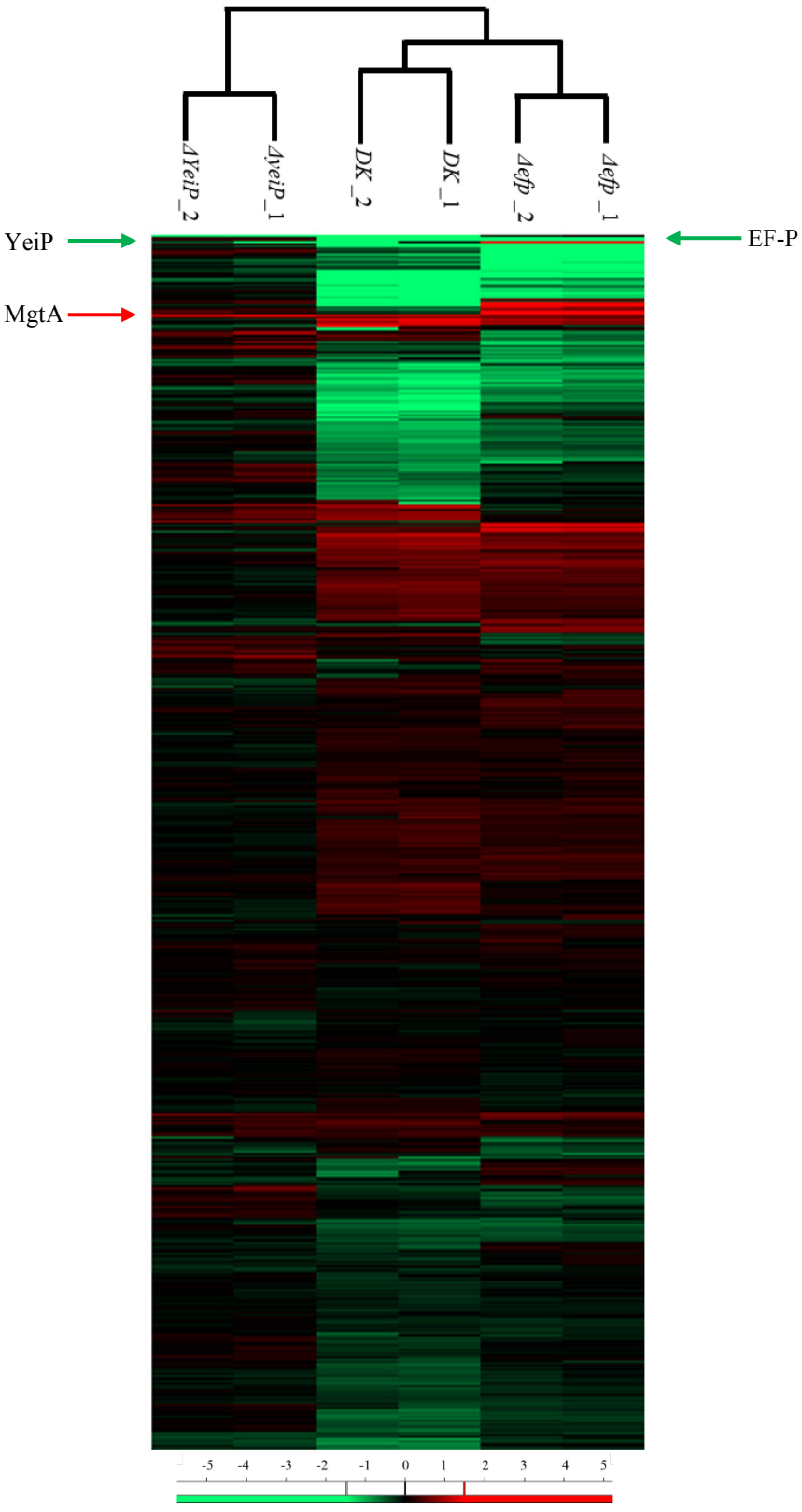

Figure 50. Hierarchical clustering of proteomics data from *Δefp*, *ΔyeiP*, and DK strains. Heat map showing all quantified proteins that are up- (red) and down- (green) regulated in two biological replicates of comparisons of *Δefp*, *ΔyeiP*, and DK strains relative to the control.

Although the absence of YeiP does not make such huge changes as EF-P at proteome of *E. coli*, the changes on the MgtA is remarkable. It is also up-regulated in the *Δefp* strain, but to a lesser extent than in *ΔyeiP* strain. And it is up-regulated with a similar extent in DK strain (Figure 48A).

The MgtA is encoded by *mgtA* gene. The initiation of *mgtA* gene transcription is regulated by the PhoP/PhoQ two-component system. PhoP is a transcriptional regulatory protein, and PhoQ is a sensor protein. PhoP is phosphorylated when PhoQ detects low Mg^{2+} concentration, the phospho-PhoP activates the P1 promoter in a *phoPQ* operon of *E. coli*, and the expression of *mgtA* is activated as a subsequent result [162, 163]. On the other side, the expression of *mgtA* is controlled by a 17 codon proline-rich peptide MgtL, of which the open reading frame and ribosome binding site presence in the 5' leader region (LR) of *mgtA*. A transcription termination at up-stream of the *mgtA* protein coding region (CR) is led by the high-efficiency translation of *mgtL*, while stalling of *mgtL* antagonizes the termination. The termination factor Rho plays an important role in the transcription. At low concentration of Mg^{2+}, the LR of *mgtA* forms stem loopC, in which the Rho-utilization (*rut*) site is hidden and the termination is inhibited, in contrast, the high Mg^{2+} concentration induces the formation of loopA and loopB, in which the rut site is exposed for Rho, and the further termination is promoted. In this regulatory model, the high Mg^{2+} concentration could overcome the translation "speed bump" of *mgtA* brought by Pro codons in *mgtL* [164].

In the previous work, SILAC medium contains a Mg^{2+} concentration which is constant at 1mM, and which can be considered as high Mg^{2+} concentration. In addition, in our data, the mentioned above proteins, PhoP, PhoQ, Rho and some other proteins involved in MgtA expression, such as Rob [165], RpmA, and RpmE [164] are almost not found that significantly regulated in all of *ΔyeiP*, *Δefp* and DK strains (Figure 51). Therefore, our observations for on the higher levels of MgtA cannot be due to an effect of the Mg^{2+} concentration. MgtL, a short and proline-rich peptide, could not be identified by the SILAC-based MS measurement.

Gene name	*ΔyeiP*_2	*ΔyeiP*_1	DK_2	DK_1	*Δefp*_2	*Δefp*_1	*ΔyeiP*_1 significant	*ΔyeiP*_2 significant	DK_1 A significant	DK_2 A significant	*Δefp*_1 significant	*Δefp*_2 significant
mgtA	1.27	1.44	1.19	1.29	0.84	0.77	+	+	+	+	+	+
phoP	-0.02	-0.14	-0.48	-0.51	-0.10	-0.06						
phoQ	0.00	-0.05	0.06	0.07	0.44	0.39						
rho	0.05	0.04	0.04	0.03	0.13	0.19						
rob	0.10	0.21	-0.36	-0.34	-0.10	0.03						
rpmA	0.45	0.05	0.68	0.50	-0.97	-0.50		+				+
rpmE	0.25	0.38	-0.63	-0.64	-0.07	-0.21						

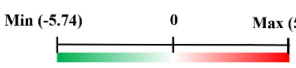

Figure 51. Changes of MgtA expression related proteins in *ΔyeiP*, *Δefp*, and DK strains *vs.* the control strain.

In previous work of Gall, et al. [164], *S. typhimurium* strain deprived of EF-P, show that the expression of *mgtA* increased nearly 10 fold at high Mg^{2+} (1.6 mM) and 4 fold at low Mg^{2+} (0.016 mM) environments, respectively. In addition, the translation of MgtL is reduced to 40% at high Mg^{2+} and 30% at low Mg^{2+} environments, respectively. However, in the 3 prolines mutant *mgtL* strains (there are 4 prolines in the wild type gene), the expression of *mgtL* and *mgtA* are not sensitive in the absence of EF-P. These results indicate that EF-P plays an important role in the regulation of *mgtA* expression through specifically acts on the expression of *mgtL*.

In the *Δefp E. coli* strain of this study, the expression of MgtA is up-regulated around 0.8 log2 fold. The ratio is not as high as in the reported *S. typhimurium* [164], but it also belongs to the significantly changed proteins in here presented experiments. In addition, for the experiment cells have been harvested in the phase between early to mid-exponential growth (~ 3×10^8 cells/ml), while the *S. typhimurium* were harvested at mid-exponential phase (~ 5×10^8 cells/ml). In *ΔyeiP* strain, the expression of MgtA is up-regulated 1.4 log2 fold.

When we focus on the alterations of PPP-containing proteins (Figure 52), it is clear that the absence of YeiP almost does not lead to significant changes in these proteins. The regulations in DK strain is showing a similar trend as *Δefp* strain. This result indicates that YeiP does not play a similar role as EF-P in the regulation of PPP-containing proteins expression.

Gene name	*ΔyeiP*_1 Fold	*ΔyeiP*_2 Fold	DK_1 Fold	DK_2 Fold	*Δefp*_1 Fold	*Δefp*_2 Fold
entF	-0.49	-0.19	-1.94	-1.72	-3.06	-3.61
rnb	-0.02	0.00	-3.31	-2.94	-1.70	-1.92
ycgR	0.18	0.17	-2.75	-2.56	-1.73	-1.91
lepA	0.06	0.00	-2.47	-2.16	-1.24	-1.43
valS	-0.04	-0.02	-2.30	-2.04	-1.25	-1.41
qorA	-0.44	-0.29	-2.67	-2.30	-1.39	-1.35
tonB	0.79	0.32	0.31	0.09	-0.70	-0.96
dppF	0.11	0.06	-0.35	-0.43	-0.62	-0.82
uvrB	-0.11	-0.24	-1.21	-1.22	-0.73	-0.59
ftsK	0.14	0.17	-0.18	-0.19	-0.29	-0.41
ppc	-0.02	-0.06	-0.45	-0.31	-0.27	-0.40
sdaC	0.29	0.13	0.01	0.10	-0.08	-0.34
hisD	-0.32	-0.12	-1.01	-0.87	-0.25	-0.26
mdC	0.11	0.05			-0.16	-0.18
gltB	0.02	-0.02	-0.31	-0.24	-0.15	-0.09
clsA	-0.04	-0.09			-0.07	-0.06
katE	-0.04	-0.14	-1.10	-0.83	0.05	0.03
cyoB	0.69	0.46	0.67	0.64	0.11	0.11
rsmA	-0.02	0.00	0.04	0.16	0.24	0.20
ydiK	-0.20	-0.01	0.20	0.39	0.06	0.23
yhbW	-0.17	-0.14	-0.52	-0.29	0.06	0.30
nuoC	0.31	0.19	-0.12	-0.07	0.37	0.31
nlpD	0.25	-0.01	0.22	0.29	0.25	0.33
ycgL	-0.03	-0.05	0.19	0.31	0.37	0.43
mrcA	-0.01	0.09	0.65	0.70	0.51	0.46
recG	-0.04	-0.12				

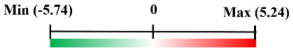

Figure 52. Heat map represents the changes of PPP-containing proteins in *ΔyeiP, Δefp,* and DK strains relative to the control strain.

Summary

Through the growth curve, we do not find the clear-cut difference between the *ΔyeiP* strain and control strain as between *Δefp* strain and control strain vs control, considering growth rate and maximal cells number. Proteomics data analysis on the *ΔyeiP* strain compared to the control strains, do not show significant changes as the *Δefp* strain vs the control counterpart. The most significantly changed protein is MgtA. The MgtA expression related proteins, PhoP, PhoQ, Rho, Rbo, RpmA, and RpmE are not significantly regulated in *ΔyeiP* strain. The up-regulated ratio of MgtA in *ΔyeiP* is more than *Δefp* strain. This indicates that YeiP is more sensitive than EF-P on the regulation of MgtA expression in *E. coli* at the high Mg^{2+} environment.

On the aspect of PPP-containing proteins expression, the *ΔyeiP* strain doesn't show similar chenges as *Δefp* strain, but the DK strain shows similar effects as *Δefp* stain.

In summary, YeiP does not play such essential role as EF-P at the *E. coli* proteome level, but it has a unique function in the regulation of MgtA expression. Since the MgtA is a very important magnesium transporter in bacterial cells, it is very meaningful to do further research about the relation between YeiP and the expression of proline-rich peptide MgtL and the mechanism of MgtA up-regulated by YeiP absence.

3 Conclusion and Outlook

In this study, we aimed to characterize the proteomics of the robustly grown WT and EF-P KO *E. coli* strains, which have been continually cultivated in GM3 device. The SILAC methodology has been successfully employed to study the proteome dynamics differences between: (i) the control strain cultured in M9 minimal medium and LB medium; (ii) adapted strains and control strain in M9 minimal media; (iii) EF-P KO strain and control strain in M9 minimal media; (iv) adapted EF-P KO strains and original EF-P KO strain in M9 minimal media; (v) YeiP KO strain and control strain in M9 minimal media.

When the *E. coli* control strain is cultured in M9 minimal medium, the ATP-dependent peptide transport systems are significantly up-regulated. A large number of amino acids transport and biosynthesis related proteins (anabolism) are significantly up-regulated too, whereas a corresponding down-regulation occurs at some amino acids degradation pathways (catabolism). In addition, a large amount of nucleotide biosynthesis especially *de novo* pathways are extremely enhanced, while a corresponding down-regulation takes place at nucleoside catabolism related proteins. All these changes clearly present a tendency to ATP-utilization import and biosynthetic pathways of the basic biomolecules such as amino acids, peptides, and nucleotides. These observations are consistent with the literature reports about the effects of nutrient limitation in the minimal medium [96]. The down-regulation of various carbon sources transport and catabolism pathways is consistent with the lack of these carbon sources in M9 minimal medium and the previous studies about carbon sources utilization in LB medium [114]. The down-regulation of protein synthesis related proteins corresponds with the slow growth of *E. coli* in the minimal medium. Since a large amount of related proteins could be efficiently quantified by the SIALC-based MS measurements, this method (in combination with genomics, transcriptomics and metabolomics methods) is the most suitable tool for the studies about *E. coli* metabolism and nutrients utilization in different culture conditions.

The adaptation experiments performed by GM3 device greatly improved the growth rate of *E. coli* in all studied strains. Interestingly, it has been reported that putrescine plays an essential role to improve growth of bacterial cells [120, 122]. The enhancement of putrescine synthesis pathway and repression of the conversion form putrescine to spermidine in the studied strains provide evidence that the adaptation process and related improved bacterial growth might be facilitated through the increase of the putrescine synthesis. The other two significantly up-regulated proteins, YgiW and OsmC could be further studied in order to elucidate their role in the bacterial growth dynamics. On the other hand, the significant down-regulation is observable in some ATP- consumption biosynthetic pathways, involved at least in a part of amino acids biosynthesis pathways and *de novo* synthetic pathway of UMP. The down-regulation of chemotaxis and flagellar assembly related proteins is plausible since in the turbidostat cultivation regime a considerable amount of the energy could be saved (due to the immediate availability of the all necessary nutrients). In the regulation of the central carbon metabolism, significant

up-regulation occurs before the conversion of pyruvate to acetyl-CoA whereas the repression affects the TCA-cycle as the main energy source of the cells. Therefore, it might exist a certain connection among the phenomenon of reducing of energy supply from TCA-cycle (associated also with the decreasing movement capacity) and the need to keep necessary energy levels for faster bacterial growth under the selective pressure. Obviously, more data and studies that include genomics (mutations in the genome), metabolomics (e.g. metabolic fluxes) are necessary to reveal the mechanism of the improved growth rate during the cultivation experiments.

The growth rate of *Δefp* strain is obviously lower than control strain. The absence of EF-P greatly inhibits the growth of *E. coli*. At proteome level, as a global regulator, the absence of EF-P leads to numerous changes. The most significantly up-regulated pathways are related to galactitol transport and catabolism. As previous knowledge, it is just known that galactitol could be adapted as a carbon source, but could not be a sole carbon source in bacterial cells. What a role does it play in *Δefp* strain, and how it is regulated by EF-P are the questions that require being answered in further study. The down-regulation of amino acids and protein biosynthetic pathways is consistent with the low growth rate of *Δefp* strain. The significant down-regulation of the enterobactin biosynthesis and transport system and the SUF Fe-S cluster assembly pathway related proteins in *Δefp* strain indicates that EF-P greatly affects iron up-take and storage in *E. coli*, thereby impacts a series of intracellular reactions that require iron to participate. A core protein in enterobactin synthesis is EntF, which is involved in the last biosynthetic step, simultaneously it is a proline-rich and PPP-containing protein. We speculate that the absence of EF-P leads to the translation stalling of EntF, and then as the effect of the positive feedback of EntF inhibition that the whole pathway of enterobactin synthesis and transport system are inhibited, even further the SUF pathway is down-regulated. In a further study, we are planning to construct EntF overexpression plasmid, and transform the plasmid to *Δefp* and control strains, respectively. If the expression level of EntF could be restored in *Δefp* strain by the overexpression plasmid, it means that the translation stalling of EntF caused by EF-P absence could be rescued by increasing the number of copies, otherwise it is not.

After the adaptation of studied strains under the conditions of cultivation in GM3 devices, the growth rate of *Δefp* strain is significantly improved. On proteome level, the up-regulation of HslVU protease complex is an interesting discovery. HslVU could be a candidate for a further study on the role of improving cell growth and division. Next, the other significantly up-regulated but uncharacterized proteins are YeeN, YghA, YghJ, and YjjU; they are also ‘hot’ candidates for further studies of their potential roles in the growth dynamics of bacterial cells. The down-regulation of the ATP-consumption pathways, *de novo* of UMP biosynthesis, chemotaxis and flagellar assembly is consistent with the observations made in the adapted WT and control strains. The significantly up-regulated proteins and the variety of energy flux related pathways should be further investigated as potential factors for overcoming the negative effects caused by the absence of EF-P and improving cells growth and division.

Certainly, the central aspect are oligo-proline containing proteins and their expression dynamics. Surprisingly, *Δefp* strain does not show a global regulation ability to the PP-containing proteins, even a part of these proteins are up-regulated in *Δefp* strain. In the data of PPP-containing proteins, the following four proteins, Vals, Rnb, LepA, and YcgR are significantly down-regulated in previous reports [32]. We also confirmed these observations in our experiments with EF-P-deficient strains. Additionally, EntF, TonB, and QorA as PPP-containing proteins are found that significantly down-regulated in *Δefp* strain uniquely in our data sets. On the other hand, in the adapted *Δefp* strains, the PPP-containing protein YcgR also serves as a flagellar brake, which is further significantly down-regulated along with the chemotaxis and flagellar related proteins. Expectedly, the proteins such as EntF, TonB, LepA and Rnb are increased to a certain extend with the adaptation. And ValS and QorA are significantly up-regulated in all cultivation experiments. It is plausible to conclude that the ribosome stalling caused by the absence of EF-P is successfully overcome though some unknown mechanisms.

In addition, in the adapted *Δefp* strains, down-regulated enterobactin synthesis and transport related proteins are not significantly restored, but the SUF pathway related proteins are indeed significantly up-regulated. The connection between the improved growth rate and the up-regulated SUF pathway should be a subject of future studies.

YeiP is the paralog of EF-P in *E. coli* [166]. The *ΔyeiP* strain does not show any similar features to the growth and proteomics of *Δefp* strain. In fact, the growth rate of *ΔyeiP* strain shows almost no difference with the control strain. Expectedly, there is not much changes in *ΔyeiP* strain when compared with *Δefp* strain at proteome level. In addition, the double knock-out strain deprived of both EF-P and YeiP is much more similar to single knockout *Δefp* strain at proteome level. Analyses of proteomics results dynamics indicate that YeiP is maybe a not suitable candidate to be paralog of EF-P protein. On the other hand, the significant up-regulation of MgtA is interesting as its translation is regulated by the short Pro-rich leader peptide MgtL. We speculate that YeiP might alleviate the translation stalling of MgtL caused by the 4Pro- sequence, thus promotes the expression of MgtL, and further inhibits the translation of MgtA. Thus, we propose a hypothetical model that YeiP or EF-P regulates the expression of a certain gene or an ORF indirectly through rescuing the translation stalling of a leader peptide or protein caused by Pro-rich sequence. Furthermore, the leader peptide or protein promotes or inhibits the expression of the core region of the gene or ORF. Thereby, the crucial question is whether this kind of regulation model is widely present in *E. coli* and other organism cells. Certainly, further data mining and analyses are required to answer this question.

In general, this study revealed beside some well-known mechanisms also novel features associated with the bacterial adaptation under the conditions of continuous cultivation. Doubtless, the changes in energy flux related pathways caused by the turbidostat model evolution are related to the observed dynamics of enterobactin biosynthesis and transport pathways affected by EF-P KO. Furthermore, SUF Fe-S pathway was down-regulated when EF-P gene is knock-outed but it could be restored by the adaptation

process. Other important changes include the up-regulation of HslVU in the adapted EF-P KO strains, and the significantly up-regulated MgtA in YeiP KO strain. In the future, these strains will be further subjected to continuous evolution with various Proline analogs in order to investigate whether their proteome-wide insertion is possible. These analogs will serve as an important building blocks for many biotechnologically high-value products such as therapeutic proteins of peptide-based antibiotics. Their large production in evolutionarily adapted strains belongs to the great promises of the biotechnology of the future.

4 Materials

4.1 Equipments

Electrophoresis	
PowerPac™ HC High-Current Power Supply	Bio-Rad (Hercules, CA, USA)
Mini-Sub® Cell GT Cell	Bio-Rad (Hercules, CA, USA)
Wide Mini-Sub Cell GT Cell	Bio-Rad (Hercules, CA, USA)
Mini-Protein® Tetra Cell	Bio-Rad (Hercules, CA, USA)
Electroporation System	
Gene Pulser Xcell™	Bio-Rad (Hercules, CA, USA)
Gene Pulser®/Micropulser™ electroporation cuvettes	Bio-Rad (Hercules, CA, USA)
Thermomixer	
Thermomixer comfort	Eppendorf (Hamburg, DE)
Thermocycler	
Peqstar 2X Gradient	Peqlab (Erlangen, DE)
Mastercycler ep Gradient S	Eppendorf (Hamburg, DE)
Incubator	
Ecotron	Infors HT (Einsbach, DE)
Multitron	Infors HT (Einsbach, DE)
New Brunswick™ Innova® 44	Eppendorf (Hamburg, DE)
Incubator series B, KB	Binder (Tuttlingen, DE)
Heraeus T6060	Thermo Scientific (Waltham, MA, USA)
Centrifuge	
Rotilabo®-mini-centrifuge	Carl Roth (Karsruhe, DE)
Centrifuge 5417R	Eppendorf (Hamburg, DE)
Centrifuge 5810R	Eppendorf (Hamburg, DE)
Spectroscopy	
Libra S 22 UV/Vis Spectrophotometer	Biochrom (Berlin, DE)
Ultrospec 6300pro	Amersham Biosciences (Buckinghamshire, UK)

BioPhotometer plus	Eppendorf (Hamburg, DE)
Microplate reader Infinite M200	Tecan (Crailsheim, DE)

Sonicator

Sonopuls HD2070	Bandelin (Berlin, DE)
Sonotrodes MS72, KE76	Bandelin (Berlin, DE)

Centrifugal vacuum concentrator

Concentrtor 5301	Eppendorf (Hamburg, DE)

Liquid Chromatography

1200 Nanoflow-HPLC	Agilent Technologies (Waldbronn, DE)

Mass spectrometry

LTQ Orbitrap XL	Thermo Scientific (Waltham, MA, USA)

Miscellaneous

Polymax 1040	Heidolph (Schwabach, DE)
Vortex mixer VV3	VWR (Radnor, PA, USA)
Gel-documentation system Felix 2050	Biostep (Jahnsdorf, DE)
Scanner ViewPix 700	Biostep (Jahnsdorf, DE)
ED224S-OCE	Sartorius (Göttingen, DE)
Column Loader Kit SP036	Proxeon Biosystems (Odense, DK)

4.2 Chemicals

Bacterial culture

LB-Medium

Tryptone	Carl Roth (Karlsruhe, DE)
Yeast extract	Carl Roth (Karlsruhe, DE)
NaCl	Carl Roth (Karlsruhe, DE)
Agar-Agar	Carl Roth (Karlsruhe, DE)

M9 minimal medium

M9 Minimal Salts (5×)	Sigma-Aldrich (Taufkirchen, DE)
Thiamine	Sigma-Aldrich (Taufkirchen, DE)
$MgSO_4$	Sigma-Aldrich (Taufkirchen, DE)
$CaCl_2$	Sigma-Aldrich (Taufkirchen, DE)
Glucose	Sigma-Aldrich (Taufkirchen, DE)
Proline	Sigma-Aldrich (Taufkirchen, DE)

L-arginine	Sigma-Aldrich (Taufkirchen, DE)
L-lysine	Sigma-Aldrich (Taufkirchen, DE)
L-[$^{13}C_6$] arginine	Eurisotop (Saarbrücken, DE)
L-[$^{2}H_4$] lysine	Eurisotop (Saarbrücken, DE)
L-[$^{13}C_6$,$^{15}N_4$] arginine	Eurisotop (Saarbrücken, DE)
L-[$^{13}C_6$,$^{15}N_2$] lysine	Eurisotop (Saarbrücken, DE)

Antibiotic

Ampicillin	Sigma-Aldrich (Taufkirchen, DE)
Kanamycin	Sigma-Aldrich (Taufkirchen, DE)

Bacterial storage

Glycerol	Sigma-Aldrich (Taufkirchen, DE)
DMSO	Sigma-Aldrich (Taufkirchen, DE)

Polymerase chain reaction (PCR)

10× Buffer E (with $(NH_4)_2SO_4$ and $MgCl_2$)	Genaxxon bioscience (Ulm, DE)
dNTPs	Genaxxon bioscience (Ulm, DE)
Taq DNA Polymerase	Genaxxon bioscience (Ulm, DE)
Agarose	Sigma-Aldrich (Taufkirchen, DE)
Gel red Nucleic Acid Stain	Biotium (Fremont, CA, USA)
6× DNA Loading Dye	Thermo Scientific (Waltham, MA, USA)
Gene Ruler 1kb DNA Ladder	Thermo Scientific (Waltham, MA, USA)

Lysis buffer

Tris	Carl Roth (Karlsruhe, DE)
Hydrochloric acid (HCl)	Carl Roth (Karlsruhe, DE)
Dithiothreitol (DTT)	Sigma-Aldrich (Taufkirchen, DE)
Ethylenediaminetetraacetic acid disodium salt dihydrate (EDTA-2Na)	Carl Roth (Karlsruhe, DE)
Lysozyme	Sigma-Aldrich (Taufkirchen, DE)
TritonX-100	Carl Roth (Karlsruhe, DE)
cOmplete™ Protease Inhibitor Cocktail	Sigma-Aldrich (Taufkirchen, DE)

Sample preparation and MS measurement

Iodoacetamide (IAA)	Sigma-Aldrich (Taufkirchen, DE)
SimplyBlue™ SafeStain	Invitrogen (Carlsbad, CA, USA)
10 x Tris/Glycine/SDS running buffer	Bio-Rad (Hercules, CA, USA)
Ammonium bicarbonate (ABC)	Sigma-Aldrich (Taufkirchen, DE)
Ethanol (100%)	LGC Standards (Middlesex, UK)
Trypsin	Promega (Fitchburg, WI, USA)
Acetic acid	LGC Standards (Middlesex, UK)
Acetonitrile	Carl Roth (Karlsruhe, DE)
Trifluoroacetic acid (TFA)	LGC Standards (Middlesex, UK)
Bovine serum albumin (BSA)	Sigma-Aldrich (Taufkirchen, DE)

4.3 Media and Supplements

LB medium: 10 g/L tryptone, 5 g/L yeast extract, 10 g/L NaCl.

M9 minimal medium (SILAC medium): M9 Minimal Salts (5×, Sigma. Components: 33.9 g/L Na_2HPO_4, 15 g/L KH_2PO_4, 5 g/L NH_4Cl, 2.5 g/L NaCl), $1/10^4$ thiamine, 1 mM $MgSO_4$, 10 μM $CaCl_2$, 0.5% glucose, 20 mg/L proline, 25 mg/L L-arginine (Arg-0) and 25 mg/L L-lysine (Lys-0) for light labeled (L) medium, 25 mg/L L-[$^{13}C_6$] arginine (Arg-6) and 25 mg/L L-[$^{2}H_4$] lysine (Lys-4) for medium labeled (M) medium, 25 mg/L L-[$^{13}C_6$,$^{15}N_4$] arginine (Arg-10) and 25 mg/L L-[$^{13}C_6$,$^{15}N_2$] lysine (Lys-8) for heavy labeled (H) medium.

Antibiotics supplementation:

Ampicillin, 100 mg/L (stock concentration is 100 mg/ml).

Kanamycin, 50 mg/L (stock concentration is 50 mg/ml).

4.4 Microbe strains

All the BU numbers in the following are the numbers used in our lab database, in order to easily remember and understand, they are referred as the following names in bold in this thesis:

E. coli BU1, **WT** strain *Escherichia coli* K-12 MG1655

E. coli GM117C1 (Evo), one adapted strain from WT by GM3 device.

E. coli GM117C3 (Evo), second adapted strain from WT by GM3 device.

P1 bacteriophage, used for gene deletion.

Control strain, *E. coli* BU173 (*ΔargAΔlysA*::*kanR*, *frt*+), *argA* and *lysA* KO from WT strain.

Evo-1, *E. coli* BU171 (Evo, *ΔargAΔlysA*::*kanR*, *frt*+), *argA* and *lysA* KO from GM117C1.

Evo-2, *E. coli* BU172 (Evo, Δ*argA*Δ*lysA*::*kanR*, *frt*+), *argA* and *lysA* KO from GM117C3.

Evo-3, *E. coli* BU174 (Δ*argA*Δ*lysA*::*kanR*, *frt*+, Evo), one adapted strain from the control strain by GM3.

Evo-4, *E. coli* BU175 (*ΔargAΔlysA::kanR*, *frt*+, Evo), another adapted strain from the control strain by GM3.

Δefp strain, *E. coli* BU62 (*ΔargAΔlysAΔefp*::*kanR*, *frt*+), *argA*, *lysA* and *efp* KO strain.

***Δefp* Evo-1**, *E. coli* BU165 (Evo, *ΔefpΔargAΔlysA::kanR*, *frt*+), one adapted *Δefp* strain by GM3, *argA* and *lysA* were KO after the evolution.

***Δefp* Evo-2**, *E. coli* BU166 (Evo, *ΔefpΔargAΔlysA*::*kanR*, *frt*+), another strain adapted from *Δefp* strain by GM3, *argA* and *lysA* were KO after evolution.

***Δefp* Evo-3**, *E. coli* BU167 (*ΔargAΔlysAΔefp*::*kanR*, *frt*+, Evo), one adapted *Δefp* strain by GM3, *argA* and *lysA* were KO before evolution.

***Δefp* Evo-4**, *E. coli* BU168 (*ΔargAΔlysAΔefp*::*kanR*, *frt*+, Evo), another adapted strain based on the *Δefp* strain, in which *argA* and *lysA* have been KO before evolution.

ΔyeiP strain, *E. coli* BU193 (*ΔargAΔlysAΔyeiP*::*kanR*, *frt*+), *yeiP* was KO based on the control strain.

DK strain*, E. coli* DK (*ΔargAΔlysAΔefpΔyeiP::kanR*, *frt+*), double knock-out of *efp* and *yeiP* based on the control strain.

4.5 Plasmids

Plasmid	Origin of replication	Resistance
pKD46	oriR101; w/repA101ts	Amp
pKD4	oriR6Kgamma	Kan
pCP20	oriR101	Amp

4.6 Primers for PCR

All the primers in this work were purchased from Sigma-Aldrich (Taufkirchen, DE) as dry desalted then diluted by ddH_2O to 100 μM. The primers more than 40 bps were purchased by HPLC purity form.

Table 20. Recombineering primer pair for FRT-kanR-FRT cassette

Primers	5' part	3'part (5'→3')	Total sequence (5'→3')
Forward primer Rec_fwd	50 nt upstream of target gene forward strand	gtgtaggctggagcttc Tm 62.5 °C	$N_{50\ up}$ gtgtaggctggagcttc
Reverse primer Rec_rev	50 nt downstream of target gene forward strand	catatgaatatcctccttag Tm 48.7 °C	$N_{50\ down}$ catatgaatatcctccttag

Table 21. Control primers for *argA* and *lysA* genes knock-out checking

Primers	Sequence	Tm (°C)
argA-C1	TAAACGACGACGGCTGATTG	62
argA-C2	CTGGCGGCGTTGTTTAGTTC	64
argA-C5	CATTAGTGACGCCCTGGGAA	64
kanR-K1	CAGTCATAGCCGAATAGCCT	61
kanR-K2	TTGTCAAGACCGACCTGTCC	63
lysA-C1	CTCTCGCAATCCGGTAATCC	62
lysA-C2	GCTGGTACGTCGTCATTCAG	62
lysA-C5	CAATGTGCATGTGAATGCCG	62

Table 22. Length of colony PCR products by checking primers.

Forward primer	Reverse primer	Length of PCR product in WT strain (bps)	Length of PCR product in gene KO strain (bps)
argA-C1	*argA*-C2	1693	445
argA-C1	*argA*-C5	919	-
argA-C1	*kanR*-K1	-	-
kanR-K2	*argA*-C2	-	-
lysA-C1	*lysA*-C2	1450	1664

lysA-C1	*lysA*-C5	691	-
lysA-C1	*kanR*-K1	-	631
kanR-K2	*argA*-C2	-	980

4.7 Kits

GeneJET Plasmid Midiprep Kit	Thermo Scientific (Waltham, MA, USA)
GeneJET PCR purification Kit	Thermo Scientific (Waltham, MA, USA)
Pierce™ BCA Protein Assay Kit	Thermo Scientific (Waltham, MA, USA)

4.8 Buffers and Solutions

1× TAE Buffer: 40mM Tris, 20mM acetic acid, and 1mM EDTA.

Bacterial lysis buffer: 125 mM Tris-HCL (pH 7.4), 150 mM NaCl, 1 mM DTT, 1 mM EDTA, 100 mg/L lysozyme, 1% Triton X-100, 1 tablet proteinase inhibitor.

ABC Buffer: 100 mM Ammonium bicarbonate, pH 7.5.

Buffer A: 0.5% Acetic acid in ddH_2O.

Buffer B: 80% Acetonitrile, 0.5% Acetic acid in ddH_2O

Buffer A*: 3% Acetonitrile, 0.3% TFA in ddH_2O

Buffer A*/A: 30% Buffer A* + 70% Buffer A

5 Methods

5.1 Gene deletion from chromosomal genes in *E. coli*.

5.1.1 Gene knock-out based on λ red system carried by plasmid pKD46

The gene deletion in *E. coli* chromosome is based on the *λ* Red system (*γ, β, exo*), which is an own homologous recombination system encoded by bacteriophage. The basic strategy is using a selectable antibiotic resistance gene to replace the target chromosomal gene. The plasmid with selected resistance gene will be templated for PCR, in which the primers contain ~50-nt extensions that are homologous to an adjacent region of the gene to be knocked out. In the template plasmids, the resistance genes are flanked by FRT (Flp recognition target). The resistance gene can be removed by a helper plasmid expressing the Flp recombinase, which is acting on the directly repeated FRT sites flanking the resistance gene [167].

5.1.1.1 PCR of FRT-kanR-FRT cassette containing fragment

In this study, the plasmid pKD46 was employed as *λ* Red function carrier. The target deletion sequence was replaced by an FRT-kanR-FRT cassette, which is amplified from the template plasmid pKD4 with the primers contain 50 bps sequence from both up- and down-stream of the target gene. The PCR products are digested with Dpn I FastDigest restriction enzymes to linear form, subsequently purified from the electrophoretic gel.

Table 23. PCR mixture for FRT-kanR-FRT cassette containing fragment.

Component	Stock concentration	Final concentration	Volume
Rec_fwd	25 pmol/µl	0.5 µM	1 µl
Rec_rev	25 pmol/µl	0.5 µM	1 µl
pKD4	20-100 ng/ µl	1-2 ng	x µl
PCR reaction buffer	10×	1×	5 µl
dNTPs	2.5 mM each	0.2 mM	4 µl
DNA polymerase	5 units/ µl	0.1-1.5 units	0.3 µl
H_2O	-	-	38.7-x µl
V_{tot}			50 µl

Table 24. PCR Progress for FRT-kanR-FRT cassette containing fragment.

Step	Temperature	Time	Cycles
Denaturation	95 °C	2 min	1
Denaturation	95 °C	30 s	30
Annealing	55 °C	1 min/kbps	
Elongation	72 °C	30 s	
End elongation	72 °C	10 min	1
Storage	4 °C	∞	-

5.1.1.2 Electrocompetent target cells preparation

The competent cells are necessary for the transformation of target replacing DNA fragments and helper plasmids. Steps of competent cells prepare are as follows: the frozen stock (-80 °C) of the cells were pre-cultured in 5 ml LB at 37 °C, 220 rpm, O/N. The pre-cultured cells were inoculated to 50 ml LB (with an inoculation rate of 1:100) in a 250 ml baffled flask as main-culture, which was incubated at 37 °C, 220 rpm until the OD_{600} reaches to 0.4. Then the cells were harvested by a centrifugation at 4000 rpm, 4 °C, with 10 min. Subsequently, the cells were washes by pre-chilled (4 °C) and sterilized 10% glycerol twice. Finally, the cells pellets were resuspended by cold 10% glycerol to the final concentration of OD_{600} be 35-45.

5.1.1.3 Transformation of pKD46 into the target cells by electroporation

50 µl of the prepared electro-component target cell was mixed with 20 ng of the salt-free pKD46 plasmid in a chilled sterile Eppi tube on ice. The mixture was transferred to a chilled 0.1 cm gap electroporation cuvette on the ice. Then electroporation was performed immediately under 1.8 kV voltage by BioRad Gene Pulser. 1 ml pre-warmed (~37 °C) LB medium was added to the cuvette after the electroporation as soon as possible. Afterward, the cells were incubated at 30 °C, 200 rpm for one hour (the plasmid would be lost at 37 °C growth condition). 50 µl of the out grown mixture was inoculated into 5 ml LB^{Amp} and incubated at 30 °C, O/N. It was verified by pKD46 plasmid isolation from target cells.

5.1.1.4 Electrocompetent target cells harboring pKD46 preparation

The cells harboring pKD46 were pre-cultured from frozen stock (-80 °C) into 5 ml LB at 30 °C, 220 rpm, o/n. The per-cultured cells were inoculated to 50 ml LB^{Amp} and incubated until OD_{600} reach to 0.2, and then 500 µl 20% (W/V) L-arabinose was added as an inducer and the cells were incubated to a final OD_{600} of 0.4-0.6. Then the cells were washed and harvested as mentioned in the first electro-competent cells preparation.

5.1.1.5 Transformation and recombination of FRT-kanR-FRT deletion cassette

50-150 ng of salt-free FRT-kanR-FRT deletion cassette mixed with 50 µl electro-competent cells harboring pKD46 in the chilled sterile Eppi tube on ice. And the electroporation was performed under same conditions and equipment as the pKD46 plasmid transformation mentioned above. The transformed cells were incubated at 37 °C (it is not required any more for the maintenance of pKD46 plasmid). A mixture of 50 µl the outgrown cells and 150 µl LB medium were plated onto an LB^{Kan} plate and incubated at 37 °C, O/N. The positive KanR recombineering clones were screened by three rounds PCR, then the stable hit colony was obtained.

5.1.1.6 Removal of the *kanR* marker by Flp recombination ("Flp-out")

After the genome replacement of FRT-kanR-FRT cassette on target gene position, the pCP20 plasmid was transformed into the target *kanR* cells (both of heat shock and electroporation are suitable) and

incubated on LB^{Amp} plate at 30 °C to "flp-out" the *kanR* label. The hit colony was streaked out three times by LB^{Amp} plate at 30 °C and changed to 41 °C to remove pCP20 plasmid. Then both of *kanR* and *ampR* would be removed and the deletion strain was verified by colony RCR.

5.1.2 Gene knock-out based on P1 transduction

Bacteriophage P1 is used for generalized transduction. The basic strategy for gene deletion by P1 transduction is that the phage is first grown on a donor strain (containing the elements to be knocked out), then the produced phage lysate is used to infect the recipient strain. The lysate contains bacterial DNA as well as phage DNA, the subsequent genetic recombination will be catalyzed by the recipient strain's enzymes, and the donor strain fragment will be incorporated into recipient chromosome (Figure 53) [168].

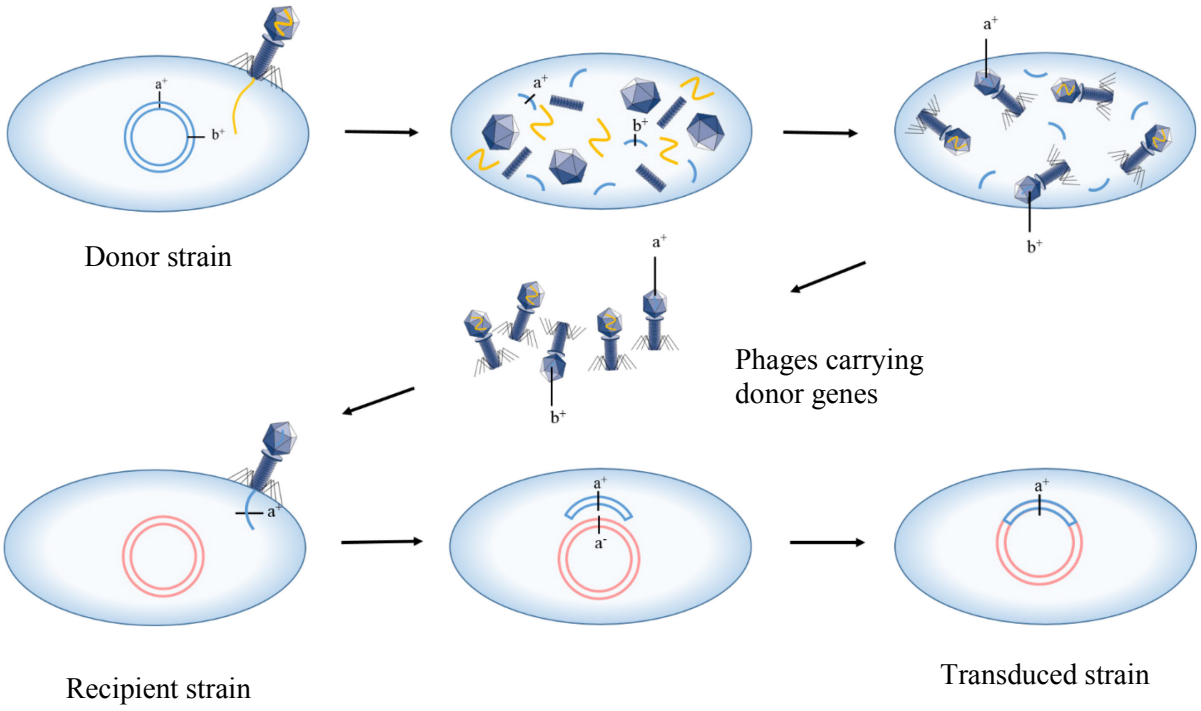

Figure 53. Phage P1 caused generalized transduction, modified from Griffiths, et al [169].

5.1.2.1 Grow phage on recipient strain

This is a preliminary step to ensure that the procedure is as clean as possible and to reduce the risk of transferring foreign DNA.

A single colony of the strain who will be receiving the genetic modification was inoculated to a liquid culture (LB medium + 5 mM $CaCl_2$ + 0.2% glucose), in which calcium facilitates the physical interaction between the phage and the bacterial cell. 100 µl phage stock was added to 5 ml bacterial liquid culture that OD_{600} of 0.1-0.2 and incubated at 37 °C three hours. The recipient cells were killed

by adding of 15 drops chloroform (3 drops per ml culture). The supernatant was removed to fresh tubes, three additional drops of chloroform were added per ml of culture and which was stored at 4 °C.

5.1.2.2 Grow phage on donor strain

The phage from the last step was grown on the *E. coli* strain whose genetic modification will be transferred. The process is same as the last step, just replaced the recipient strain to donor strain.

5.1.2.3 Transfer genetic modification to recipient strain

The genetic modification was transferred to the recipient strain through the phage obtained from the donor strain in above step.

A liquid culture (LB medium + 5 mM $CaCl_2$ + 0.2% glucose) was inoculated with a single colony of recipient strain. Centrifuge the culture was centrifugedat 5000 rpm with10 min when the OD_{600} of 0.8-1.0. Afterward, the cell pellet was resuspended in a ¼ volume of LB medium with 5 mM $CaCl_2$ and 100 mM $MgSO_4$. Set up four reactions in 1.5 ml Eppendorf tubes were set up as follows:

a. 100 µl recipient cells with 100 µl undiluted phage
b. 100 µl recipient cells with 100 µl 1/10 dilution of phage in LB, add 5 mM $CaCl_2$ and 100 mM $MgSO_4$ (10 µl phage + 90 µl LB + 5 mM $CaCl_2$ + 100 mM $MgSO_4$).
c. 100 µl recipient cells with 100 µl LB, add 5 mM $CaCl_2$ and 100 mM $MgSO_4$ (control for spontaneous resistance)
d. 100 µl phage with 100 µl LB, add 5 mM $CaCl_2$ and 100 mM $MgSO_4$ (control for the presence of any un-killed donor cells).

The settings were incubated at 37 °C without shaking for 30 min. 200 µl 1M sodium citrate (pH 5.5) was added, which is a chelator of calcium and is used to disrupt the physical interaction between the phage and bacterial cell. The mixture with 1 ml LB medium was shaken at 37 °C for 1 hour. The culture was centrifuged and the pellet was resuspended in 100 µl LB with 100 mM sodium citrate and then plated on LB with antibiotic plates O/N.

If the transduction works well, several colonies should be conspicuously observed on the test plates (reaction mixture “an” and “b”) in the following day. On the contrary, if no colonies grown on the plates during 24-48 hours, it means the transduction did not work, and it should be repeated. And the two control plates (reaction mixture “c” and “d”) should be clean within 48 hours. Sometimes, spontaneous antibiotic resistance mutant might appear on the first control plate (reaction mixture “c”) after 48 hours. If there are colonies appear on the second control plate (reaction mixture “d”), then the phage stock could be contaminated with cells from the recipient strain.

5.1.2.4 Isolating transductants

Once we observed colonies from the test plates and no colonies on the control plates, it means that we obtain the positive result. Then pick up single transductant and streak on the LB with an antibiotic plate, incubate at 37 °C O/N.

5.1.2.5 Verification of transductants via PCR

Two pairs of primers are necessary for the verification of the correct genetic modification. One pair of primers will need to recognize a region of DNA outside of modification on the genome of the recipient, and the other pair will need to recognize the genetic modification itself. For the Keio strains that we used in this project, the second pair of primers will recognize the kan resistance cassette.

5.2 Automated evolution with GM3

The automated continuous evolution cultures were performed in MS-glucose medium with additional 80 mg/L L-arginine and 80 mg/L L-lysine at 30 °C. In the turbidostat mode, the chambers were sterilized 2-4 times per day, pulsed with 30% of the culture volume and a density threshold of 80 (OD_{600} 0.8 E). Every week, the samples were taken and froze at -80 °C for safety storage and further study.

5.3 SILAC applied to *E. coli* cell culture

5.3.1 Bacterial growth in SILAC media

The first step of bacterial culture is the activation and enrichment of cells, in which the single colonies of experimental strains were streaked from the standard plates and inoculated into 12 ml sterile culture tubes with 5 ml liquid LB medium with appropriate antibiotics, and the cells were incubated at 37 °C O/N. The second step is the SILAC pre-culture, in which 50 µl of the O/N cultured bacterial solution was inoculated to 5ml SILAC-M9 minimal medium (the inoculation ratio is 1:100) supplemented with appropriate antibiotics, and bacteria were grown to the mid-logarithmic phase (OD_{600} is between 0.3 and 0.5). Afterward, the third step is the main culture, where the SILAC pre-culture is inoculated with an initial OD_{600} between 0.03 and 0.05 to 50 ml SILAC-M9 minimal medium in 300 ml Erlenmeyer flasks. After the strains were incubated to the desired OD_{600} of 0.3 to 0.5. Finally, the cells were harvested by centrifuging at 4 °C at 4000 rpm during 15 min, discarding the supernatant, and the bacterial pellets were stored at -80 °C until sample preparation. The composition of the SILAC-M9 minimal medium is described in Section 4.3.

5.3.2 Preparation of proteome samples

5.3.2.1 Bacterial lysis

Bacterial pellets were washed with water twice, and dissolved in 500 µl lysis buffer (see Section 4.8) and incubated at 37 °C, during 30 minutes. Lysis was achieved by sonication using 6 cycles of 30 seconds and 40% amplitude, on an ice bath. Cell debris was removed by centrifugation at 14000 rpm and 4°C during 10 minutes, and supernatants were transferred to new Eppendorf tubes.

5.3.2.2 Determination of protein concentration

The total protein concentration was determined by Pierce™ BCA Protein Assay Kit (Thermo Scientific).

5.3.2.3 MS samples preparation

A sample mixture contains 100 µg each set of isotope labeled bacterial proteins, of which the volume was calculated depending on the total protein concentration. Samples were supplemented with Lämmli buffer (6×) and DTT (a final concentration of 1 mM), and then the sample mixtures were incubated at 97 °C for 10 min. Subsequently, IAA was added to a final concentration of 5.5 mM once the samples are cooled down to room temperature. Then the samples were kept in dark and at the RT 30 min.

The samples were loaded on a 4-12 % acrylamide gradient gel (Mini-PROTEAN® TGX™ Precast Gels, BIO-RAD), and after an electrophoresis run between 150-200 V, the gel was washed twice by water for 10 min and stained by SimplyBlue™ SafeStain (Thermo Scientific) 15 min. Afterward, the stained gel was washed by water until the blue sample bands can be clearly seen, and then each sample lane was fractionated into 10 gel pieces and performed in-gel digestion by trypsin at 37 °C O/N [170]. Subsequently, the resulting peptides were desalted by C18 stage tips protocol [171]. Then the MS samples are ready and could be stored in -80 °C for measurement.

5.3.3 MS measurement and data analysis

All samples were measured on an Agilent 1200 nanoflow-HPLC (Agilent Technologies GmbH, Waldbronn, DE) coupled on an LTQ Orbitrap XL mass spectrometer (ThermoFisher Scientific, Bremen, DE). For the chromatographical separation of the peptides, we employed a fused silica HPLC column tip with 75 µm inner diameter were self-packed [172] with ReproSil-Pur 120 C18-AQ 3 µm resin (Dr. Maisch GmbH, Ammerbuch, DE) to a length of 20 cm. Peptides were injected into the column at a flow rate of 0.5 µl/min in 98 % buffer A (0.5% acetic acid) and 2% buffer B (80% acetonitrile in 0.5% acetic acid). Separation was achieved by a linear gradient from 10% to 30% of buffer B at a flow rate of 0.25 µl/min. The mass spectrometer was operated in the data-dependent mode and switched automatically between MS (max. of 1 x10 ions) and MS/MS. Each MS scan was followed by a maximum of five MS/MS scans in the linear ion trap using normalized collision energy of 35% and a target value of 5,000. Parent ions with charge states of z = 1 and unassigned charge states were excluded from fragmentation.

The mass range for MS was m/z = 370 to 2,000. The resolution was set to 60,000. MS parameters were as follows: spray voltage 2.3 kV; no sheath and auxiliary gas flow; ion transfer tube temperature 125°C.

Data analysis

All MS raw data were processed with the MaxQuant software suite version 1.4.1.2 [84, 173] which performs peak and SILAC-pair detection, generates peak lists of mass error corrected peptides and data base searches. The SILAC labeling parameter was set to a multiplicity of three (Light: Arg-0 and Lys-0, Medium: Arg-6 and Lys-4, Heavy: Arg-10 and Lys-8). A database search was performed by the search engine Andromeda [174], which has been integrated into MaxQuant. Trypsin/P was required as enzyme specificity, with an allowance of up to three miss cleavages. MS/MS spectra were searched against the FASTA file of UniProt *Escherichia coli* K12 MG1655 database (taxonomy reference: 83333), which complete proteome set containing 4306 proteins entries, was down loaded July 16, 2015. The variable modifications were set as N-terminal acetylation and Methionine oxidation. Cysteine carbamidomethylation was defined as a fixed modification. MS/MS tolerance was set to 0.5 Da. The average mass precision of identified peptides was, in general, less than 1 ppm after recalibration. Peptide lists were further used by MaxQuant to identify and relatively quantify proteins using the following parameters: peptide and protein false discovery rates (FDR) were set to 0.01, maximum peptide posterior error probability (PEP) was set to 0.1, minimum peptide length was set to 7, minimum number peptides for identification and quantitation of proteins was set to two of which one must be unique, and identified proteins have been re-quantified. The “match-between-run” option (1 min) was used.

The software Perseus (version 1.4.0.8) [175] was employed for the following data analysis: Log2 transform of the data, the generation of the histograms for the proteome changed ratios, scatter plot graphs for the correlation of the replicates, and the heat maps of hierarchical clustering.

The biological function descriptions are according to UniProt (www.uniprot.org). The interactions of proteins are analyzed by String (string-db.org).

6 References

[1] G. N. Ramachandran, C. Ramakrishnan and V. Sasisekharan, "Stereochemistry of polypeptide chain configurations," *Journal of molecular biology ,* vol. 7, no. 1, pp. 95-99, 1963.

[2] G. N. Ramachandran and V. Sasisekharan, "Conformation of polypeptides and proteins," *Adv Protein Chem,* vol. 23, pp. 283-438, 1968.

[3] F. A. Momany, R. F. McGuire, A. W. Burgess and H. A. Scheraga, "Energy parameters in polypeptides. VII. Geometric parameters, partial atomic charges, nonbonded interactions, hydrogen bond interactions, and intrinsic torsional potentials for the naturally occurring amino acids," *J. Phys. Chem.,* vol. 79, no. 22, pp. 2361-2381, 1975.

[4] Y. K. Kang and H. Y. Choi, "Cis–trans isomerization and puckering of proline residue," *Biophys. Chem.,* vol. 111, pp. 135-142, 2004.

[5] Y. K. Kang, "Puckering Transition of Proline Residue in Water," *J. Phys. Chem. B ,* vol. 111, pp. 10550-10556, 2007.

[6] S. M. Weiss, A. Jabs and R. Hilgenfeld, "Peptide bonds revisited," *Nat. Struct. biol,* vol. 5, no. 8, p. 676, 1998.

[7] M. D. Shoulders and R. T. Raines, "Collagen Structure and Stability," *Annu. Rev. Biochem.,* vol. 78, p. 929–958, 2009.

[8] W. J. Wedemeyer, E. Welker and H. A. Scheraga, "Proline Cis-Trans Isomerization and Protein Folding," *Biochemistry,* vol. 41, pp. 14637-14644, 2002.

[9] S. Fischer, R. L. Dunbrack and M. Karplus, "Cis- Trans Imide Isomerization of the Proline Dipeptide," *J. Am. Chem. Soc.,* vol. 116, pp. 11931-11937, 1994.

[10] T. M. H. Bach and H. Takagi, "Properties, metabolisms, and applications of L-proline analogues," *Appl Microbiol Biotechnol,* vol. 97, p. 6623–6634, 2013.

[11] A. J. Delauney and D. P. S. Verma, "Proline biosynthesis and osmoregulation in plants," *The Plant Journal,* vol. 4, no. 2, pp. 215-223, 1993.

[12] L. N. Csonka and A. D. Hanson, "Prokaryotic osmoregulation: genetics and physiology," *Annu Rev Microbiol,* vol. 45, p. 569–606, 1991.

[13] A. S. Rudolph and J. H. Crowe, "Membrane stabilization during freezing: The role of two natural cryoprotectants, trehalose and proline," *Cryobiology,* vol. 22, no. 4, pp. 367-377, 1985.

[14] H. Takagi, K. Sakai, K. Morida and S. Nakamori, "Proline accumulation by mutation or disruption of the proline oxidase gene improves resistance to freezing and desiccation stresses in Saccharomyces cerevisiae," *FEMS Microbiol Lett,* vol. 184, no. 1, pp. 103-108, 2000.

[15] J. F. Carpenter and J. H. Crowe, "Modes of stabilization of a protein by organic solutes during desiccation," *Cryobiology,* vol. 25, no. 5, pp. 459-470, 1988.

[16] T. Hottiger, C. De Virgilio, M. N. Hall, et al., "The role of trehalose synthesis for the acquisition of thermotolerance in yeast," *Eur. J. Biochem,* vol. 219, pp. 187-193, 1994.

[17] J. Matysik, Alia, B. Bhalu and P. Mohanty, "Molecular mechanisms of quenching of reactive oxygen species by proline under stress in plants," *Current Science,* vol. 82, no. 5, pp. 525-532, 2002.

[18] B. Schobert and H. Tschesche, "Unusual solution properties of proline and its interaction with proteins," *Biochimica et Biophysica Acta,* vol. 541, no. 2, pp. 270-277, 1978.

[19] D. Samuel, G. Ganesh, P.-W. Yang, et al., "Proline inhibits aggregation during protein refolding," *Protein Science,* vol. 9, no. 2, pp. 344-352, 2000.

[20] Z. Ignatova and L. M. Gierasch, "Inhibition of protein aggregation in vitro and in vivo by a natural osmoprotectant," *PNAS,* vol. 103, no. 36, p. 13357–13361, 2006.

[21] L. K. Doerfel, I. Wohlgemuth, K. Vladimir, et al., "Entropic Contribution of Elongation Factor P to Proline Positioning at the Catalytic Center of the Ribosome," *J. Am. Chem. Soc. ,* vol. 137, pp. 12997-13006, 2015.

[22] M. V. Rodnina, "The ribosome as a versatile catalyst: reactions at the peptidyl transferase center," *Curr. Opin. Struc. Biol.,* vol. 23, no. 4, pp. 595-602, 2013.

[23] D. N. Wilson, S. Arenz and R. Beckmann, "Translation regulation via nascent polypeptide-mediated ribosome stalling," *Curr. Opin. Stru. Biol,* vol. 37, pp. 123-133, 2016.

[24] M. Y. Pavlov, R. E. Watts, Z. Tan, et al., "Slow peptide bond formation by proline and other N-alkylamino acids in translation," *PNAS,* vol. 106, no. 1, pp. 50-54, 2009.

[25] S. Melnikov, J. Mailliot, L. Rigger, et al., "Molecular insights into protein synthesis with proline residues," *EMBO reports,* p. e201642943, 2016.

[26] I. Wohlgemuth, S. Brenner, M. Beringer and M. V. Rodnina, "Modulation of the Rate of Peptidyl Transfer on the Ribosome by the Nature of Substrates," *J. Biol. Chem.,* vol. 283, no. 47, pp. 32229-32235, 2008.

[27] H. Muto and K. Ito, "Peptidyl-prolyl-tRNA at the ribosomal P-site reacts poorly with puromycin," *Biochem Biophys Res Commun,* vol. 366, no. 4, pp. 1043-1047, 2008.

[28] M. Johansson, K.-W. Ieong, S. Trobro, et al., "pH-sensitivity of the ribosomal peptidyl transfer reaction dependent on the identity of the A-site aminoacyl-tRNA," *PNAS,* vol. 108, no. 1, pp. 79-84, 2011.

[29] S. Ude, J. Lassak, A. L. Starosta, et al., "Translation Elongation Factor EF-P Alleviates Ribosome Stalling at Polyproline Stretches," *Science,* vol. 339, pp. 82-85, 2013.

[30] L. K. Doerfel, I. Wohlgemuth, C. Kothe, et al., "EF-P Is Essential for Rapid Synthesis of Proteins Containing Consecutive Proline Residues," *Science,* vol. 339, pp. 85-88, 2013.

[31] C. J. Woolstenhulme, N. R. Guydosh, R. Green and A. R. Buskirk, "High-Precision Analysis of Translational Pausing by Ribosome Profiling in Bacteria Lacking EFP," *Cell Reports,* vol. 11, pp. 13-21, 2015.

[32] L. Peil, A. L. Starosta, J. Lassak, et al., "Distinct XPPX sequence motifs induce ribosome stalling, which is rescued by the translation elongation factor EF-P," *PNAS,* vol. 110, no. 38, p. 15265–15270, 2013.

[33] B. R. Glick and M. C. Ganoza, "Identification of a soluble protein that stimulates peptide bond synthesis," *PNAS,* vol. 72, no. 11, pp. 4257-4260, 1975.

[34] N. C. Kyrpides and C. R. Woese, "Universally conserved translation initiation factors," *PNAS,* vol. 95, no. 1, pp. 224-228, 1998.

[35] M. Bailly and V. de Crécy-Lagard, "Predicting the pathway involved in post-translational modification of Elongation factor P in a subset of bacterial species," *Biology Direct,* vol. 5, p. 3, 2010.

[36] G. An, B. R. Glick, J. D. Friesen and M. C. Ganoza, "Identification and quantitation of elongation factor EF-P in Escherichia coli cell-free extracts," *Canadian Journal of Biochemistry,* vol. 58, no. 11, pp. 1312-1314, 1980.

[37] K. Hanawa-Suetsugu, S.-i. Sekine, H. Sakai, et al., "Crystal structure of elongation factor P from Thermus thermophilus HB8," *PNAS,* vol. 101, no. 26, p. 9595–9600, 2004.

[38] G. Blaha, R. E. Stanley and T. A. Steitz, "Formation of the First Peptide Bond: The Structure of EF-P Bound to the 70S Ribosome," *Science,* vol. 325, pp. 966-970, 2009.

[39] J.-H. Park, H. E. Johansson, H. Aoki, et al., "Post-translational Modification by β-Lysylation Is Required for Activity of Escherichia coli Elongation Factor P (EF-P)," *J. Biol. Chem.,* vol. 287, pp. 2579-2590, 2012.

[40] W. W. Navarre, S. B. Zou, H. Roy, et al., "PoxA, YjeK, and Elongation Factor P Coordinately Modulate Virulence and Drug Resistance in Salmonella enterica," *Molecular Cell,* vol. 39, no. 2, pp. 209-221, 2010.

[41] T. Yanagisawa, T. Sumida, R. Ishii, et al., "A paralog of lysyl-tRNA synthetase aminoacylates a conserved lysine residue in translation elongation factor P," *Nat. Struct. Mol. Biol.,* vol. 17, pp. 1136-1143, 2010.

[42] T. J. Bullwinkle, S. B. Zou, A. Rajkovic, et al., "(R)-β-Lysine-modified Elongation Factor P Functions in Translation Elongation," *J. Biol. Chem.,* vol. 288, pp. 4416-4423, 2013.

[43] J. Lassak, E. C. Keilhauer, M. Fürst and e. al., "Arginine-rhamnosylation as new strategy to activate translation elongation factor P," *Nat. Chem. Biol,* vol. 11, pp. 266-270, 2015.

[44] A. Rajkovic, S. Erickson, A. Witzky, et al., "Cyclic Rhamnosylated Elongation Factor P Establishes Antibiotic Resistance in Pseudomonas aeruginosa," *mBio,* vol. 6, no. 3, pp. e00823-15, 2015.

[45] T. Yanagisawa, H. Takahashi, T. Suzuki, et al., "Neisseria meningitidis Translation Elongation Factor P and Its Active-Site Arginine Residue Are Essential for Cell Viability," *PLoS ONE,* vol. 11, no. 2, p. e0147907, 2016.

[46] S. J. Hersch, M. Wang, S. B. Zou and e. al., "Divergent Protein Motifs Direct Elongation Factor P-Mediated Translational Regulation in Salmonella enterica and Escherichia coli," *mBio,* vol. 4, no. 2, pp. e00180-13, 2013.

[47] K. L. Gorres and R. T. Raines, "Prolyl 4-hydroxylase," *Crit Rev Biochem Mol Biol.,* vol. 45, no. 2, pp. 106-124, 2010.

[48] J. J. Hutton and S. Udenfriend, "Soluble collagen proline hydroxylase and its substrates in several animal tissues," *PNAS,* vol. 56, pp. 198-202, 1966.

[49] R. E. Rhoads and S. Udenfriend, "Decarboxylation of α-ketoglutarate coupled to collagen proline hydroxylase," *PNAS,* vol. 62, p. 1473–1478, 1968.

[50] H. Dickens, A. Ullrich, D. Runge, et al., "Anticancer drug cis-4-hydroxy-L-proline: Correlation of preclinical toxicology with clinical parameters of liver function," *Mol. Med. Rep,* vol. 1, pp. 459-464, 2008.

[51] E. M. Tan, L. Ryhänen and J. Uitto, "Proline Analogues Inhibit Human Skin Fibroblast Growth and Collagen Production in Culture," *J. Invest. Dermatol.,* vol. 80, no. 4, pp. 261-267, 1983.

[52] T. Nakajima and B. E. Volcani, "3,4-Dihydroxyproline: A New Amino Acid in Diatom Cell Walls," *Science,* vol. 164, no. 3886, pp. 1400-1401, 1969.

[53] A. Buku, T. Wieland, H. Bodenmüller and H. Faulstich, "Amaninamide, a new toxin ofAmanita virosa mushrooms," *Experientia,* vol. 36, no. 1, pp. 33-34, 1980.

[54] R. Laursen, "Reflection on the structure of mussel adhesive protein," *Results Probl Cell Differ,* vol. 19, pp. 52-72, 1992.

[55] G. W. Fleet, A. Karpas, R. A. Dwek, et al., "Inhibition of HIV replication by amino-sugar derivatives," *FEBS Letters,* vol. 237, no. 1-2, pp. 128-132, 1988.

[56] T. Baumann, J. H. Nickling, M. Bartholomae, et al., "Prospects of In vivo Incorporation of Non-canonical Amino Acids for the Chemical Diversification of Antimicrobial Peptides," *Front Microbiol,* vol. 8, p. Article 124, 2017.

[57] K. Lang and J. W. Chin, "Cellular Incorporation of Unnatural Amino Acids and Bioorthogonal Labeling of Proteins," *Chem. Rev.,* vol. 114, p. 4764−4806, 2014.

[58] F. Zinoni, A. Birkmann, W. Leinfelder and A. Böck, "Cotranslational insertion of selenocysteine into formate dehydrogenase from Escherichia coli directed by a UGA codon," *PNAS,* vol. 84, pp. 3156-3160, 1987.

[59] D. G. Longstaff, R. C. Larue and J. E. Faust, "A natural genetic code expansion cassette enables transmissible biosynthesis and genetic encoding of pyrrolysine," *PNAS,* vol. 104, no. 3, pp. 1021-1026, 2007.

[60] N. Budisa, C. Minks, S. Alefelder, et al., "Toward the experimental codon reassignment in vivo: protein building with an expanded amino acid repertoire," *The FASEB Journal,* vol. 13, no. 1, pp. 41-51, 1999.

[61] N. Terasaka, Y. Iwane, A.-S. Geiermann, et al., "Recent Developments of Engineered Translational Machineries for the Incorporation of Non-Canonical Amino Acids into Polypeptides," *Int. J. Mol. Sci.,* vol. 16, no. 3, pp. 6513-6531, 2015.

[62] D. D. Buechter, D. N. Paolella, B. S. Leslie, et al., "Co-translational Incorporation ofTrans-4-Hydroxyproline into Recombinant Proteins in Bacteria," *J. Biol. Chem,* vol. 278, pp. 645-650, 2003.

[63] C. Catherine, S. J. Oh, K.-H. Lee and S.-E. Min, "Engineering thermal properties of elastin-like polypeptides by incorporation of unnatural amino acids in a cell-free protein synthesis system," *Biotechnol. Bioproc,* vol. 20, pp. 417-422, 2015.

[64] J. T.-F. Wong, "Membership mutation of the genetic code: loss of fitness by tryptophan," *PNAS,* vol. 80, no. 20, pp. 6303-6306, 1983.

[65] Z. D. Blount, C. Z. Borland and R. E. Lenski, "Historical contingency and the evolution of a key innovation in an experimental population of Escherichia coli," *PNAS,* vol. 105, no. 23, p. 7899–7906, 2008.

[66] J. M. Bacher and A. D. Ellington, "Selection and Characterization of Escherichia coliVariants Capable of Growth on an Otherwise Toxic Tryptophan Analogue," *J. Bacteriol,* vol. 183, no. 18, pp. 5414-5425, 2001.

[67] M. G. Hoesl, S. Oehm, P. Durkin, et al., "Chemical Evolution of a Bacterial Proteome," *Angew. Chem. Int. Ed.,* vol. 54, pp. 10030-10034, 2015.

[68] A. Kuthning, P. Durkin, S. Oehm, et al., "Towards Biocontained Cell Factories: An Evolutionarily Adapted Escherichia coli Strain Produces a New-to-nature Bioactive Lantibiotic Containing Thienopyrrole-Alanine," *Sci. Rep.,* vol. 6, p. 33447, 2016.

[69] A. H. Badran and D. R. Liu, "In vivo continuous directed evolution," *Curr. Opin. Chem. Biol.,* vol. 24, pp. 1-10, 2015.

[70] K. M. Esvelt, J. C. Carlson and D. R. Liu, "A system for the continuous directed evolution of biomolecules," *Nature,* vol. 472, pp. 499-503, 2011.

[71] N. Ziv, N. J. Brandt and D. Gresham, "The Use of Chemostats in Microbial Systems Biology," *Journal of Visualized Experiments,* vol. 80, p. e50168, 2013.

[72] L. Avrahami-Moyal, D. Engelberg, J. W. Wenger, et al., "Turbidostat culture of Saccharomyces cerevisiae W303-1A under selective pressure elicited culture of Saccharomyces cerevisiae W303-1A under selective pressure elicited," *FEMS Yeast Res,* vol. 12, pp. 521-533, 2012.

[73] E. Toprak, A. Veres, J.-B. Michel, et al., "Evolutionary paths to antibiotic resistance under dynamically sustained drug selection," *Nat. Genet.,* vol. 44, pp. 101-105, 2011.

[74] D. Gresham and M. J. Dunham, "The enduring utility of continuous culturing in experimental evolution," *Genomics,* vol. 104, pp. 399-405, 2014.

[75] R. Mutzel and P. Marliere, "Experimentelle Evolution in vivo in kontinuierlicher Suspensionskultur," *Biospektrum,* vol. 16, no. 6, pp. 660-662, 2010.

[76] P. Marliere, J. Patrouix, V. Döring and et, al., "Chemical Evolution of a Bacterium's Genome," *Angew. Chem.,* vol. 123, pp. 1-7, 2011.

[77] S.-E. Ong and M. Mann, "Mass spectrometry–based proteomics turns quantitative," *Nature Chemical Biology,* vol. 1, pp. 252-262, 2005.

[78] G. L. Corthals, V. C. Wasinger, D. F. Hochstrasser and J.-C. Sanchez, "The dynamic range of protein expression: a challenge for proteomic research," *Proteins,* vol. 21, pp. 1104-1115, 2000.

[79] M. Ünlü, M. E. Morgan and J. Minden, "Difference gel electrophoresis: A single gel method for detecting changes in protein extracts," *Electrophoresis,* vol. 18, pp. 2071-2077, 1997.

[80] S. E. Ong, B. Blagoev, I. Kratchmarova, et al., "Stable isotope labeling by amino acids in cell culture, SILAC, as a simple and accurate approach to expression proteomics," *Molecular & cellular proteomics,* vol. 1, no. 5, pp. 376-386, 2002.

[81] G. Dittmar and M. Selbach, "SILAC for biomarker discovery," *Proteomics Clin. Appl.,* vol. 9, pp. 301-306, 2015.

[82] S.-E. Ong and M. Mann, "A practical recipe for stable isotope labeling by amino acids in cell culture (SILAC)," *Nature Protocol,* vol. 1, no. 6, pp. 2650-2660, 2006.

[83] T. Geiger, J. R. Wisniewski, J. Cox, et al., "Use of stable isotope labeling by amino acids in cell culture as a spike-in standard in quantitative proteomics," *Nature Protocols,* vol. 6, p. 147–157, 2011.

[84] J. Cox and M. Mann, "MaxQuant enables high peptide identification rates, individualized p.p.b.-range mass accuracies and proteome-wide protein quantification," *Nature Biotechnology,* vol. 26, no. 12, pp. 1367-1372, 2008.

[85] D. Gutnick, J. M. Calvo, T. Klopotowski and B. N. Ames, "Compounds Which Serve as the Sole Source of Carbon or Nitrogen for Salmonella typhimurium LT-2," *Journal of Bacteriology,* vol. 100, no. 1, pp. 215-219, 1969.

[86] J. W. payne, "Transport and utilization of peptides by bacteria," in *Microorganisms and nitrogen sources*, Chichester, UK, JW Wiley, 1980, pp. 211-256.

[87] B. G. Hogarth and C. F. Higgins, "Genetic Organization of the Oligopeptide Permease (opp) Locus of Salmonella typhimurium and Escherichia coli," *Journal of bacteriology,* vol. 153, no. 3, pp. 1548-1551, 1983.

[88] C. F. Higgins and M. M. Hardie, "Periplasmic protein associated with the oligopeptide permeases of Salmonella typhimurium and Escherichia coli.," *Journal of Bacteriology,* vol. 155, no. 3, pp. 1434-1438, 1983.

[89] W. N. Abouhamad, M. Manson, M. M. Gibson and C. F. Higgins, "Peptide transport and chemotaxis in Escherichia coli and Salmonella typhimurium: characterization of the dipeptide permease (Dpp) and the dipeptide-binding protein," *Molecular microbiology,* vol. 5, no. 5, pp. 1035-1047, 1991.

[90] I. D. Hiles, L. M. Powell and C. F. Higgins, "Peptide transport in Salmonella typhimurium: Molecular cloning and characterization of the oligopeptide permease genes," *Molecular and General Genetics MGG,* vol. 206, no. 1, pp. 101-109, 1987.

[91] E. W. Goodell and C. F. Higgins, "Uptake of Cell Wall Peptides by Salmonella typhimurium and Escherichia coli," *journal of Bacteriology,* vol. 169, no. 8, pp. 3861-3865, 1987.

[92] J. W. Payne and M. W. Smith, "Peptide Transport by Micro-organisms," *Advances in Microbial Physiology,* vol. 36, pp. 1-80, 1994.

[93] D. P. Zimmer, E. Soupene, H. L. Lee, et al., "Nitrogen regulatory protein C-controlled genes of Escherichia coli: Scavenging as a defense against nitrogen limitation," *PNAS,* vol. 97, no. 26, pp. 14674-14679, 2000.

[94] M. L. Urbanowski , L. T. Stauffer and G. V. Stauffer, "The gcvB gene encodes a small untranslated RNA involved in expression of the dipeptide and oligopeptide transport systems in Escherichia coli.," *Molecular Microbioiogy,* vol. 37, no. 4, pp. 856-568, 2000.

[95] E. R. Olson, D. S. Dunyak, L. M. Jurss and R. A. Poorman, "Identification and characterization of dppA, an Escherichia coli gene encoding a periplasmic dipeptide transport protein.," *Journal of bacteriology,* vol. 173, no. 1, pp. 234-244, 1991.

[96] M. V. Baev, D. Baev, A. J. Radek and J. .. W. Campbell, "Growth of Escherichia coli MG1655 on LB medium: monitoring utilization of amino acids, peptides, and nucleotides with transcriptional microarrays," *Applied Microbiology and Biotechnology,* vol. 71, no. 3, p. 317–322, 2006.

[97] D. Weitz, D. Harder, F. Casagrande, et al., "Functional and Structural Characterization of a Prokaryotic Peptide Transporter with Features Similar to Mammalian PEPT1," *J. B. Chem,* vol. 282, pp. 2832-2839, 2006.

[98] D. Harder, J. Stolz, F. Casagrande, et al., "DtpB (YhiP) and DtpA (TppB, YdgR) are prototypical proton-dependent peptide transporters of Escherichia coli," *FEBS J.,* vol. 275, pp. 3290-3298, 2008.

[99] H.-Y. Steiner, F. Naider and J. M. Becker, "The PTR family: a new group of peptide transporters," *Molecular Microbiology,* vol. 16, no. 5, pp. 825-834, 1995.

[100] H. Daniel, B. Spanier, G. Kottra and D. Weitz, "From Bacteria to Man: Archaic Proton-Dependent Peptide Transporters at Work," *Physiology,* vol. 21, pp. 93-102, 2006.

[101] L. Reitzer, "Nitrogen Assimilation and Global Regulatin in Escherichia coli," *Annu. Rev. Microbiol. ,* vol. 57, pp. 155-176, 2003.

[102] A. Sekowska, H.-F. Kung and A. Danchin, "Sulfur Metabolism in Escherichia coli and Related Bacteria: Facts and Fiction," *J. Mol. Microbiol. Biotechnol.,* vol. 2, no. 2, pp. 145-177, 2000.

[103] J. M. Berg, J. L. Tymoczko and L. Stryer, "Section 25.2 Purine Bases Can Be Synthesized de Novo or Recycled by Salvage Pathways," in *Biochemistry. 5th edition.*, New York, W H Freeman, 2002.

[104] J. M. Berg, J. L. Tymoczko and L. Stryer, "Section 25.1In de Novo Synthesis, the Pyrimidine Ring Is Assembled from Bicarbonate, Aspartate, and Glutamine," in *Biochemistry, 5th edition*, New York, W H Freeman, 2002.

[105] P. Nygaard , "Chapter 26 : Purine and Pyrimidine Salvage Pathways," in *Bacillus subtilis and Other Gram-Positive Bacteria: Biochemistry, Physiology, and Molecular Genetics*, Washington, D. C., American Society for Microbiology, 1993, p. 359.

[106] G. Koellner, A. Bzowska, B. W.-K. Wielgus-Kutrowska, et al., "Open and closed conformation of the E. coli purine nucleoside phosphorylase active center and implications for the catalytic mechanism," *Journal of Molecular Biology,* vol. 315, no. 3, pp. 351-371, 2002.

[107] D. T. Logan, E. Mulliez, K.-M. Larsson, et al., "A metal-binding site in the catalytic subunit of anaerobic ribonucleotide reductase," *PNAS,* vol. 100, no. 7, p. 3826–3831, 2002.

[108] B. Jochimsen, P. Nygaard and T. Vestergaard, "Location on the chromosome of Escherichia coli of genes governing purine metabolism," *Molec. gen. Genet,* vol. 143, pp. 85-91, 1975.

[109] B.-H. Song and J. Neuhard , "Chromosomal location, cloning and nucleotide sequence of the Bacillus subtilis cdd gene encoding cytidine/deoxycytidine deaminase," *Mol. Gen. Genet.,* vol. 216, pp. 462-468, 1989.

[110] C. F. Beck, J. .. L. Ingraham, J. Neuhard and E. Thomassen, "Metabolism of Pyrimidines and Pyrimidine Nucleosides by Salmonella typhimurium," *Journal of bacteriology,* vol. 110, no. 1, pp. 219-228, 1972.

[111] J. C. Leer, K. Hammer-Jespersen and M. Schwartz, "Uridine phosphorylase from Escherichia coli," *The FEBS Journal,* vol. 75, no. 1, p. 217–224, 1977.

[112] L. Gonzales-Siles, R. Karlsson, D. Kenny, et al., "Proteomic analysis of enterotoxigenic Escherichia coli (ETEC) in neutral and alkaline conditions," *BMC Microbiology,* vol. 17, no. 11, 2017.

[113] S. Schwarz and P. Van Dijck, "Trehalose metabolism: A sweet spot for Burkholderia pseudomallei virulence," *Virulence,* vol. 8, no. 1, pp. 5-7, 2017.

[114] M. V. Baev, D. Baev, A. J. Radek and J. W. Campbell, "Growth of Escherichia coli MG1655 on LB medium: monitoring utilization of sugars, alcohols, and organic acids with transcriptional microarrays," *Appl Microbiol Biotechnol,* vol. 71, p. 310–316, 2006.

[115] B. Perroud and D. Le Rudulier, "Glycine betaine transport in Escherichia coli: osmotic modulation," *Journal of Bacteriology,* vol. 161, no. 1, pp. 393-401, 1985.

[116] C. F. Higgins, C. J. Dorman, D. A. Stirling, et al., "A physiological role for DNA supercoiling in the osmotic regulation of gene expression in S. typhimurium and E. coli," *Cell,* vol. 52, no. 4, pp. 569-584, 1988.

[117] N. Gul and B. Poolman, "Functional reconstitution and osmoregulatory properties of the ProU ABC transporter from Escherichia coli," *Molecular Membrane Biology,* vol. 30, no. 2, pp. 138-148, 2013.

[118] J. Cairney, I. R. Booth and C. F. Higgins, "Osmoregulation of gene expression in Salmonella typhimurium: proU encodes an osmotically induced betaine transport system," *Journal of Bacteriology,* vol. 164, no. 2, pp. 1224-1232, 1985.

[119] C. W. Tabor and H. Tabor, "Polyamines," *Annu. Rev. Biochem.,* vol. 53, p. 749–790, 1984.

[120] K. Igarashi and K. Kashiwagi, "Polyamine Modulon in Escherichia coli: Genes Involved in the Stimulation of Cell Growth by Polyamines," *J. Biochem.,* vol. 139, p. 11–16, 2006.

[121] Z.-G. Qian, X.-X. Xia and S. Y. Lee, "Metabolic Engineering of Escherichia coli for the Production of Putrescine: A Four Carbon Diamine," *Biotechnology and Bioengineering,* vol. 104, no. 4, pp. 651-662, 2009.

[122] Y. Sugiyama, A. Nakamura, M. Matsumoto, et al., "A Novel Putrescine Exporter SapBCDF of Escherichia coli," *Journal of Biological Chemistry,* vol. 291, no. 51, pp. 26343-26351, 2016.

[123] S. Bi and L. Li, "Bacterial chemoreceptors and chemoeffectors," *Cell. Mol. Life Sci,* vol. 72, pp. 691-708, 2015.

[124] M. R. Kehry and F. W. Dahlquist, "The methyl-accepting chemotaxis proteins of Escherichia coli. Identification of the multiple methylation sites on methyl-accepting chemotaxis protein I.," *The Journal of Biological Chemistry,* vol. 257, pp. 10375-10386, 1982.

[125] A. I. M. S. Ud-Din and A. Roujeinikova, "Methyl-accepting chemotaxis proteins: a core sensing element in prokaryotes and archaea," *Cell. Mol. Life Sci.,* pp. 1-11, 2017.

[126] J. S. Parkinson, G. L. Hazelbauer and J. J. Falke, "Signaling and sensory adaptation in Escherichia coli chemoreceptors: 2015 update," *Trends in microbiology,* vol. 23, no. 5, p. 257–266, 2015.

[127] V. Sourjik and N. S. Wingreen, "Responding to chemical gradients: bacterial chemotaxis," *Current opinion in cell biology,* vol. 24, p. 262–268, 2012.

[128] W. B. John and K. O. Nathan, "Hexitol Metabolism in Escherichia coli," *J. Bacteriol,* vol. 71, no. 5, p. 557–564., 1955.

[129] J. W. Lengeler, "Mutations affecting transport of the hexitols D-mannitol, D-glucitol, and galactitol in Escherichia coli K-12: isolation and mapping.," *J. Bacteriol.,* vol. 124, no. 1, pp. 26-38, 1975.

[130] L. Volpon, C. R. Young, A. Matte and K. Gehring, "NMR structure of the enzyme GatB of the galactitol-specific phosphoenolpyruvate-dependent phosphotransferase system and its interaction with GatA," *Protein Science,* vol. 15, pp. 2435-2441, 2006.

[131] P. W. Postma, J. W. Lengeler and G. R. Jacobson, "Phosphoenolpyruvate:carbohydrate phosphotransferase systems of bacteria.," *Microbiol. Rev.,* vol. 57, no. 3, pp. 543-594, 1993.

[132] A. Brinkkötter, A. Shakeri-Garakani and J. W. Lengeler, "Two class II D-tagatose-bisphosphate aldolases from enteric bacteria," *Arch. Microbiol.,* vol. 177, pp. 410-419, 2002.

[133] J. W. Lengeler, "Analysis of Mutations Affecting the Dissimilation of Galactitol (Dulcitol) in Escherichia coli K 12," *Molec. Gen. Genet.,* vol. 152, pp. 83-91, 1977.

[134] B. Nobelmann and J. W. Lengeler, "Sequence of the gat operon for galactitol utilization from a wild-type strain EC3132 of Escherichia coli," *Biochimica et Biophysica Acta,* vol. 1262, pp. 69-72, 1995.

[135] B. Nobelmann and J. W. Lengeler, "Molecular Analysis of the gat Genes from Escherichia coli and of Their Roles in Galactitol Transport and Metabolism," *J. Baceriol.,* vol. 178, no. 23, pp. 6790-6795, 1996.

[136] G. Grass, "Iron Transport in Escherichia Coli: All has not been said and Done," *Biometals,* vol. 19, no. 2, pp. 159-172, 2006.

[137] K. Hantke, "Is the bacterial ferrous iron transporter FeoB a living fossil?," *Trends in Microbiology,* vol. 11, no. 5, pp. 192-195, 2003.

[138] H. Makui, E. Roig, S. T. Cole and et, al., "Identification of the Escherichia coli K-12 Nramp orthologue (MntH) as a selective divalent metal ion transporter," *Molecular Microbiology,* vol. 35, no. 5, pp. 1065-1078, 2000.

[139] M. L. Guerinot, "Microbial Iron Transport," *Annu. Rev. Microbiol.,* vol. 48, pp. 743-772, 1994.

[140] N. Noinaj, M. Guillier, T. J. Barnard and S. K. Buchanan, "TonB-Dependent Transporters: Regulation, Structure, and Function," *Annu. Rev. Microbiol.,* vol. 64, pp. 43-60, 2010.

[141] G. S. Moeck and J. W. Coulton, "TonB-dependent iron acquisition: mechanisms of siderophore-mediated active transport," *Molecular Microbiology,* vol. 28, no. 4, pp. 675-681, 1998.

[142] J. P. McHugh, F. Rodríguez-Quiñones, H. Abdul-Tehrani, et al., "Global Iron-dependent Gene Regulation in Escherichia coli," *J. Biol. Chem,* vol. 278, pp. 29478-29486, 2003.

[143] K. N. Raymond, E. A. Dertz and S. S. Kim, "Enterobactin: An archetype for microbial iron transport," *PNAS,* vol. 100, no. 7, pp. 3584-3588, 2003.

[144] A. Gehring, K. Bradley and C. Walsh, "Enterobactin Biosynthesis in Escherichia coli: Isochorismate Lyase (EntB) Is a Bifunctional Enzyme That Is Phosphopantetheinylated by EntD and Then Acylated by EntE Using ATP and 2,3-Dihydroxybenzoate," *Biochemistry ,* vol. 36, pp. 8495-8503, 1997.

[145] F. Rusnak, M. Sakaitani, D. Drueckhammer, et al., "Biosynthesis of the Escherichia coli Siderophore Enterobactin: Sequence of the entF Gene, Expression and Purification of EntF, and Analysis of Covalent Phosphopantetheine," *Biochemistry,* vol. 30, no. 11, pp. 2916-2927, 1991.

[146] D. Leduc, A. Battesti and E. Bouveret, "The Hotdog Thioesterase EntH (YbdB) Plays a Role In Vivo in Optimal Enterobactin Biosynthesis by Interacting with the ArCP Domain of EntB," *J. Bacteriol.,* vol. 189, no. 19, pp. 7112-7126, 2007.

[147] H. Beinert and P. J. Kiley, "Fe-S proteins in sensing and regulatory functions," *Curr. Opin. Chem. Biol,* vol. 3, no. 2, pp. 152-157, 1999.

[148] E. N. Marinoni, J. S. de Oliveira, Y. Nicolet, et al., "(IscS-IscU)2 Complex Structures Provide Insights into Fe2S2 Biogenesis and Transfer," *Angew. Chem., Int. Ed.,* vol. 51, p. 5439−5442, 2012.

[149] M. Fontecave, S. Ollagnier de Choudens, B. Py and F. Barras, "Mechanisms of iron–sulfur cluster assembly: the SUF machinery," *J. Biol. Inorg. Chem.,* vol. 10, pp. 713-721, 2005.

[150] M. Bühning, A. Valleriani and S. Leimkühler, "The Role of SufS Is Restricted to Fe−S Cluster Biosynthesis in Escherichia coli," *Biochemistry,* vol. 56, pp. 1987-2000, 2017.

[151] C. J. Schwartz, J. L. Gie, T. Patschkowski, et al., "IscR, an Fe-S cluster-containing transcription factor, represses expression of Escherichia coli genes encoding Fe-S cluster assembly proteins," *PNAS,* vol. 98, no. 26, p. 14895–14900, 2001.

[152] F. W. Outten, O. Djaman and G. Storz, "A suf operon requirement for Fe–S cluster assembly during iron starvation in Escherichia coli," *Molecular Microbiology,* vol. 52, no. 3, pp. 861-872, 2004.

[153] C. Ayala-Castro, A. Saini and F. W. Outten, "Fe-S Cluster Assembly Pathways in Bacteria," *Microbiol. Mol. Biol. Rev.,* vol. 72, no. 1, pp. 110-125, 2008.

[154] S. Bandyopadhyay, K. Chandramouli and M. K. Johnson, "Iron–sulfur cluster biosynthesis," *Biochem. Soc. Trans. ,* vol. 36, pp. 1112-1119, 2008.

[155] L. Loiseau, S. Ollagnier-de Choudens, D. Lascoux, et al., "Analysis of the heteromeric CsdA-CsdE cysteine desulfurase, assisting Fe-S cluster biogenesis in Escherichia coli," *J. Biol. Chem.,* vol. 280, p. 26760–26769, 2005.

[156] M. Y. Galperin and E. V. Koonin, "From complete genome sequence to 'complete' understanding?," *Trends in Biotechnology,* vol. 28, pp. 389-406, 2010.

[157] M. Rohrwild, O. Coux, H. Huanf, et al., "HslV-HslU: A novel ATP-dependent protease complex in Escherichia coli related to the eukaryotic proteasome," *PNAS,* vol. 93, no. 12, pp. 5808-5813, 1996.

[158] M. M. Khattar, "Overexpression of the hslVU operon suppresses SOS-mediated inhibition of cell division in Escherichia coli," *FEBS Letters ,* vol. 414, pp. 402-404, 1997.

[159] M. Kanemori, H. Yanagi and T. Yura, "The ATP-Dependent HslVU/ClpQY Protease Participates in Turnover of Cell Division Inhibitor SulA in Escherichia coli," *J. Bacteriol.,* vol. 181, no. 12, pp. 3674-3680, 1999.

[160] I. S. Seong, J. Y. Oh, S. J. Yoo, et al., "ATP-dependent degradation of SulA, a cell division inhibitor, by the HslVU protease in Escherichia coli," *FEBS Letters,* vol. 456, no. 1, pp. 211-214, 1999.

[161] W. Nishii and T. Kenji, "Determination of the cleavage sites in SulA, a cell division inhibitor, by the ATP-dependent HslVU protease from Escherichia coli," *FEBS Letters,* vol. 553, no. 3, pp. 351-354, 2003.

[162] A. Kato, H. Tanabe and R. Utsumi, "Molecular Characterization of the PhoP-PhoQ Two-Component System in Escherichia coli K-12: Identification of Extracellular Mg2+-Responsive Promoters," *J. Bacteriol.,* vol. 181, no. 17, pp. 5516-5520, 1999.

[163] S.-Y. Park, M. J. Cromie, E.-J. Lee and E. A. Groisman, "A bacterial mRNA leader that employs different mechanisms to sense disparate intracellular signals," *Cell,* vol. 142, pp. 737-748, 2010.

[164] A. R. Gall, K. A. Datsenko, N. Figueroa-Bossi, et al., "Mg2+ regulates transcription of mgtA in Salmonella Typhimurium via translation of proline codons during synthesis of the MgtL peptide," *PNAS,* p. e:1612268113, 2016.

[165] J. Barchiesi, M. E. Castelli,, F. C. Soncini and E. G. Véscovi, "mgtA Expression Is Induced by Rob Overexpression and Mediates a Salmonella enterica Resistance Phenotype," *J. Bacteriol.,* vol. 190, no. 14, pp. 4951-4958, 2008.

[166] S. B. Zou, The Role of Elongation Factor P in Salmonella enterica serovar Typhimurium Stress Response and Pathogenesis, University of Toronto (Canada), 2015.

[167] K. A. Datsenko and B. L. Wanner, "One-step inactivation of chromosomal genes in Escherichia coli K-12 using PCR products," *PNAS,* vol. 97, no. 12, pp. 6640-6645, 2000.

[168] L. C. Thomason, N. Costantino and D. L. Court, "E. coli Genome manipulation by P1 Transduction," *Curr. Protoc. Mol. Biol.,* vol. 79, pp. 1.17.1-1.17.8, 2007.

[169] A. J. Griffiths, S. R. Wessler, R. C. Lewontin, et al., An Introduction to Genetic Analysis Eighth Edition, Freeman, W. H. & Company, 2004.

[170] A. Shevchenko , H. Tomas, J. Havlis, et al., "In-gel digestion for mass spectrometric characterization of proteins and proteomes.," *Nat Prot.,* vol. 1, no. 6, pp. 2856-2860, 2006.

[171] J. Rappsilber, Y. Ishihama, M. Mann, et al., "Stop and Go Extraction Tips for Matrix-Assisted Laser Desorption/Ionization, Nanoelectrospray, and LC/MS Sample Pretreatment in Proteomics," *Anal. Chem.,* vol. 75, pp. 663-670, 2003.

[172] O. J. V. M. S. e. a. Gruhler A, "Quantitative phosphoproteomics applied to the yeast pheromone signaling pathway," *Molecular & Cellular Proteomics,* vol. 4, no. 3, pp. 310-327, 2005.

[173] S. Tyanova, M. Mann and J. Cox, "MaxQuant for in-depth analysis of large SILAC datasets," *MaxQuant for in-depth analysStable Isotope Labeling by Amino Acids in Cell Culture (SILAC) Methods and Protocols,* pp. 351-364, 2014.

[174] J. Cox, N. Neuhauser, A. Michalski, et al., "Andromeda: A Peptide Search Engine Integrated into the MaxQuant Environment," *J. Proteome Res. ,* vol. 10, pp. 1794-1805, 2011.

[175] J. Cox and M. Mann, "D and 2D annotation enrichment: a statistical method integrating quantitative proteomics with complementary high-throughput data," *BMC bioinformatics,* vol. 13, no. 16, p. S12, 2012.

7 Appendix

Sequence of the FRT-kanR-FRT deletion cassette from priming sites P1 to P2 (1477 bps)

Priming site P1

GTGTAGGCTGGAGCTGCTTCGAAGTTCCTATACTTTCTAGAGAATAGGAACTTCGGAATAGGAACT
TCAAGATCCCCTCACGCTGCCGCAAGCACTCAGGGCGCAAGGGCTGCTAAAGGAAGCGGAACACG
TAGAAAGCCAGTCCGCAGAAACGGTGCTGACCCCGGATGAATGTCAGCTACTGGGCTATCTGGAC
AAGGGAAAACGCAAGCGCAAAGAGAAAGCAGGTAGCTTGCAGTGGGCTTACATGGCGATAGCTAG
ACTGGGCGGTTTTATGGACAGCAAGCGAACCGGAATTGCCAGCTGGGGCGCCCTCTGGTAAGGTTG
GGAAGCCCTGCAAAGTAAACTGGATGGCTTTCTTGCCGCCAAGGATCTGATGGCGCAGGGGATCA
AGATCTGATCAAGAGACAGGATGAGGATCGTTTCGCATGATTGAACAAGATGGATTGCACGCAGG
TTCTCCGGCCGCTTGGGTGGAGAGGCTATTCGGCTATGACTGGGCACAACAGACAATCGGCTGCTC
TGATGCCGCCGTGTTCCGGCTGTCAGCGCAGGGGCGCCCGGTTCTTTTTGTCAAGACCGACCTGTCC
GGTGCCCTGAATGAACTGCAGGACGAGGCAGCGCGGCTATCGTGGCTGGCCACGACGGGCGTTCC
TTGCGCAGCTGTGCTCGACGTTGTCACTGAAGCGGGAAGGGACTGGCTGCTATTGGGCGAAGTGCC
GGGGCAGGATCTCCTGTCATCTCACCTTGCTCCTGCCGAGAAAGTATCCATCATGGCTGATGCAAT
GCGGCGGCTGCATACGCTTGATCCGGCTACCTGCCCATTCGACCACCAAGCGAAACATCGCATCGA
GCGAGCACGTACTCGGATGGAAGCCGGTCTTGTCGATCAGGATGATCTGGACGAAGAGCATCAGG
GGCTCGCGCCAGCCGAACTGTTCGCCAGGCTCAAGGCGCGCATGCCCGACGGCGAGGATCTCGTCG
TGACCCATGGCGATGCCTGCTTGCCGAATATCATGGTGGAAAATGGCCGCTTTTCTGGATTCATCG
ACTGTGGCCGGCTGGGTGTGGCGGACCGCTATCAGGACATAGCGTTGGCTACCCGTGATATTGCTG
AAGAGCTTGGCGGCGAATGGGCTGACCGCTTCCTCGTGCTTTACGGTATCGCCGCTCCCGATTCGC
AGCGCATCGCCTTCTATCGCCTTCTTGACGAGTTCTTCTGAGCGGGACTCTGGGGTTCGAAATGACC
GACCAAGCGACGCCCAACCTGCCATCACGAGATTTCGATTCCACCGCCGCCTTCTATGAAAGGTTG
GGCTTCGGAATCGTTTTCCGGGACGCCGGCTGGATGATCCTCCAGCGCGGGGATCTCATGCTGGAG
TTCTTCGCCCACCCCAGCTTCAAAAGCGCTCTGAAGTTCCTATACTTTCTAGAGAATAGGAACTTCG
GAATAGGAACTAAGGAGGATATTCATATG

Priming site P2

FRT

NEOKAN promoter

kanR

Amino acids sequence of EF-P

MATYYSNDFRAGLKIMLDGEPYAVEASEFVKPGKGQAFARVKLRRLLTGTRVEKTFKSTDSAEGADV
VDMNLTYLYNDGEFWHFMNNETFEQLSADAKAIGDNAKWLLDQAECIVTLWNGQPISVTPPNFVELEI
VDTDPGLKGDTAGTGGKPATLSTGAVVKVPLFVQIGEVIKVDTRSGEYVSRVK

Amino acids sequence of YeiP

MPRANEIKKGMVLNYNGKLLLVKDIDIQSPTARGAATLYKMRFSDVRTGLKVEERFKGDDIVDTVTLT
RRYVDFSYVDGNEYVFMDKEDYTPYTFTKDQIEEELLFMPEGGMPDMQVLTWDGQLLALELPQTVDL
EIVETAPGIKGASASARNKPATLSTGLVIQVPEYLSPGEKIRIHIEERRYMGRAD

Homolog block

Table S1. Proteins of up-regulated in all of the four adapted strains, and significantly changed in at least one adapted strain compared to control strain.

Gene name	Evo1 Fold	Evo2 Fold	Evo3 Fold	Evo4 Fold	Annotation	KEGG pathway
speB	1.09	1.31	1.42	0.61	Agmatinase	Arg and Pro metabolism
speC	0.75	1.09	0.74	0.42	Ornithine decarboxylase, constitutive	Arg and Pro metabolism
gpmA	0.90	1.01	0.20	0.74	Phosphoglyceromutase 1	Glycolysis
pfkB	0.55	1.15	0.97	1.98	6-phosphofructokinase II	Glycolysis; Pentose phosphate pathway
eno	0.87	1.28	0.29	0.39	Enolase	Glycolysis; RNA degradation
pgi	0.83	1.10	0.21	0.34	Glucosephosphate isomerase	Glycolysis; Pentose phosphate pathway
tktB	0.07	1.50	0.93	0.60	Transketolase 2, thiamine triphosphate-binding	Pentose phosphate pathway
aroA	0.33	0.15	1.09	0.01	5-enolpyruvylshikimate-3-phosphate synthetase	Phe, Tyr, Trp biosynthesis
rpsS	0.75	0.62	0.59	3.27	30S ribosomal subunit protein S19	Ribosome
rpsQ	1.07	0.40	0.17	1.93	30S ribosomal subunit protein S17	Ribosome
rraA	0.80	1.26	0.11	0.95	Ribonuclease E inhibitor protein	RNA degradation
rnr	0.53	1.29	0.05	0.63	Exoribonuclease R, rnase R	RNA degradation
yqjG	0.84	2.26	0.74	1.55	Putative S-transferase	No description
rnk	1.33	0.51	1.05	1.70	Regulator of nucleoside diphosphate kinase	No description
qorA	0.58	1.43	0.44	0.81	Quinone oxidoreductase, NADPH-dependent	No description
cysQ	0.77	0.87	0.86	0.91	3'(2'),5'-bisphosphate nucleotidase	No description
elaB	0.24	1.31	0.64	1.02	Putative membrane-anchored DUF883 family ribosome-binding protein	No description
ybdF	0.60	1.05	1.04	1.23	DUF419 family protein	No description
ecnB	0.49	1.29	0.77	1.16	Entericidin B membrane lipoprotein	No description
ahpF	0.76	0.36	0.22	0.98	Alkyl hydroperoxide reductase, F52a subunit, FAD/NAD(P)-binding	No description
yigI	0.90	0.98	0.11	0.50	4HBT thioesterase family protein	No description
yqjD	0.38	1.34	0.15	1.38	Membrane-anchored ribosome-binding protein	No description
hchA	0.34	1.35	0.47	1.51	Glyoxalase III and Hsp31 molecular chaperone	No description
msyB	0.45	1.70	0.43	1.87	Multicopy suppressor of secy and seca	No description
uspD	0.66	1.41	0.35	1.40	Stress-induced protein	No description
ycgM	0.97	1.17	0.58	1.32	Putative isomerase/hydrolase	No description
hdhA	0.53	1.22	1.02	1.47	7-alpha-hydroxysteroid dehydrogenase, NAD-dependent	No description
dps	0.55	1.87	0.43	1.42	Fe-binding and storage protein; stress-inducible DNA-binding protein	No description

Table S2. Proteins of down-regulated in all of the four adapted strains, and at least significantly changed in two adapted strain compared to control strain.

Gene name	Evo1 Fold	Evo2 Fold	Evo3 Fold	Evo4 Fold	Annotation	KEGG pathway
modA	-1.63	-1.57	-2.05	-2.07	Molybdate ABC transporter periplasmic binding protein; chlorate resistance protein	ABC transporters
livJ	-0.24	-0.05	-1.12	-1.20	Branched-chain amino acid ABC transporter periplasmic binding protein	ABC transporters
gdhA	-1.48	-1.08	-1.27	-2.18	Glutamate dehydrogenase, NADP-specific	Ala, Asp, Glu metabolism; Arg and Pro metabolism
glnA	-0.79	-0.45	-1.30	-1.25	Glutamine synthetase	Ala, Asp, Glu metabolism; Arg and Pro metabolism
gltB	-0.91	-0.23	-1.00	-1.35	Glutamate synthase, large subunit	Ala, Asp, Glu metabolism
pyrI	-4.67	-4.78	-0.81	-5.43	Aspartate carbamoyltransferase, regulatory subunit	Ala, Asp, Glu metabolism Pyrimidine metabolism
pyrB	-4.44	-4.18	-3.53	-5.18	Aspartate carbamoyltransferase, catalytic subunit	Ala, Asp, Glu metabolism Pyrimidine metabolism
carA	-2.45	-2.32	-2.25	-3.17	Carbamoyl phosphate synthetase small subunit, glutamine amidotransferase	Ala, Asp, Glu metabolism Pyrimidine metabolism
carB	-2.48	-2.04	-2.41	-3.02	Carbamoyl-phosphate synthase large subunit	Ala, Asp, Glu metabolism Pyrimidine metabolism
codA	-1.95	-1.74	-2.21	-2.57	Cytosine/isoguanine deaminase	Arg and Pro metabolism; Pyrimidine metabolism
cheZ	-4.54	-4.57	-3.05	-4.47	Chemotaxis regulator, protein phosphatase for chey	Bacterial chemotaxis
fliN	-1.76	-1.78	-2.51	-2.93	Flagellar motor switching and energizing component	Bacterial chemotaxis; Flagellar assembly
cheY	-5.04	-5.20	-3.70	-5.27	Chemotaxis regulator transmitting signal to flagellar motor component	Bacterial chemotaxis
cheW	-5.53	-5.64	-4.61	-5.73	Purine-binding chemotaxis protein	Bacterial chemotaxis
cheA	-4.84	-4.64	-3.65	-3.52	Fused chemotactic sensory histidine kinase in two-component regulatory system with cheb and chey: sensory histidine kinase/signal sensing protein	Bacterial chemotaxis
tar	-4.74	-4.87	-3.23	-3.90	Methyl-accepting chemotaxis protein II	Bacterial chemotaxis
tsr	-5.23	-4.88	-3.77	-5.05	Methyl-accepting chemotaxis protein I, serine sensor receptor	Bacterial chemotaxis
tap	-4.43	-2.99	-1.77	-2.13	Methyl-accepting protein IV	Bacterial chemotaxis
sdhD	-0.81	-0.65	-1.76	-1.44	Succinate dehydrogenase, membrane subunit, binds cytochrome b556	TCA cycle
sdhA	-0.42	-0.59	-1.45	-1.53	Succinate dehydrogenase, flavoprotein subunit	TCA cycle
sdhB	-0.66	-1.10	-1.33	-1.47	Succinate dehydrogenase, fes subunit	TCA cycle
pykF	-4.95	-4.98	-0.78	-1.19	Pyruvate kinase I	Glycolysis
flgE	-4.55	-4.37	-2.98	-4.94	Flagellar hook protein	Flagellar assembly
flgH	-1.25	-1.26	-2.49	-1.88	Flagellar protein of basal-body outer-membrane L ring	Flagellar assembly

fliF	-1.38	-1.43	-0.93	-4.26	Flagellar basal-body MS-ring and collar protein	Flagellar assembly
fliC	-5.29	-5.16	-4.22	-4.98	Flagellar filament structural protein (flagellin)	Flagellar assembly
gatY	-2.88	-3.72	-2.18	-3.30	D-tagatose 1,6-bisphosphate aldolase 2, catalytic subunit	Galactose metabolism
gatA	-2.67	-4.04	-2.27	-1.98	Galactitol-specific enzyme IIA component of PTS	Galactose metabolism; Phosphotransferase system (PTS)
aldA	-0.85	-0.71	-1.69	-1.52	Aldehyde dehydrogenase A, NAD-linked	Glyoxylate and dicarboxylate metabolism; Pyruvate metabolism
aroF	-1.90	-2.09	-1.95	-2.83	3-deoxy-D-arabino-heptulosonate-7-phosphate synthase, tyrosine-repressible	Phe, Tyr, Trp biosynthesis
trpE	-1.57	-2.60	-0.83	-0.27	Component I of anthranilate synthase	Phe, Tyr, Trp biosynthesis
pyrD	-1.82	-2.02	-1.88	-1.91	Dihydro-orotate oxidase, FMN-linked	Pyrimidine metabolism
pyrC	-1.61	-1.92	-0.88	-1.46	Dihydro-orotase	Pyrimidine metabolism
rpmE	-0.96	-1.62	-1.25	-2.86	50S ribosomal subunit protein L31	Ribosome
ycgR	-4.37	-4.98	-2.88	-4.34	Flagellar velocity braking protein	No description
gntR	-3.47	-2.69	-2.84	-7.67	D-gluconate inducible gluconate regulon transcriptional repressor	No description
ridA	-1.68	-1.30	-1.98	-1.70	Enamine/imine deaminase, reaction intermediate detoxification	No description
fliL	-1.71	-3.54	-3.24	-1.86	Flagellar biosynthesis protein	No description
miaB	-2.02	-3.71	-0.06	-0.59	Trna-i(6)A37 methylthiotransferase	No description
yebO	-0.33	-0.30	-0.86	-1.81	Putative inner membrane protein	No description
yahK	-1.49	-1.55	-0.11	-1.55	Broad specificity NADPH-dependent aldehyde reductase, Zn-containing	No description
msrB	-0.66	-0.95	-1.06	-1.54	Methionine sulfoxide reductase B	No description

Table S3. Changes of PPP-containing proteins in *Δefp* strain compared to control strains.

Gene name	Exp1 Fold	Exp2 Fold	Exp1 significant	Exp2 significant	Annotation
entF	-3.06	-3.61	+	+	Enterobactin synthase multienzyme complex component, ATP-dependent
valS	-1.25	-1.41	+	+	Valyl-trna synthetase
rnb	-1.70	-1.92	+	+	Ribonuclease II
lepA	-1.24	-1.43	+	+	Back-translocating elongation factor EF4, gtpase
ycgR	-1.73	-1.91	+	+	Flagellar velocity braking protein, c-di-GMP-regulated
qorA	-1.39	-1.35	+	+	Quinone oxidoreductase, NADPH-dependent
tonB	-0.70	-0.96		+	Membrane spanning protein in tonb-exbb-exbd transport complex
ftsK	-0.29	-0.41			DNA translocase at septal ring sorting daughter chromsomes
gltB	-0.15	-0.09			Glutamate synthase, large subunit
katE	0.05	0.03			Catalase HPII, heme d-containing

mrcA	0.51	0.46	Penicillin-binding protein 1a, murein transglycosylase and transpeptidase
ppc	-0.27	-0.40	Phosphoenolpyruvate carboxylase
nuoC	0.37	0.31	NADH: ubiquinone oxidoreductase, fused CD subunit
uvrB	-0.73	-0.59	Exision nuclease of nucleotide excision repair, DNA damage recognition component
nlpD	0.25	0.33	Activator of amic murein hydrolase activity, lipoprotein
cyoB	0.11	0.11	Cytochrome o ubiquinol oxidase subunit I
agp	0.06	0.10	Glucose-1-phosphatase/inositol phosphatase
dppF	-0.62	-0.82	Dipeptide/heme ABC transporter atpas
hisD	-0.25	-0.26	Bifunctional histidinal dehydrogenase/ histidinol dehydrogenase
clsA	-0.07	-0.06	Cardiolipin synthase 1
rsmA	0.24	0.20	16S rrna m(6)A1518, m(6)A1519 dimethyltransferase, SAM-dependent
yhbW	0.06	0.30	Putative luciferase-like monooxygenase
ydiK	0.06	0.23	UPF0118 family inner membrane protein
sdaC	-0.08	-0.34	Putative serine transporter
nudC	-0.16	-0.18	NADH pyrophosphatase
ycgL	0.37	0.43	UPF0745 family protein

Exp_1 represents the first experiment of *Δefp*: Control_1; Exp_2 represents the second experiment of *Δefp*: Control_2.

Table S4. The proteins are significantly up-regulated in at least two of the four adapted *Δefp* strains.

Gene name	Annotation	KEGG pathway
cysQ	3'(2'),5'-bisphosphate nucleotidase	No description
prlC	Oligopeptidase A	No description
pyrE	Orotate phosphoribosyltransferase	Pyrimidine metabolism
sufA	Fe-S cluster assembly protein	No description
yeeN	UPF0082 family; Probable transcriptional regulatory protein	No description
argB	Acetylglutamate kinase	Arg and Pro metabolism
ghrB	Glyoxylate/hydroxypyruvate reductase B	Pentose phosphate pathway
grcA	Autonomous glycyl radical cofactor	No description
malE	Maltose transporter subunit	ABC transporters
qorA	Quinone oxidoreductase, NADPH-dependent	No description
sufS	Cysteine desulfurase, stimulated by sufe; Selenocysteine lyase, PLP-dependent	Selenocompound metabolism; Thiamine metabolism
valS	Valyl-trna synthetase	Aminoacyl-tRNA biosynthesis; Val, Leu and Ile biosynthesis
yhjJ	Putative periplasmic M16 family chaperone	No description
argH	Argininosuccinate lyase	Ala, Asp and Glu metabolism; Arg and Pro metabolism
bcsG	DUF3260 family cellulose production inner membrane protein	No description
fiu	Catecholate siderophore receptor	No description
hslU	Molecular chaperone and atpase component of hsluv protease	No description
hslV	Peptidase component of the hsluv protease	No description
malP	Maltodextrin phosphorylase	Insulin signaling pathway;

		Starch and sucrose metabolism
nanA	N-acetylneuraminate lyase	Amino sugar and nucleotide sugar metabolism
yghA	Putative oxidoreductase	No description
yghJ	Putative secreted and surface-associated lipoprotein mucinase	Vibrio cholerae pathogenic cycle
yjjU	Putative patatin-like family phospholipase	No description

8 Acknowledgements

Confucius said, “The wise man finds pleasure in water, the virtuous man finds pleasure in hills.”

Several years ago, I just chose to take the road of scientific research with my own interests. I was very curious about the unknown road. I didn’t know whether it will be beautiful or dangerous on this road. Fortunately, until today, I am still traveling in the ocean of knowledge and climbing on the mountain of science. I am still on the road to the wise and virtuous. On this long journey, I have to thank those who have been with me to grow up. They are the most beautiful scenery on this road.

First and foremost, I would like to thank my supervisor, Prof. Nediljko Budisa, for the opportunity to study in this warm and positive group. His patience and wise guidance make me like bathing in the spring breeze. His desire for knowledge and rigorous attitude toward scientific research that set an example for me. I am really grateful his great support.

The deepest gratitude would be expressed to my additional supervisor, Dr. Verónica Dumit. She brought me to the beautiful world of proteomics. She gives me kind help in both of study and life. Her decisive work style and responsible work attitude benefit me a lot. I would like to give her the most sincere thanks and wishes.

I would also like to thank my dear colleagues of Biocatalysis Group in Technische Universität Berlin, especially for Dr. Ying Ma, Christian Schipp, and Huan Sun, we supported each other and cooperated very happy in this project. The same thanks to other members of my laboratory family in Berlin: Federica Agostini, Saba Nojoumi, Tuyet-Mai To, Isabella Tolle, Jessica Nickling, Maxi Marock, Dr. Tobias Baumann, and Dr. Jan-Stefan Völler.

At the same time, I have to thank the dear members of my laboratory family in Freiburg, the colleagues of Core facility of Proteomics (CFP) in University of Freiburg: Lisa Winner, Dr. Simon Stephan, Daniel Vogele, and the students I guided during my research, Gizem Kilic and Almena López. Great gratitude for your contribution to my work. Additionally, I appreciate the support and advice from Prof. Jörn Dengjel and his group, Zehan Hu, Regine Tölle, Michal Rackiewicz, Christine Gretzmeier, Dr. Britta Diedrich, and Dr. Kerstin Thriene.

The Berlin International Graduate School of Natural Science and Engineering (BIG-NSE) also supplied me great help in both of study and life, which prompted me to adapt to the life in Germany as soon as possible. I thank the BIG-NSE friends: Dr. Xuan Li, Nils Lindenmaier, Stefan Wahlefeld, Linda Sukmarini, Ha Vu Le, Dr. Genwen Tan, Dr. Linyu Jiao, Dr. Xunhua Zhao, Dr. Xinrui Zhou and the managing director Dr. Jean-Philippe Lonjaret.

The financial support from China Scholarship Council (CSC) is essential for my whole doctoral process. I am extremely grateful the opportunity supplied by CSC.

I would like to thank some old friends. Prof. Chun Li who led me to enter the gate of life science world. My best friend, Yucheng Jin, since childhood we support each other and grow together. And the lovely friends who accompanied me with a good time in Germany: Tobias Pilz and his family, Tianyi Lian, Man Zhang, Xudong Zhang, Xiaoyu Jia and Kefei Chen.

Finally, I would like to thank my dear parents. In fact, no words can express the gratitude for the greatest love of the world.

The road ahead will be long. Our climb will be steep. I will be on the road, I am looking forward to traveling with you.

Eidesstattliche Erklärung

Hiermit versichere ich, dass ich die vorliegende Arbeit eigenständig und ohne fremde Hilfe angefertigt habe. Insbesondere habe ich hierfür nicht die entgeltliche Hilfe von Vermittlungs- bzw. Beratungsdiensten in Anspruch genommen. Niemand hat von mir unmittelbarer mittelbar geldwerte Leistungen für Arbeiten erhalten, die im Zusammenhang mit dem Inhalt der vorgelegten Dissertation stehen. Es wurden ausschließlich die angegebenen Quellen und Hilfsmittel genutzt. Alle Ergebnisse, die in Kooperation mit anderen Arbeitsgruppen erhalten wurden und in anderen Arbeiten zu finden sind, sind dementsprechend gekennzeichnet. Diese Arbeit wurde in dieser oder ähnlicher Form bisher bei keiner anderen Prüfungsbehörde einer Hochschule, weder im Inland noch im Ausland, eingereicht.

Berlin, 15, August 2017